UNIVERSIDADE D
COIMBRA

Cátia Sofia Leite Pereira

Metabolomic and Proteomic Approaches to Characterize the Role of Epigenetics on *Pinus halepensis* Mill. Somatic Embryogenesis

Tese no âmbito do Doutoramento em Biociências, especialidade em Biotecnologia, orientada pelo Professor Doutor Jorge Manuel Pataca Leal Canhoto e pela Doutora Paloma Moncaleán Guillén e apresentada ao departamento de Ciências da Vida da Faculdade de Ciências e Tecnologia da Universidade de Coimbra.

Abril de 2023

Faculdade de Ciências e Tecnologia
da Universidade de Coimbra

METABOLOMIC AND PROTEOMIC APPROACHES TO CHARACTERIZE THE ROLE OF EPIGENETICS ON *PINUS HALEPENSIS* MILL. SOMATIC EMBRYOGENESIS

Cátia Sofia Leite Pereira

Tese no âmbito do Doutoramento em Biociências, especialidade em Biotecnologia, orientada pelo Professor Doutor Jorge Manuel Pataca Leal Canhoto e pela Doutora Paloma Moncaleán Guillén e apresentada ao Departamento de Ciências da Vida da Faculdade de Ciências e Tecnologia da Universidade de Coimbra.

Abril de 2023

1 2 9 0

UNIVERSIDADE D
COIMBRA

Agradecimentos

A realização deste trabalho nunca teria sido possível sem toda a ajuda recebida e, por isso, deixo um agradecimento sincero a todos os que contribuíram para que se tornasse uma realidade.

Como não poderia deixar de ser, começo por agradecer aos meus orientadores, professor Jorge Canhoto e Doutora Paloma Moncaleán, por toda a direção, ajuda, disponibilidade e ensinamentos fornecidos desde o primeiro dia.

Já passaram uns bons anos desde que o professor Jorge me aceitou como estagiária no laboratório de Biotecnologia de Plantas da UC. Estar-lhe-ei eternamente grata por ter acreditado em mim, por aceitar o meu pedido de orientação, e me ter guiado e apoiado ao longo de todos os altos e baixos desta minha jornada científica. Sem o professor, nada disto teria acontecido. À Doutora Paloma, agradeço-lhe profundamente ter aceite esta portuguesa, caída do nada no seu laboratório da NEIKER-BRTA, e por tudo o que me proporcionou. Obrigada por todo o incentivo, carinho, e confiança depositados em mim, mesmo quando eu própria não os tinha. Grata, de coração!

Deixo, ainda, um especial e forte agradecimento à Doutora Itziar Montalbán. Quem, apesar de não ser orientadora oficial deste trabalho, me "adotou" de braços abertos como se fosse transmitindo-me uma quantidade imensurável de conhecimento! Obrigada por tanto, Itzi!

Ao professor Miroslav Strnad e ao Doutor Ondrej Novák, por me receberem no Laboratório de Reguladores de Crescimento da Universidade de Palacký, na República Checa. Assim como a todos os que aí trabalham e tão bem me acolheram. Em especial à Doutora Iva Pavlović e Jitka Široká, pela ajuda no laboratório e pela amizade fora dele.

Ao Doutor Bruno Manadas e à Vera Mendes, do Centro de Neurociências e Biologia Celular da UC, e à Doutora Sandra Correia e à Ana Pedrosa, do Centro de Ecologia Funcional da UC, pela ajuda, disponibilidade e trabalho entregues nas análises do proteoma e transcritos.

À professora María Jesús Cañal e à Doutora Mónica Meijón, e a todos aqueles que me acolheram e ajudaram no laboratório de Fisiologia Vegetal da Universidade de Oviedo, Espanha.

À professora Ester Sales da Universidade de Zaragoza, por me receber no seu laboratório no Departamento de Ciências Agrárias e do Meio Ambiente, em Huesca, Espanha. Pelos ensinamentos de PCR e genes, pela hospitalidade e pelo "Gewürztraminer".

Aos meus colegas e amigos do laboratório de Biotecnologia Vegetal da UC, muito obrigada por me acompanharem nesta jornada… "Meus anjos!".

A todos os que fazem parte da NEIKER-BRTA. Por me terem recebido tão amavelmente. Por me ensinarem pacientemente o Espanhol e Euskera (ainda que sem muitos frutos). Pelos cafés, "Pintxo-potes", passeios e conversas… por fazerem de Vitória uma agradável segunda casa durante estes anos. Eskerrik asko!

Finalmente, um agradecimento especial aos, agora doutores, que me acompanharam desde o primeiro dia. Ao Doutor João Martins, obrigada, isto foi sem dúvida uma montanha-russa e tive o melhor colega de viagem… que venha a seguinte. Ao Doutor Ander Castander, gracias chugggiiiii.. a amizade que cresceu entre pinheiros e laboratórios diversos, durará, entre cantigas espetacularmente desafinadas e felizes, por muitos anos.

Para finalizar, à minha família e amigos. Aos de sempre e para sempre, e aos que chegaram no entretanto. Pelo amor e suporte, por existirem na minha vida e estarem incondicionalmente ao meu lado, mesmo quando não estava fisicamente presente.

Para a Luísa e o Marco, meus pais… e para o João e o Guilherme, meus irmãos… porque vos amo e não existem palavras suficientes para vos agradecer.

Funding

The Portuguese Foundation for Science and Technology (FCT) supported the PhD fellowship of Cátia Pereira (SFRH/BD/123702/2016).
ReNATURE (CENTRO-01-0145-FEDER-000007), F4F-Forest for the future (CENTRO-08-5864-FSE-000031), and CULTIVAR (CENTRO-01-0145-FEDER-000020), co-financed by the Regional Operational Programme Centro 2020, Portugal 2020, and the European Union, through the European Regional Development Fund (ERDF); PINEM (AGL2016-76143-C4-3R), MINECO (Spanish Government); DECO (Basque government, Ayudas de formación a jóvenes investigadores y tecnólogos); VARIFOR (PID2020-112627RB-C32), Ministerio de Ciencia e Innovación (Spanish Government); BIOALI-CYTED (P117RT0522); and MULTIFOREVER (Project MULTIFOREVER is supported under the umbrella of ERA-NET cofund Forest Value by ANR (FR), FNR (DE), MINCyT (AR), MINECO-AEI (ES), MMM (FI), and VINNOVA (SE)).

This work was carried out at the Center for Functional Ecology—Science for People and the Planet (CFE), TERRA Associate Laboratory, Department of Life Sciences, University of Coimbra (Portugal), and the Department of Forestry Science of NEIKER-BRTA, Member of Basque Research and Technology Alliance (Basque Country, Spain).

Resumo

As árvores são parte fundamental de um dos mais importantes ecossistemas terrestres: as florestas. O elevado valor ecológico e socioeconómico que as florestas apresentam, acompanhado das ameaças climáticas e antropológicas que regularmente enfrentam, torna imperativo melhorar a qualidade e produtividade das árvores florestais. Assim, entender como os fatores climáticos impactam o seu funcionamento, sobrevivência e adaptação é crucial para antecipar as consequências que eventos ambientais extremos podem ter sobre esses ecossistemas.

A cultura *in vitro* é um conjunto de técnicas biotecnológicas que permite, entre outras coisas, clonar plantas. Ainda que o desenvolvimento embrionário represente um período muito curto na vida de uma árvore, a embriogénese somática, uma técnica de propagação em larga escala, provou ser uma ferramenta importante para caracterizar os vários mecanismos envolvidos na resposta ao stresse e adaptação das plantas.

As coníferas são as árvores mais comuns em vastas áreas do Hemisfério Norte, sendo o género *Pinus* crucial para a indústria madeireira e de grande importância ecológica devido à sua ampla distribuição mundial. O pinheiro-do-Alepo (*Pinus halepensis*), a espécie em estudo, é uma espécie mediterrânica com uma plasticidade ecológica significativa, o que tem contribuído para a sua utilização em programas de (re)florestação.

Assim sendo, o principal objetivo deste trabalho foi a indução de uma "memória" epigenética ao stresse, através da aplicação de elevadas temperaturas na fase de iniciação da embriogénese somática de *P. halepensis* para estudar os efeitos do stresse térmico na eficiência da embriogénese somática, e como ferramenta para compreender os mecanismos subjacentes à resposta ao stresse das coníferas. Para isso, diferentes tratamentos foram aplicados durante a indução das massas embrionárias (40 ℃ por 4 h, 50 ℃ por 30 min e 60 ℃ por 5 min).

Para avaliar como o stresse térmico pode afetar o sucesso das diferentes etapas da embriogénese somática, foram recolhidos dados ao longo das diferentes fases. Da mesma forma, para compreender os mecanismos de resposta ao stresse térmico, a análise dos efeitos dos tratamentos aplicados na concentração endógena de citocininas, na caracterização morfológica das culturas embriogénicas, no proteoma e na concentração relativa de carboidratos e aminoácidos das massas embrionárias obtidas foram analisados. Foram ainda avaliadas as taxas de metilação do DNA e a expressão diferencial de quatro genes relacionados ao stresse em massas embrionárias e agulhas de plantas somáticas *in vitro*.

Todos os tratamentos de indução permitiram a obtenção de plantas, sugerindo a possibilidade de induzir embriogénese somática sob stresse térmico em *P. halepensis*, e não se detetaram diferenças significativas entre as taxas de iniciação, proliferação, maturação ou germinação; os tratamentos aplicados durante a fase de iniciação da embriogénese somática não levaram à perda de variedade genética comparativamente às condições controlo (23 ℃ por 9 semanas). No entanto, uma diferença significativa foi encontrada no que toca à produção de embriões somáticos, tendo o maior número de embriões sido obtido em amostras induzidas a 60 ℃ (5 min). Deste modo, este

tratamento térmico parece ter desencadeado um efeito positivo na eficiência do processo, reforçando-a.

A análise da concentração endógena de citocininas mostrou que as diferentes condições aplicadas durante a fase de iniciação da embriogénese somática levaram a diferentes perfis hormonais. Não foram encontrados níveis de metilação do DNA significativamente diferentes, mas as pequenas flutuações encontradas podem estar relacionadas com o processo embriogénico, e variações na expressão diferencial de genes relacionados ao stresse foram obtidas ao longo de diferentes fases da embriogénese. Finalmente, foram identificadas 27 proteínas relacionadas com a resposta ao stresse térmico, sendo que a maioria das proteínas acumuladas em massas embrionárias induzidas a temperaturas mais elevadas estarão envolvidas na regulação do metabolismo, ligação ao DNA, divisão celular, regulação da transcrição e no ciclo de vida das proteínas. Além disso, foram encontradas diferenças significativas nas concentrações de sacarose, glutamina, glicina e cisteína.

Em conclusão, a aplicação do stresse térmico na fase inicial da embriogénese somática provocou efeitos que se mantiveram ao longo de diferentes fases do processo, e permitiu a identificação de citocininas, proteínas, genes relacionados ao stresse e metabólitos específicos envolvidos nos intrincados mecanismos subjacentes à resposta ao stresse e/ou ao processo embriogénico das coníferas.

Paralelamente, tentou-se desenvolver protocolos eficientes de embriogénese somática e organogénese para material adulto. Neste sentido, a primeira descrição de um protocolo de regeneração *in vitro* de árvores adultas de *P. halepensis*, por meio de organogénese, foi concretizada no âmbito desta tese.

Palavras-chave: fito-hormonas; pinheiro-do-Alepo; priming; proteínas; resposta ao stresse.

Abstract

Trees are fundamental players of one of the most important terrestrial ecosystems: forests. The immeasurable ecological and socio-economic value that forests represent, accompanied by the anthropological and climatic threats they regularly face, makes it imperative to improve forest trees quality and productivity. On this matter, a deeper understanding on how climatic factors impact tree's function, survival and adaptation is crucial for anticipating the consequences that the extreme environmental events foreseen may have on these ecosystems.

The *in vitro* culture is a set of biotechnological techniques that allows, among other things, to clone plants. Even though embryogenesis is a very short period at the lifespan of a tree, somatic embryogenesis, a large-scale propagation technique, proved to be a valuable tool to characterize the various mechanisms involved in stress response and adaptation of plants.

Conifers are the most common trees in some vast areas of the Northern Hemisphere and the *Pinus* genus, of crucial importance for the wood-based industries, has high ecological importance due to its wide distribution around the globe. Aleppo pine (*Pinus halepensis*), the species under study, is a Mediterranean species with significant ecological plasticity, which has contributed to its use in (re)afforestation programs.

With this as background, the main goal of this work was to trigger the formation of a long-lasting epigenetic "stress memory", through the application of high temperatures during the initiation stage of *P. halepensis* somatic embryogenesis to study the influence of heat stress regarding the success of the somatic embryogenesis process, and as a tool to understand the mechanisms underlying stress-response in conifers. For this matter, different temperature treatments were applied during the induction of embryonal masses (40 ℃ for 4 h, 50 ℃ for 30 min, and 60 ℃ for 5 min).

To assess how heat stress could affect the success of the different stages of the process, data were collected along the different steps of somatic embryogenesis. Likewise, to understand the mechanisms underlying temperature stress response, analyses regarding the effect of the temperature treatments applied on the endogenous concentration of cytokinins, the morphological characterization of the embryogenic cultures, the proteome and the relative concentration of soluble sugars, sugar alcohols and amino acids of the obtained embryonal masses were performed. Also, changes in the DNA methylation rates and the differential expression of four stress-related genes in embryonal masses and needles from *in vitro* somatic plants were evaluated.

It was possible not only to obtain plants from all induction treatments, suggesting the opportunity to induce somatic embryogenesis under heat stress in *P. halepensis,* but also to assess that there were no significant differences between initiation, proliferation, maturation, or germination rates for the different treatments assayed; the high temperature pulses applied during the initiation phase of somatic embryogenesis did not translate into genetic variety loss when compared to the standard conditions (23 ℃ for 9 weeks). Though, a significant difference was found at the production of somatic embryos, and the highest number was obtained at samples

induced at 60 ºC (5 min). In this sense, this specific temperature treatment appeared to have triggered a positive effect on the efficiency of the process, strengthening it.

The analysis of endogenous concentration of cytokinins showed that different conditions applied during the initiation phase of somatic embryogenesis led to different hormonal profiles. No significantly different levels of DNA methylation were found, but small fluctuations were seemingly related with the embryogenic process, and long-lasting variations in the differential expression of stress-related genes were obtained. Finally, 27 proteins related to heat stress response were identified, with the majority of the proteins up-accumulated in embryonal masses induced at higher temperatures being involved in the regulation of metabolism, DNA binding, cellular division, transcription regulation and the life-cycle of proteins. Also, significant differences in the concentrations of sucrose, glutamine, glycine and cysteine were found.

In conclusion, the application of heat stress at the initial stage of somatic embryogenesis provoked long-lasting effects throughout the process, and allowed to identify specific cytokinins, proteins, stress-related genes and metabolites involved in the intricate mechanisms underlying stress response and / or the embryogenic process in conifers.

In parallel, the establishment of efficient protocols for somatic embryogenesis and organogenesis of mature material was attempted. In this regard, the first report of a successful protocol for *in vitro* regeneration of *P. halepensis* adult trees through organogenesis was developed in the framework of this thesis.

Keywords: Aleppo pine; phytohormones; priming; proteins; stress-response.

Table of contents

List of Tables

List of Figures

Abbreviations

ABA	Abscisic acid
AC	Activated charcoal
BA	N^6-Benzyladenine
BAR	N^6-Benzyladenosine
BA7G	N^6-Benzyladenine-7-glucoside
BA9G	N^6-Benzyladenine-9-glucoside
BARMP	N^6-benzyladenosine-50monophosphate
CKs	Cytokinins
cZ	*cis*-Zeatin
*c*ZR	*cis*-Zeatin riboside
*c*ZOG	*cis*-Zeatin *O*-glucoside
*c*Z7G	*cis*-Zeatin-7-glucoside
*c*Z9G	*cis*-Zeatin-9-glucoside
*c*ZROG	*cis*-Zeatin riboside *O*-glucoside
*c*ZRMP	*cis*-Zeatin riboside-50-monophosphate
DHZ	Dihydrozeatin
DHZR	Dihydrozeatin riboside
DHZOG	Dihydrozeatin *O*-glucoside
DHZ7G	Dihydrozeatin-7-glucoside
DHZ9G	Dihydrozeatin-9-glucoside
DHZROG	Dihydrozeatin riboside *O*-glucoside
DHZRMP	Dihydrozeatin riboside-50-monophosphate
DI19	*DEHYDRATION INDUCED PROTEIN 19*
ECs	Embryogenic cells
ECLs	Embryogenic cell lines
EFS (%)	Explants forming shoots (%)
EMs	Embryonal masses
HSPs	Heat shock proteins
IBA	Indole-3-butyric acid
iP	N^6-Isopentenyladenine
iP7G	N^6-Isopentenyladenine-7-glucoside
iP9G	N^6-Isopentenyladenine-9-glucoside
iPMP	N^6-Isopentenyladenosine-50monophosphate
Kn	Kinetin
KR	Kinetin riboside
K9G	Kinetin-9-glucoside

LB	Lipid bodies
*m*T	*meta*-Topolin
*m*TR	*meta*-Topolin riboside
*m*T7G	*meta*-Topolin-7-glucoside
*m*T9G	*meta*-Topolin-9-glucoside
NAA	1-naphthaleneacetic acid
NADP-ME1-4	NADP-malic enzymes genes 1 to 4
NS/E	Number of shoots formed per explant
*o*T	*ortho*-Topolin
*o*TR	*ortho*-Topolin riboside
*o*T7G	*ortho*-Topolin-7-glucoside
*o*T9G	*ortho*-Topolin-9-glucoside
*p*T	*para*-Topolin
*p*TR	*para*-Topolin riboside
*p*T7G	*para*-Topolin-7-glucoside
*p*T9G	*para*-Topolin-9-glucoside
PCs	Phenolic compounds
PGRs	Plant growth regulators
PEMs	Proembryogenic masses
PLS-DA	Partial least square-discriminant analysis
PV	Provacuoles
P439	*CHLOROPLAST SMALL HEAT PROTEIN*
P444	*HSP20 FAMILY PROTEIN*
ROS	Reactive oxygen species
SCs	Suspensor cells
SE	Somatic embryogenesis
SE	Standard error
SOD	*SUPEROXIDE DISMUTASE [Cu–Zn]*
*t*Z	*trans*-Zeatin
*t*ZR	*trans*-Zeatin riboside
*t*ZOG	*trans*-Zeatin *O*-glucoside
*t*Z7G	*trans*-Zeatin-7-glucoside
*t*Z9G	*trans*-Zeatin-9-glucoside
*t*ZROG	*trans*-Zeatin riboside *O*-glucoside
*t*ZRMP	*trans*-Zeatin riboside-50-monophosphate
TLCs	Tube-like cells
V	Vacuole
VIP	Variable influence on projections

2,4-D	2,4-dichlorophenoxyacetic acid
5mC	5-methylcytosine
5hmC	5-hydroxymethylcytosine

General Introduction

1. Forests, conifers and pine trees

Forests cover approximately one-third of the Earth's land surface and comprise the majority of terrestrial biodiversity (FAO 2022). They provide a diversity of commercial products from raw materials like wood, latex, resins, fruits and oils, which are used in a variety of purposes such as building, construction, creation of reusable and recyclable biomaterials, production of paper and energy, medicines and human nutrition (Walter et al. 2005; Harfouche et al. 2011; Weiss et al. 2020). Accordingly, these products allow the maintenance of various industries and job careers with strong socioeconomic impact. Alongside its socioeconomic value, the ecological importance of forests regarding the planet itself is enormous. They have a central role in global water resources, protection of land and biogeochemical cycles, mitigation of the increasing carbon dioxide levels and climate change effects, and biodiversity preservation (Pan et al. 2013; Rank et al. 2022). In this sense, it is well established that forests are natural landscapes of critical importance to satisfy social, economic and ecological needs.

In the last decades, the massive growth of the world population, which reached 8 billion at the end of 2022, and its associated economic development have contributed for urban progress and, consequently, for deforestation and the reduction of natural habitats. At the same time, in order to satisfy the needs of this developed society the demand for forest products/services has significantly increased (Lewis et al. 2015). Additionally, forests are one of the most affected environments by climate change, mostly due to the long lifespan of trees that do not allow them to rapidly adapt, and the projected increase of frequency and intensity of forest fires (Lindner et al. 2010). Climate warming has been projected to increase the frequency and magnitude of extreme climatic events, and the fate of many forest ecosystems will depend on its rate of adaptation to such occurrences (FAO 2022).

The direct climate change effects on ecosystems throughout the impacts on plant physiology are accompanied by its indirect impact through changes on the composition and diversity of plant communities (Morin et al. 2018). A better understanding of how climatic factors, which are the main determinants in vegetation distribution and climate dynamics, influence plant function and survival is crucial for predicting the consequences of environmental variation at the ecosystems working (González-Zamora et al. 2021; Rank et al. 2022).

In the northern forests, conifers are the most common trees covering, almost exclusively, the Boreal Climate Zone and vast areas in North America and Eurasia. The Pinaceae, comprising 232 species, attracts attention among the conifers for its economic and ecological importance, with particular emphasis to the genus *Pinus* (Farjon 2018). Pine species are crucial for the wood-based industries above-mentioned and have a direct influence on water and biogeochemical cycles due to its wide distribution around the globe (Sánchez-González 2008; Farjon 2018). The Mediterranean basin is particularly susceptible to climate change, since intensification of drought and extreme

events, such as heat waves, are expected in the years ahead (Lindner et al. 2010; Sarris et al. 2011; Olivar et al. 2022). Also, due to their first position in the successional evolution of Mediterranean ecosystems, pine species seem to be potentially vulnerable (Carnicer et al. 2013).

Considering the above-mentioned reasons, there is an immediate need to improve forest trees´ quality and productivity. Traditional breeding methods and conventional forestry practices have meaningly contributed to the improvement of forest tree species in the past and will continue to have a considerable impact (Canhoto, 2010; Rodríguez et al. 2022). Notwithstanding, conifers´ trees have long-lasting life cycles, the traits they present as juveniles are not always the ones they show at their mature phase (Weng et al. 2008), and techniques like rooting of cuttings become impracticable at their mature stage (Bonga et al. 2015). Accordingly, the selection of specific traits in these species by traditional methods is a slow and difficult process. In this sense, plant biotechnology appears as a tool that exploits fundamental discoveries in the field of plant tissue culture for clonal forestry, gene transfer techniques, molecular biology and genomics which provides an extended way for improvement of traits that have previously been considered difficult to reach (Nehra et al. 2005; Canhoto 2010; Montalbán et al. 2020).

2. *In vitro* culture in conifers and *Pinus* spp.

In vitro culture commonly refers to a set of techniques of plant propagation in which a new plant is regenerated from small portions of tissues, organs or plant cells under aseptic and controlled conditions (Davis and Becwar, 2007). One of the central concepts of plant regeneration is the totipotency of plant cells, their ability to grow, divide, and differentiate into an entire plant; their cellular plasticity allows differentiated cells to switch its differentiation process and to acquire new fates from their regained juvenile state (Vasil 2008; Canhoto 2010; Sugiyama 2015).

Another main factor promoting *in vitro* regeneration is the culture medium, particularly the presence of plant growth regulators (PGRs). Since the pioneer works of Skoog and Miller (1957) in tobacco, it is well accepted that a combination of auxins and cytokinins controls the organogenic behavior of tissues in culture and that the auxin-cytokinin ratio can regulate organ differentiation. Variations in this ratio are often the primary empirical approach to the optimization of *in vitro* cultures. However, various species do not respond to this common approach and require added physical or chemical stimuli (Ramage and Williams 2002). Endogenous and environmental factors, such as genotype, excision tissue and timing, phenology, and tree maturation are other factors influencing *in vitro* regeneration (Bonga et al. 2010).

Two of the most common techniques of *in vitro* propagation for conifer species are organogenesis and somatic embryogenesis (SE) (Rodríguez et al. 2022). Organogenesis, usually occurring in the presence of cytokinins alone or together with auxins; *de novo* formation of adventitious shoots is stimulated, requiring further development of adventitious roots from shoots and, finally, the development of an entire plant (Zhang and Lemaux 2004). Organogenesis has been successfully applied to several conifers like *Juniperus* spp. (Gomez and Segura 1995; Hazubska-Przybył 2019), *Taxus* sp. (Chang et al. 2001), *Picea* spp. (von Arnold and Eriksson 1984; Lu et al.

1991; López-Escamilla et al. 2000), *Cedrus* spp. (Renau-morata et al. 2005), and it has been widely employed at the genus *Pinus*, such as in *P. brutia* (Abdullah et al. 1987), *P. canariensis* (Pulido et al. 1994), *P. ponderosa* (Lin et al. 1991), *P. pinea* (Moncaleán et al. 2005) and *P. halepensis* (Lambardi et al. 1993). Our research group has successfully carried out organogenesis in *P. pinaster* (De Diego et al. 2008), *P. sylvestris* (De Diego et al. 2010), *Pinus pinea* (Cortizo et al. 2009) and *P. radiata* (Montalbán et al. 2011b; Rojas-Vargas et al. 2022). Accordingly, organogenesis can be used to clone elite trees and to study the aging process. However, numerous problems associated with this technique such as reduced *in vitro* rooting, poor growth and low acclimatization percentages make it difficult to use as a large-scale vegetative propagation method (Montalbán et al. 2020).

On the other hand, SE is a process by which a somatic embryo develops from a single and/or group of somatic cells resembling a zygotic embryo, without endosperm and outer covering (Von Arnold et al. 2002). An exogenous stimulus to these somatic cells, accompanied by the induction of gene transcription required for embryogenesis and metabolism reorganization, leads them to enter the dedifferentiation process and, further, embryogenesis (Stasolla and Yeung 2003; Smertenko and Bozhkov 2014). As previously mentioned here, and reviewed by Ragonezi et al. (2010), there are two main groups of inductive conditions which allow differentiated cells to change into competent dedifferentiated cells: PGRs and stress factors.

SE can be a direct or an indirect process: SE with an intermediary stage of callus formation is referred to as indirect SE while in the direct SE the formation of somatic embryos occurs directly in the vegetative cells (Smertenko and Bozhkov 2014).

The sequence of events for SE *in vitro* are characterized by distinct biochemical and molecular events which occur during the main phases: initiation, proliferation (multiplication), maturation and germination (Pullman and Buchanan 2003). The first phase of SE is the induction stage in which differentiated somatic cells acquire embryogenic competence (Zavattieri et al. 2010). Then, early-stage embryos, or proembryogenic masses (PEMs) (Filonova et al. 2000), start developing and proliferating. Lastly, during maturation, somatic embryos anticipate germination by desiccation and reserve accumulation (Dodeman et al. 1997). Culture and storage conditions, such as the presence of PGRs, their concentration and which one to use, as well as the culture media, pH, temperature, water availability, light, etc. may be adapted and improved for each of the different SE stages and species during this process (Stasolla and Yeung 2003; Klimaszewska et al. 2007; Oseni et al. 2018; von Arnold et al. 2019).

SE was first reported in *Daucus carota* in the late 1950s (Reinert 1959; Steward 1958) and numerous protocols have been developed for different plant species ever since. In conifers, the first report of somatic embryos able to convert into plantlets through SE, from immature embryos as explants, was in *Picea abies* (Chalupa, 1985; Hakman et al., 1985). As expected, several protocols for SE improvement of various pine trees had been developed over the last decades (Gupta and Durzan 1986; Pullman and Buchanan 2003; Yildirim et al. 2006; Klimaszewska et al. 2007; Varis

et al. 2018; Maruyama and Hosoi 2019; Salaj et al. 2019; Castander-Olarieta et al. 2020a; Montalbán et al. 2021).

It has been widely recognized that SE offers several advantages and applications to biotechnology compared to other techniques: it has great potential for a large-scale propagation system for superior specimens, because of the large quantities of somatic embryos produced from just one explant; it is low-priced and less time-consuming than organogenesis; it is possible to grow embryogenic cultures in bioreactors; it enables tree improvement thru the formation of genetically modified crops; allows the implementation of genomic selection for multi-varietal forestry; the production of artificial seeds; and, cryoconservation, when applied to embryogenic tissues, allows to preserve its potentiality and the combination of both techniques makes the development of high value forestry reachable (Park 2002; Celestino et al. 2005; Charity et al. 2005; Weng et al. 2010; Lelu-Walter et al. 2013; Bonga 2015; Park et al. 2019).

Organogenesis and SE have been widely applied as model systems for plant regeneration investigation and as propagation systems for coniferous cloning (Von Aderkas and Bonga 2000; Klimaszewska et al. 2007; von Arnold et al. 2019). However, recalcitrance is still one of the main constrictions in conifers, especially when cloning adult specimens. Bearing in mind the most effective explants, organogenesis is generally restricted to the zygotic embryo or young seedling, while SE generally depends on immature or mature zygotic embryos (Bonga et al. 2010; Bonga 2017; Sarmast 2018). Regeneration from embryonary explants is less valuable for cloning because it rules out the selection of specific traits that can only be seen after phase-change (when trees have entered the mature phase). In this sense, apart from the success obtained in some adult specimens of *Picea* spp. (Klimaszewska et al. 2011; Varis et al. 2018), the scientific community efforts are still aligned in order to develop large-scale SE protocols to clone mature coniferous trees.

3. *Pinus halepensis* Mill.

Pinus halepensis Mill., commonly referred to as Aleppo Pine, is a member of the Pinaceae family native to the Mediterranean region.

The Aleppo pine tree, is a medium-sized tree with an average height of 20 m and 150 cm of trunk diameter, presents a light-gray bark, an irregular shaped crown (Figure 1a) and light green needles (Figure 1b) with 6-12 cm arranged in groups of two (Simón et al. 2012; Mauri et al. 2016).

It is a monoecious species, which presents both female and male cones in separate clusters; female cones can be found in different developmental stages in the same tree, because of their biennial maturation, and usually appear alone or in clusters of two or three (Figure 1c). When mature, female cones turn from green to brown, are symmetrical and pedunculated, and can reach to 6-12 x 3.5-4.5 cm, while male cones are smaller, 3-4 x 5-8 mm, dingy and grouped in large numbers (Figure 1d; Simón et al. 2012).

The seeds are usually 5-6 mm long and this species, like most of the Mediterranean conifers, has its regeneration mandatory by seed because it does not present regrowth from the trunk and branches. The seeds are resistant to high temperatures, even requiring this stimulus to germinate,

which can be an ecological strategy of post-fire colonization (Skordilis and Thanos, 1997; Calvo et al. 2013). Strategies like early reproduction and a heavy production of serotinous cones give this tree an advantage in post-fire regeneration (Escudero et al. 1999; Mauri et al. 2016) and this capacity has been widely addressed at the Mediterranean area (Osem et al. 2013).

Figure 1. Morphological characteristics of *P. halepensis* Mill. **(a)** Aleppo pine tree; **(b)** apical shoot buds and needles; **(c)** two clustered female cones; **(d)** several clusters of male cones (from: euforgen.org).

Pinus halepensis is native from the Mediterranean basin (Figure 2a) and largely distributed in Europe and North Africa (Botella et al. 2010), being the most naturally widespread pine in this area (Ayari and Khouja 2014). It has very specific precipitation and temperature requirements (Klein et al. 2011), growing mainly on calcareous soils and in lower altitudes at arid or semiarid to humid bioclimates (Escudero et al. 1999; Klein et al. 2011; Mauri et al. 2016).

In Spain, it is largely distributed, being autochthonous and abundant in Balearic Islands and by the Mediterranean coast. Due to its important ecological plasticity, it has been intensively used for afforestation in north-western areas (Botella et al. 2010), extending to other autonomous regions as the Basque Country, Valencian Community, Castilla la Mancha and Catalonia (MITECO, 2015). In Portugal, small populations have been introduced at the coast, especially in the areas of Figueira da Foz, Lisbon and Algarve (Figure 2b).

Figure 2. Geographical distribution of *P. halepensis* Mill. **(a)** Natural distribution zone, mostly confined to the Mediterranean area (Mauri et al. 2016); **(b)** occurrence of introduced specimens in Portugal (from: flora-on.pt).

This species, contrary to other pine species, has more ecological than economic importance. As a pioneer species, the introduction of *P. halepensis* to restore degraded areas might enable the long-term colonization and expansion of late-successional species (Gil and Aránzazu Prada 1993; Montero and Alcanda, 1993). Its eco-physiological characteristics such as a fast-growing radical system, a solid water-save strategy and the resistance to water-drought interaction, allows it to live in poor calcareous soils were others arboreous species have difficulties to establish (Puértolas Simón et al., 2012). Though *P. halepensis* is considered a species adapted to fire and drought, the interaction between warm temperatures and precipitation can modify the success of its post-fire recovery patterns, restraining its resilience in the future (Elvira et al. 2021).

Another interesting characteristic of this species is that, even though it can be a host, *P. halepensis* has a moderate resistance to *Bursaphelenchus xylophilus*, the pine wilt nematode that has been destroying pine forests around the globe (Evans et al. 1996; Trindade et al. 2022).

Despite the fact that it is not used as much for economic purposes in Europe, in Tunisia for instance, its cones provide the only appropriate seed source used for many human and forestry purposes. In this country, in addition to their direct consumption as a pastry cream, several food products including yoghurt, aromatic ice creams and vegetable oil are based in *P. halepensis* seeds (Ayari et al. 2012; Ayari and Khouja 2014; Jaouadi et al. 2019).

For all the above-mentioned motives, Aleppo pine has been described as of great importance economically and ecological. Also, considering the global drying and warning conjecture, there is some concern about the physiological ability of *P. halepensis* to grow, adapt, and endure throughout these difficult circumstances.

4. Abiotic stress in plants and how SE can help – the case of *P. halepensis*

Trees, as long-lived sessile organisms subjected to recurrent environmental constraints during their long and complex lifetimes, have to develop different mechanisms of protection and adaptation for an extensive variety of biotic and abiotic stresses in order to maximize growth, reproduction, and survival *in situ* (Edreva et al. 2008; Baránek et al. 2010; Sow et al. 2018). As previously stated, climate change is expected to be one of the major ecological threats worldwide, and the Mediterranean basin is considered particularly susceptible (Lindner et al. 2010; Sánchez-Salguero et al. 2012; Morin et al. 2018).

The rise of the minimum temperatures seems to have improved the growth of *P. halepensis* in recent years (Sarris et al. 2011; Sánchez-Salguero et al. 2012). Notwithstanding, its capacity to endure drought displays strong variations across the species distribution area (Gazol et al. 2017) and the impacts, frequency, and scale of future extreme events are uncertain. In this sense, the understanding of how this species responds to stress, as well as how the application of heat during the induction stage of SE can improve its response to stress, is the groundwork of this research.

Stress stands as a condition that constrains normal growth and development of plants, which may be severely harmful or even lethal (Bäurle 2018). Accordingly, heat stress is frequently defined as a period in which temperatures are substantially high during a sufficient amount of time that cause permanent damage to functions or the development of plants (Hemantaranjan et al. 2014).

In plants, all abiotic stresses induce a cascade of physiological and molecular events that may lead to similar responses that impact metabolic pathways (alterations in the levels of crucial metabolites, proteins or transcriptions factors) and epigenetic memory (Bruce et al. 2007; Crisp et al. 2016). Heat is usually accompanied by drought, and recent studies showed that both stresses have overlying roles (García-Mendiguren et al. 2016b; Jia et al. 2017; Moncaleán et al. 2018). Metabolic memory may appear as a possible consequence of epigenetic regulations and is related to changes of metabolites, enzymes, and proteins that may result in phenotypic changes (do Nascimento et al. 2020; Auler et al. 2021).

Regarding epigenetics, alterations in epigenetic marks are reversible enzyme-mediated modifications of DNA and/or associated histones that regulate transcriptional activity of genes as well as their sequences (Hauser et al. 2011; Us-Camas et al. 2014; Amaral et al. 2020). The most studied epigenetic mark is the DNA methylation because of its stability, its incidence in both plants and mammals, and its influence on gene expression and genome structure regulation (Amaral et al. 2020).

Most epigenetics marks are reverted when the environmental constraints that triggered them are no longer present. Still, higher plants appear to be able to recollect some "stress memory" or "stress imprinting", given that a first stress exposure frequently leads to an improved resistance to a later stress (Bruce et al. 2007; Conrath 2011). Several authors have shown that environmental conditions incite epigenetic changes in plants, which can be permanent and/or hereditary, supporting their adaptation to different stress situations through the development of an adaptive

epigenetic memory (Johnsen et al. 2005b; Yakovlev et al. 2016; Lämke and Bäurle 2017; Ling et al. 2018).

Moreover, epigenetic regulation plays a critical role in modulation of multiple aspects of plant development through the adjustment of gene expression in response to environmental factors (Hauser et al. 2011). As a result, integrative studies may be performed in order to understand its role on phenotypic adaptation and plasticity (Sow et al. 2018).

The stimulation of induced defense and adaptation responses by "priming" plants with stressful temperatures during both zygotic (Johnsen et al. 2005a) and SE (Castander-Olarieta et al. 2020b; Pérez-Oliver et al. 2021) seems to favor plants resilience to extreme temperature conditions through a "memory" formation. In this sense, embryo development appears to be a key step for the development of stable epigenetic marks and stress memory. SE has become more than a propagation technique and has been widely used as a model system for studying the processes occurring during embryo development (Smertenko and Bozhkov 2014; Trontin et al. 2016), and to learn the effects of different abiotic factors in plants as well as to attempt stress memory acquisition for said stresses (Eliášová et al. 2017; do Nascimento et al. 2021).

In short, the use of controlled stress application during SE, seems to have become a useful instrument not only to study the mechanisms involved in the stress response itself (along with the negative consequences it brings), as well as a successful tool to modulate stress response in plants; the development of this report grounded in this idea.

Several studies concerning the development and optimization of SE protocols, as well as the effect of different stressful conditions at the SE process for *P. radiata* and *P. halepensis* have been carried out at Neiker-BRTA (Montalbán et al. 2011b, a, 2012, 2013a, b; Garcia-Mendiguren et al. 2015; García-Mendiguren et al. 2016b; Montalbán and Moncaleán 2017). The collaboration between Neiker-BRTA and the Centre for Functional Ecology started with the study of the protein profiles of somatic embryos of *P. radiata* induced under different temperatures and water availability (García-Mendiguren et al. 2016a), and continued with the study of the effect of the same conditions during the initial stages of Aleppo pine SE (Pereira et al. 2016, 2017). The results showed that different temperatures and water availability at different stages of SE generate long-lasting effects that determine the success of further steps of the process, as well as the somatic embryo´s profiles of stress-related proteins and hormones (Moncaleán et al. 2018).

In this context, two parallel lines of investigation have been conducted in our lab with the aim of understanding the mechanisms underlying heat stress through the induction of SE in *P. radiata* (Castander-Olarieta et al. 2019, 2020b, 2021a, b, c, 2022) and in *P. halepensis*.

5. Objectives

In view of all the above-mentioned information, using *P. halepensis* SE as a model system, the main goal of this thesis is:

_ To trigger the formation of a long-lasting epigenetic "stress memory", through the application of high temperatures during the initiation stage of *P. halepensis* somatic embryogenesis, to study the influence of heat stress regarding the success of the SE process in itself, and as a tool to understand the mechanisms underlying abiotic stress response in conifers trees.

In order to achieve the above-mentioned main objective, seven main goals were established:

1. To successfully induce SE under heat stress in *P. halepensis*.

2. To assess the effect of heat stress, during the initial stage of SE, in the success of the different stages of the process (initiation, proliferation, maturation, germination).

3. To evaluate the morphological characteristics of the embryonal masses induced under high temperatures at a cellular level.

4. To analyze the profiles of endogenous cytokinins in embryonal masses induced at different temperature conditions and their implication in the success of the SE process and in heat stress response.

5. To investigate if there were epigenetic changes at the embryogenic tissue and the somatic plants produced, and to determine if these possible changes are transitory and lead to the differential expression of stress-related genes.

6. To study the profiles of proteins and the metabolites (amino acids and sugars) present at the embryonal masses produced under heat stress, in order to study their roles in the success of the SE process and in heat stress response.

7. To develop successful protocols for both organogenesis and SE from adult explants, in order to obtain plants with the same genetic information as the donor tree for stress experiments.

CHAPTER 1: Embryonal Masses Induced at High Temperatures in Aleppo Pine: Cytokinin Profile and Cytological Characterization

(Pereira C, Castander-Olarieta A, Montalbán IA, Pěnčík A, Petřík I, Pavlović I, Oliveira EDM, Fraga HPF, Guerra MP, Novák O, Strnad M, Canhoto J, Moncaleán P (2020) Embryonal masses induced at high temperatures in Aleppo pine: cytokinin profile and cytological characterization. *Forests* 11:807.)

1. Abstract

Aleppo pine (*Pinus halepensis* Mill.), a native species of the Mediterranean region, has been suggested as a species that when introduced in degraded areas could facilitate the long-term colonization and expansion of late-successional species. Due to climate changes, plants need to withstand extreme environmental conditions through adaptation and changings in developmental pathways. Among other paths, plants undergo changes in developmental pathways controlled by phytohormones. At the same time, somatic embryogenesis has been widely used as a model to understand the mechanisms involved in plant response to different stresses. In this study, in order to induce a strong effect of temperature stress on plants regenerated from somatic embryos, higher temperatures (40 ℃ for 4 h, 50 ℃ for 30 min, and 60 ℃ for 5 min) than the control (23 ℃) were applied during the induction stage of somatic embryogenesis in *Pinus halepensis*. A morphological characterization of the embryogenic cultures showed small differences in the number of starch rains, lipid bodies, and phenolic compounds between treatments. Results showed that high temperatures (60 ℃) led to higher rates at the maturation stage of somatic embryogenesis when compared to the control (23 ℃), strengthening the productivity through the increase in the number of somatic embryos obtained. Finally, analysis of endogenous concentration of cytokinins showed that different conditions applied during the initiation phase of somatic embryogenesis led to different hormonal profiles; isoprenoid cytokinins showed a clearly defined pattern with the higher total hormone concentration being found in embryonal masses induced at 50 ℃ for 30 min, while different aromatic cytokinins presented different individual responses to the treatments applied. These differences corroborate the idea that cytokinins could be potential regulators of stress–response processes during initial steps of somatic embryogenesis.

Keywords: abiotic stress; phytohormones; *Pinus halepensis*; somatic embryogenesis; TEM analysis

2. Introduction

Aleppo pine (*Pinus halepensis* Mill.) is native of the Mediterranean basin and the most important and broadly distributed pine tree in the area, covering ca. 3.5 million hectares of forest area both as natural stands and in reforestation programs (Ne'eman et al. 2004; Botella et al. 2010). It prevails in the driest and warmest sites, especially in the western Mediterranean, due to its tolerance to high temperatures and drought stress (Escudero et al. 1999; Klein et al. 2011; Mauri et al. 2016).

Pine species appear to be very sensitive to climate warming because of their first position in the successional evolution of Mediterranean ecosystems (Carnicer et al. 2013). As a pioneer species, Aleppo pine has been suggested as a species that when introduced in degraded areas could facilitate the long-term colonization and expansion of late-successional species (Gil and Aránzazu 1993). Models predict that climate change will be one of the major environmental and economic threats worldwide, with the Mediterranean basin particularly vulnerable, since strong drought and intensification of extreme events, such as heat waves, are expected in the area in the upcoming years (Lindner et al. 2010; Sarris et al. 2011). Despite the fact that recent increase in the minimum temperature seems to improve the growth of *P. halepensis* (Sarris et al. 2011; Sánchez-Salguero et al. 2012) its capacity to withstand drought displays strong variations across the species distribution area (Gazol et al. 2017) and the impacts, frequency and magnitude of extreme events are uncertain. The capacity of forest ecosystems to cope with this problem will rely on the relationship between how fast these changes occur and how fast forest trees can adapt to them (Klein et al. 2011).

Plant stress stands as a condition that inhibits normal growth and development that may be severely damaging or even lethal and could be caused, among other factors, by extreme temperatures. As sessile organisms, plants need to withstand extreme environmental conditions *in situ* through adaptation and modification of developmental pathways (Bäurle 2018). Moreover, it was observed that *Picea abies* plants keep a memory of temperatures (Johnsen et al. 2005a) and photoperiod (Johnsen et al. 2005b) experienced during zygotic embryogenesis and further seed maturation through the development of an adaptive epigenetic memory. To this respect, several authors have shown that environmental conditions can induce epigenetic changes in plants, favoring their adaptation to different stress situations, which can be permanent and even hereditary (Mirouze and Paszkowski 2011; Mahdavi-Darvari et al. 2015; Gallusci et al. 2017).

Phytohormones, like cytokinins (CKs), are defined as naturally occurring compounds that function at very low concentrations and control various cellular processes and plant responses to environmental conditions (Frébort et al. 2011; Fahad et al. 2015). Among other different factors involved in stress signaling, they can have multiple effects and prompt different responses depending on various factors such as nutrient and water availability, environmental conditions and interactions with other phytohormones (Ferguson and Grafton-Cardwell 2014).

CKs are the mobile adenine derivatives that carry N^6-linked isopentenyl or aromatic side chains and they serve as hormonal signals functioning in countless biological processes (Sakakibara 2010). These plant hormones are involved, through modulation of its levels either by upregulation

of synthesis or deregulation of their degradation (Podlešáková et al. 2019), in abiotic stress responses (Moncaleán et al. 2018) as well as to regulate a number of aspects of plant growth and development, such as cytokinesis, cell differentiation, growth, quiescence, and senescence (Ciura and Kruk 2018).

Somatic embryogenesis (SE) brings great advantages and applications to biotechnology because it can be used for large-scale propagation of plant species and it can be combined with other techniques such as cryopreservation or conservation at low temperatures (Montalbán and Moncaleán 2017). Also, it allows the selection of clones in field tests and has been widely used as a model system for understanding the physiological and biochemical events occurring in response to different abiotic stresses (Eliášová et al. 2017). The first report of SE in *P. halepensis* was carried out in our laboratory (Montalbán et al. 2013b). Later conducted experiments in our group in *P. halepensis* showed that changes in temperature and water availability at initial steps of SE affect the success of the process in this species (Pereira et al. 2016, 2017). Considering these previous results, the main goal of this work was to evaluate the effect of high temperatures (40, 50, and 60 °C) applied for different induction periods (4 h, 30 min, and 5 min, respectively) in the initiation stage of *P. halepensis* SE in terms of the success of the process itself (initiation, proliferation, maturation and germination rates) as well as in the quantity and quality of somatic embryos obtained. In line with this goal and in order to study the involvement of CKs in temperature stress, levels of isoprenoid and aromatic cytokinins were analyzed. Moreover, morphological and ultrastructural alterations on the embryogenic cultures coming from different treatments was also evaluated.

3. Material and Methods

Plant Material and Temperature Experiment

One-year-old green female cones, enclosing immature seeds of *P. halepensis* from five open pollinated trees (17-1, 17-2, 17-3, 17-4 and 17-5) were sampled on July, at Manzanos (Spain; latitude: 42º44029" N, longitude: 2º52035" O). Cones from each mother tree were separately stored at 4 °C for three months following the method described in Montalbán et al. (2015). Whole megagametophytes containing immature embryos, corresponding to early cleavage polyembryony and the first "bullet" stages with a dominant embryo (Montalbán et al. 2012), were used as initial explants.

Initiation of Embryonal Masses

Initiation medium was DCR (Gupta and Durzan 1986) supplemented with 30 g L^{-1} sucrose and 3.5 g L^{-1} gellan gum (Gelrite®, Duchefa Biochemie, Amsterdam, Netherlands), with a combination of 9.0 µM 2,4-dichlorophenoxyacetic acid and 2.7 µM kinetin, at pH 5.7. After autoclaving, a filter-sterilized solution containing EDM amino acid mixture (Walter et al. 2005) was added to the cooled medium. For temperature treatments, sealed Petri dishes containing initiation medium were

preheated for 30 min. For the induction of embryonal masses (EMs) the procedure described in Montalbán et al. (2013b) was followed. In brief, immature megagametophytes were cultured at 40, 50, and 60 ºC for 4 h, 30 min, and 5 min, respectively. As control conditions, 23 ºC were used. After the application of the different treatments, all the megagametophytes were kept at 23 ºC for 9 weeks in darkness. Four to eight megagametophytes per 26 Petri dish per treatment were cultured.

Proliferation of Embryonal Masses

After 9 weeks on the initiation medium, proliferating EMs with an approximate diameter of 16 mm were detached from the megagametophyte. Before the first subculture on the proliferation medium, fresh tissues from all treatments were immersed in liquid nitrogen and immediately stored at -80 ºC for further analysis. Proliferation medium had the same composition to that used in the initiation stage, but a higher gellan gum concentration (4.5 g L^{-1}). EMs were subcultured every 2 weeks and kept in the dark. Following three subcultures, actively growing EMs were recorded as established embryogenic cell lines (ECLs). Proliferation and the subsequent stages of the SE process were carried out at the same temperature (23 ± 2 ºC).

Maturation of Embryogenic Cell Lines

Maturation of somatic embryos was carried out following the procedure described in Montalbán et al. (2013b). Thus, after 4 subcultures on the proliferation medium, 75 mg of EMs per dish from different treatments were used. Maturation medium was the DCR medium supplemented with 60 g L^{-1} sucrose, 75.0 µM abscisic acid (ABA), the EDM amino acid mixture (Walter et al. 2005) and 9 g L^{-1} Gelrite®. Eight or nine ECLs per treatment and eight Petri dishes per ECL were cultured in the dark for 18 weeks. To analyze their morphology 160 of the produced somatic embryos, 10 from four ECLs per temperature treatment, were selected. For this purpose, two measurements were made using a Leica DMS 1000 microscope and the LAS V4.12 (Leica Application Suite, Wetzlar, Germany) software: the total length of the somatic embryos and the width, measured just below the cotyledonary intersection (Figure 3).

Somatic Embryo Germination

Somatic embryos were transferred to half-strength macronutrients LP medium (Quoirin and Lepoivre 1977; Aitken-Christie et al. 1988) supplemented with 2 g L^{-1} of activated charcoal and 9.5 g L^{-1} Difco® granulated agar (Becton Dickinson, Franklin Lakes, USA). Twenty embryos per Petri dish and four Petri dishes per 8 ECLs of each treatment were tested. Cultures were placed partially covered for 7 days, and afterwards were kept under a 16:8 h photoperiod at 100 µmol m^{-2} s^{-1} provided by cool white fluorescent tubes (TFL 58 W/33, Philips, France). The obtained plantlets were subcultured onto fresh medium of the same composition every 4 weeks.

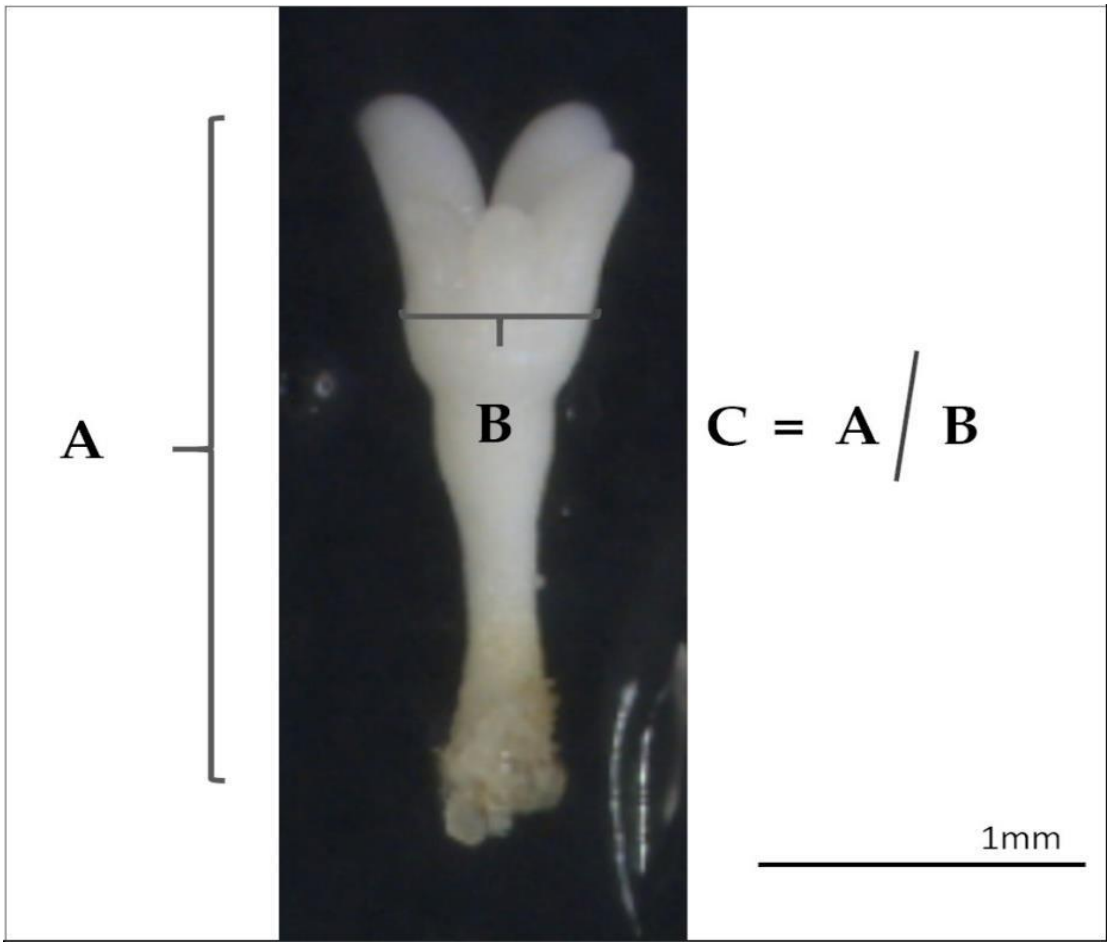

Figure 3 – Somatic embryo showing how the measurements were performed: (A) Length, (B) width, and (C) the ratio between (A) and (B).

Cytological Characterization of Embryogenic Cultures

Micromorphological Study

EMs at the end of the initiation phase, right before the first subculture on the proliferation medium, were used for light microscopy analyses following the procedure described in Fraga et al. (2015). Two ECLs per treatment, comprising a total of 8 ECLs were analyzed. Samples of 3–5 mm in diameter were collected and fixed in formaldehyde 2.5% (*v*/*v*) in 0.1 M sodium phosphate buffer (pH 7.2) overnight at 4 °C. The material was washed twice for 15 min in buffer without fixative and then dehydrated in an increasing series of ethanol aqueous solutions (30–100% *v*/*v*), comprising a total of six different solutions, for 30 min. Samples were then infiltrated with Historesin (Leica Historesin, Heidelberg, Germany) and sections of 5 µm were obtained using a rotatory microtome (Slee Technik, Mainz, Germany). After adhesion to histological slides, sections were stained with 1% (*w*/*v*) toluidine blue in an aqueous solution of 1% Borax, pH 9. Samples were analyzed and photographed using an Olympus BX 40 microscope equipped with a computer-controlled Olympus DP 71 digital camera (Olympus, Tokyo, Japan).

Ultrastructural Analysis

Part of the ECLs used for the micromorphological studies were also subjected to transmission electron microscopy (TEM) analysis. Samples of 3–5 mm in diameter were fixed in 2.5% (*v*/*v*) glutaraldehyde in 0.1% (*w*/*v*) sodium cacodylate buffer and 0.6% (*w*/*v*) sucrose overnight. After five washing steps of 20 min, with decreasing concentrations of 0.1% (*w*/*v*) sodium cacodylate buffer (1; 0.75; 0.50; 0.25; 0) and increasing concentrations of 0.6% sucrose (*w*/*v*) (1; 1.25; 1.50; 1.75; 2) in 2.5% (*v*/*v*) glutaraldehyde, the samples were post-fixed using 1% (*w*/*v*) osmium tetroxide prepared in 0.1 M sodium cacodylate for 4 h. Samples were washed again three times with the same buffer and dehydrated in an increasing series of acetone aqueous solutions from 30 to 100% (*v*/*v*) following the same procedure described above for light microscopy assays. Finally, the material was embedded in Spurr's resin (Spurr 1969) and ultrathin sections (60 nm) were collected and contrasted on grinds using aqueous uranyl acetate followed by lead citrate (Reynolds 1963). The samples were then examined under a TEM JEM 1011 electron microscope (JEOL Ltd., Tokyo, Japan, at 80 kV).

Extraction, Purification and Quantification of Endogenous Cytokinins

Liquid nitrogen frozen EMs at the end of the initiation phase, right before the first subculture on the proliferation medium, were used for the CKs analysis. Three or four ECLs per treatment, comprising a total of 13 ECLs, including the 8 ECLs studied at microscopy, were analyzed. The isoprenoids CKs studied were: *cis*-Zeatin (*c*Z), *cis*-Zeatin riboside (*c*ZR), *cis*-Zeatin *O*-glucoside (*c*ZOG), *cis*-Zeatin-7-glucoside (*c*Z7G), *cis*-Zeatin-9-glucoside (*c*Z9G), cis-Zeatin riboside *O*-glucoside (*c*ZROG), *cis*-Zeatin riboside-50-monophosphate (*c*ZRMP), *trans*-Zeatin (*t*Z), *trans*-Zeatin riboside (*t*ZR), *trans*-Zeatin *O*-glucoside (*t*ZOG), *trans*-Zeatin-7-glucoside (*t*Z7G), *trans*-Zeatin-9-glucoside (*t*Z9G), *trans*-Zeatin riboside *O*-glucoside (*t*ZROG), *trans*-Zeatin riboside-50-monophosphate (*t*ZRMP), Dihydrozeatin (DHZ), Dihydrozeatin riboside (DHZR), Dihydrozeatin *O*-glucoside (DHZOG), Dihydrozeatin-7-glucoside (DHZ7G), Dihydrozeatin-9-glucoside (DHZ9G), Dihydrozeatin riboside *O*-glucoside (DHZROG), Dihydrozeatin riboside-50-monophosphate (DHZRMP), N^6-Isopentenyladenine (iP), N^6-Isopentenyladenosine (iPR), N^6-Isopentenyladenine-7-glucoside (iP7G), N^6-Isopentenyladenine-9-glucoside (iP9G), N^6-Isopentenyladenosine-50monophosphate (iPMP); and the aromatic CKs studied were: N^6-Benzyladenine (BA), N^6-Benzyladenosine (BAR), N^6-Benzyladenine-7-glucoside (BA7G), N^6-Benzyladenine-9-glucoside (BA9G), N^6-benzyladenosine-50monophosphate (BARMP), *ortho*-Topolin (*o*T), *ortho*-Topolin riboside (*o*TR), *ortho*-Topolin-7-glucoside (*o*T7G), *ortho*-Topolin-9-glucoside (*o*T9G), *meta*-Topolin (*m*T), *meta*-Topolin riboside (*m*TR), *meta*-Topolin-7-glucoside (*m*T7G), *meta*-Topolin-9-glucoside (*m*T9G), *para*-Topolin (*p*T), *para*-Topolin riboside (*p*TR) *para*-Topolin-7-glucoside (*p*T7G), *para*-Topolin-9-glucoside (*p*T9G), Kinetin (Kn), Kinetin riboside (KR), and Kinetin-9-glucoside (K9G).

Two technical replicates of 10 mg per ECL were analyzed, using miniaturized purification (pipette tip solid-phase extraction), according to the protocol described by Svačinová et al. (2012).

Samples were extracted in 1 mL of modified Bieleski solvent and homogenized using a MM 301 vibration mill (Retsch GmbH & Co. KG, Haan, Germany) (27 Hz, 5 min, 4 ℃) after addition of 3 zirconium oxide beads. Samples were extracted with the addition of stable isotope-labeled internal standards (0.2 pmol for base, ribosides, 9- and 7-glucoside CKs and 0.5 for *O*-glucoside and CK nucleotides). The extracts were ultrasonicated for 3 min and incubated at 4 ℃ with continuous shaking for 30 min at 20 rpm. After centrifugation (15 min, 20,000 rpm, 4 ℃) from the supernatants of each sample, another 3 technical replicates of 300 µL per sample were transferred onto Stage Tips and purified according to the aforementioned protocol, with C18, SDB-RPS, and Cation-SR sorbents.

Previously to the loading of the sample the StageTip sorbents were conditioned with 50 µL acetone (by centrifugation at 2,000 rpm, 10 min, 8 ℃), 50 µL methanol (2,000 rpm, 10 min, 8 ℃), 50 µL water (2,200 rpm, 15 min, 8 ℃), equilibrated with 50 µL 50% (*v*/*v*) nitric acid (2,500 rpm, 20 min, 8 ℃), 50 µL water (2,500 rpm, 20 min, 8 ℃) and 50 µL modified Bieleski solvent (Bieleski 1964) (2,500 rpm, 20 min, 8 ℃). After the application of 300 µL of sample (3,500 rpm, 30 min, 8 ℃), the tips were washed using 50 µL of water and methanol (3,500 rpm, 20 min, 8 ℃). Samples were then eluted with 50 µL of 0.5 M NH4OH in 60% (*v*/*v*) methanol (3,500 rpm, 20 min, 8 ℃) and elutes were collected into new clean microcentrifuge tubes, evaporated to dryness and dissolved in 30 µL of mobile phase prior to UHPLC-MS/MS analyses.

Mass analysis was carried out following the procedure described by Moncaleán et al. (2018), using an Acquity UPLC® System and a triple-quadrupole mass spectrometer Xevo™ TQ-S MS (Waters MS Technologies, Manchester, United Kingdom). All MS data were processed using the MassLynx™ software with TargetLynx™ program (version 4.2., Waters, Milford, USA), and compounds were quantified by standard isotope dilution analysis (Rittenberg and Foster 1940).

Data Collection and Statistical Analysis

After 7–9 weeks on initiation medium, the number of initiated EMs per Petri dish was registered and the initiation percentages were calculated. Following three subcultures, actively growing EMs were recorded as ECLs and the percentage of proliferation with respect to the EMs initiated was calculated. After 18 weeks from the beginning of the maturation stage, the number of ECLs able to form somatic embryos and the number of mature somatic embryos produced per ECLs were registered. The percentage of mature somatic embryos per gram of ECLs and morphology data were also assessed. In the second subculture on germination medium, the number of germinated somatic embryos was evaluated to calculate germination rates.

A one-way analysis of variance was carried out to assess the effect of temperature on SE stages percentages, mature somatic embryos produced per gram as well as their morphology data, and different concentration of endogenous cytokinins produced (GraphPad Prism 8.4.1 (676)). Following confirmation of the homogeneity of variances and normality of the samples an ANOVA was made. Whenever the analysis of variance did not fulfill the normality hypothesis, the corresponding non-parametric test, Kruskal–Wallis test, was applied. When significant differences

were found ($p < 0.05$), the Tukey HSD post hoc test or Dunn's multiple comparison test, respectively, were carried out to find out which treatments were statistically different.

4. Results

Temperature Experiment

Induction at the control temperature (23 ℃) presented the lowest initiation rate. The highest initiation (Figure 4a) and proliferation percentages were achieved when megagametophytes were induced at 40 ℃ and the lowest proliferation rate was obtained at EMs (Figure 4b) induced at 60 ℃ for 5 min. Despite the fact that there were no significant differences between treatments at initiation and proliferation rates (Tables 1 and 2), a decreasing pattern could be seen as the temperature rose along the high induction temperatures applied during initiation.

Table 1. One-way analysis of variance for initiation, proliferation, number of somatic embryos (SES) produced per gram of embryonal mass, and germination of *Pinus halepensis* megagametophytes induced under different temperature treatments (23 ℃, 9 weeks; 40 ℃, 4 h; 50 ℃, 30 min; 60 ℃, 5 min).

Temperature (T) ANOVA	**d*f***	**F value**	***P* value**
Initiation	3	0.1301	n.s.[1]
Kruskal-Wallis	**d*f***	**X^2 test**	***P* value**
Proliferation	3	2.742	n.s.
Nº of SES g^{-1} EM	3	27.90	< 0.0001
Germination	3	5.862	n.s.

[1] not statistically significant.

Table 2. Embryonal mass initiation, proliferation, maturation and germination (%) as well as the number of somatic embryos (SES) produced per gram of embryogenic mass in *P. halepensis* megagametophytes cultured at different temperature treatments.

Treatment	**%Initiation**	**%Proliferation**	**%Maturation**	**SES g^{-1} EM**	**%Germination**
23 ℃ (9 weeks)	51.80 ± 6.1 [a]	76.00 ± 7.0 [a]	100	176.2 ± 18.0 [ab]	66.58 ± 4.4 [a]
40 ℃ (4 h)	56.25 ± 5.3 [a]	79.17 ± 5.0 [a]	100	141.1 ± 18.8 [b]	63.77 ± 4.0 [a]
50 ℃ (30 min)	56.06 ± 5.7 [a]	71.07 ± 7.1 [a]	100	135.2 ± 21.47 [b]	76.20 ± 3.7 [a]
60 ℃ (5 min)	54.09 ± 6.3 [a]	62.79 ± 8.2 [a]	100	317.4 ± 35.91 [a]	73.29 ± 3.1 [a]

Data are presented as mean values ± SE. Significant differences at $p < 0.05$ are indicated by different letters

Concerning the effect of different temperatures during initiation on somatic embryo maturation all ECLs transferred to maturation conditions were able to produce somatic embryos (Table 2).

No statistically significant differences were found for initiation, proliferation, or maturation capacity. Nevertheless, statistically significant differences were found when the number of somatic embryos per gram were analyzed, with the treatment of 60 ℃ for 5 min presenting the highest values (Table 2), regardless of the fact that this treatment showed lowered rates of initiation when compared to other treatments. Control temperature showed an intermediate value (Table 2).

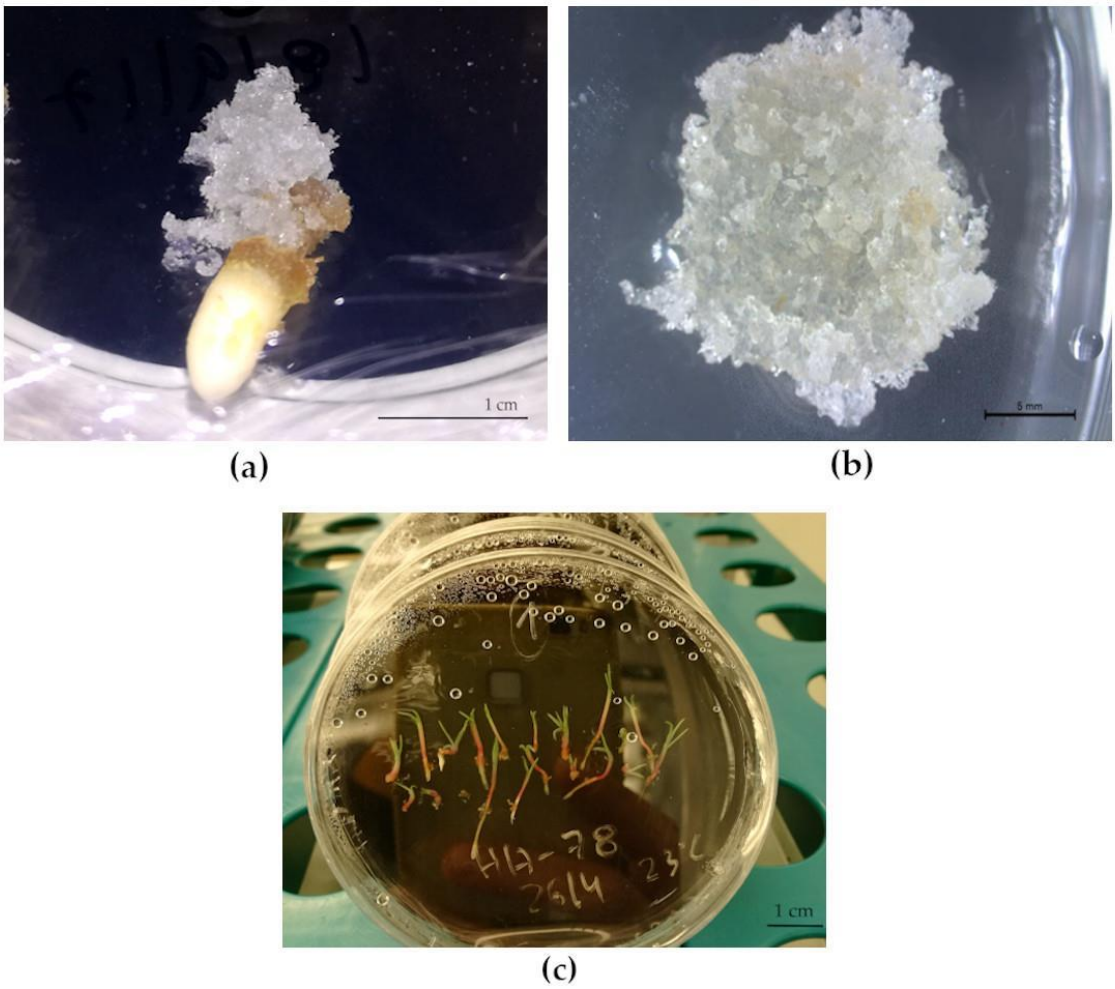

Figure 4. Plant material at different stages of the embryogenic process **(a)** embryonal mass initiation; **(b)** proliferating embryonal masses; **(c)** developing plantlets on germination medium.

When the morphological aspects of somatic embryos produced were analyzed (Figure 3), the results showed that those produced from the ECLs initiated under control (23 ℃) temperatures and at the highest temperature tested (60 ℃) were significantly longer compared to somatic embryos resulting from other treatments. Regarding the ratio between length and width, somatic embryos from EMs induced at 60 ℃ for 5 min were significantly more elongated than those from EMs induced at 40 ℃ for 4 h and 50 ℃ for 30 min that presented a more barrel-shape form (Tables 3 and 4).

Table 3. One-way analysis of variance for length, width and ratio between length and width of somatic embryos (SES) produced from *P. halepensis* megagametophytes induced under different temperature treatments (23 °C, 9 weeks; 40 °C, 4 h; 50 °C, 30 min; 60 °C, 5 min).

Temperature (T) **Kruskal-Wallis**	***Df***	**X^2 Test**	***p* Value**
SES length	3	54.03	< 0.0001
SES width	3	6.413	n.s. [1]
SES length / width	3	16.45	0.0009

[1] not statistically significant.

Table 4. Length, width and ratio between length and width of somatic embryos (mm) produced from *P. halepensis* megagametophytes induced under different temperature treatments.

Treatment	Length	Width	Length / Width
23 °C (9 weeks)	2.46 ± 0.05 [a]	0.83 ± 0.02 [a]	2.97 ± 0.11 [ab]
40 °C (4 h)	2.15 ± 0.02 [b]	0.77 ± 0.02 [a]	2.86 ± 0.07 [b]
50 °C (30 min)	2.20 ± 0.03 [b]	0.79 ± 0.02 [a]	2.81 ± 0.05 [b]
60 °C (5 min)	2.58 ± 0.05 [a]	0.82 ± 0.02 [a]	3.17 ± 0.06 [a]

Data are presented as mean values ± S.E. Significant differences at $P < 0.05$ are indicated by different letters

No significant differences were found for the percentage of germination (Figure 4c) (Table 1). The highest germination rates were achieved in somatic embryos from ECLs initiated at 50 °C for 30 min followed by 60 °C for 5 min (Table 2).

In contrast with somatic embryos length and the ratio between length and width, no significant differences could be found between somatic embryos width coming from different temperature treatments (Table 4).

Cytological Characterization of Embryogenic Cultures

Three cell types were revealed in the embryogenic cultures analyzed by light microscopy: (1) Small round-shaped embryogenic cells (ECs) strongly stained and displaying a dense cytoplasm, a high ratio nucleus/cytoplasm, a conspicuous nucleoli and where mitotic figures were often seen; (2) highly vacuolated elongated suspensor cell (SCs), which have a reduced cytoplasm between the cell membrane and the tonoplast and (3) tube-like cells (TLCs) that seemed to be in transition between ECs and SCs sharing characteristics of both cell types (Figure 5a–e). All three types of cells could be found in all samples analyzed. These different types of cells usually appeared in clusters forming proembryogenic masses (PEM).

Two different stages of development were found: PEM I (Figure 5a) with smalls groups of ECs associated with one or two SCs; and PEM II, with a higher number of ECs and SCs in the cluster (Figure 5b). No PEM III, which consists of larger clusters of ECs and SCs, were found.

Despite the organized and clear cell polarization of PEM II found in some sections (Figure 5b) the majority of PEMs found in the analyzed samples showed poor cellular organization. However, although all three types of cells were present (ECs, SCs, and TLCs), all of them tangled together without defined polarization and an unbalanced proportion between embryonal areas and suspensors, with a big number of TLCs and SCs, was often observed (Figure 5c,e). Both polarized and non-polarized areas were detected for all treatments, therefore, it seems that there are no differences with respect to cellular organization between treatments.

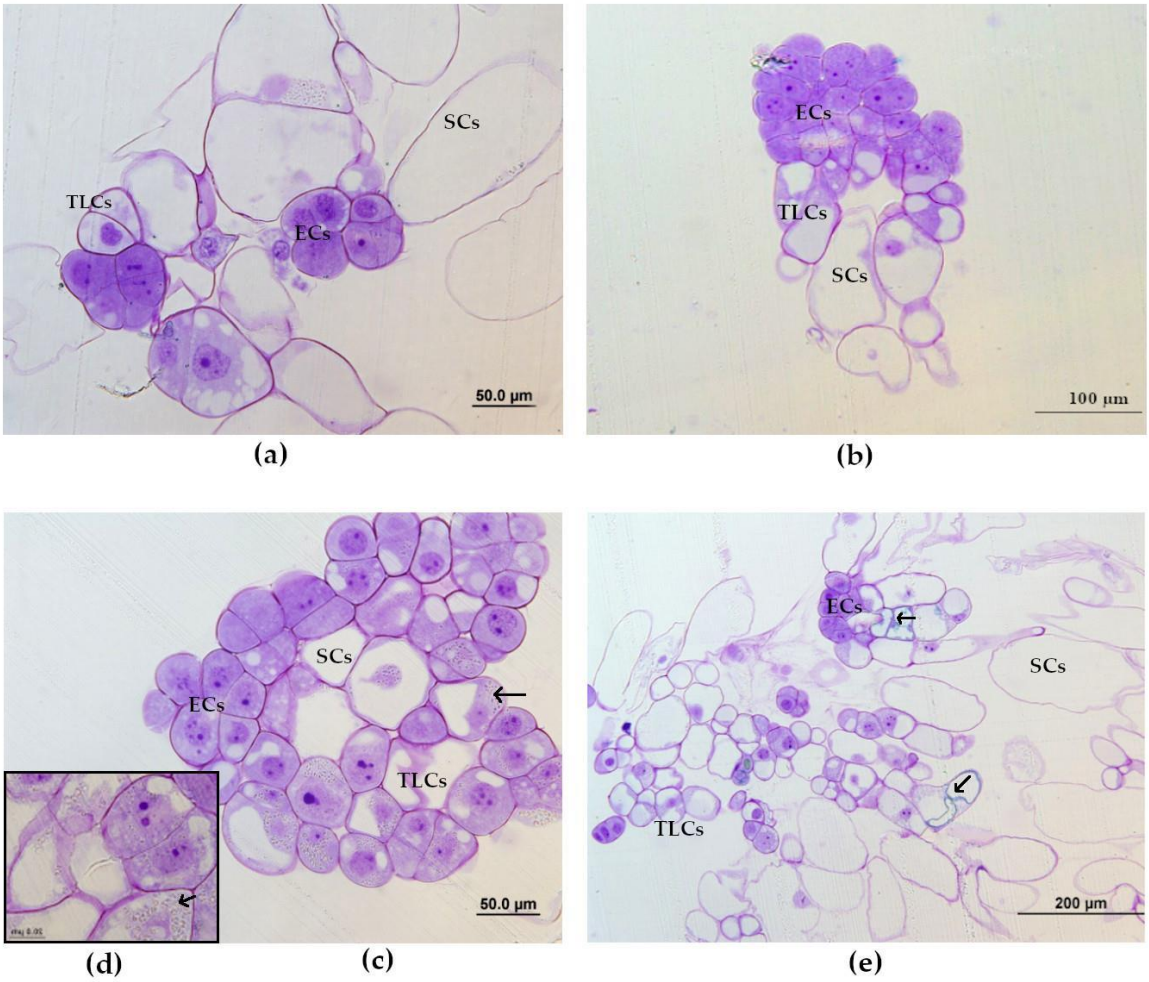

Figure 5. Light microscopy of embryogenic cultures from *P. halepensis* **(a)** proembryogenic masses (PEM) I with four embryogenic cells (ECs) linked to one suspensor cell (SCs), surrounded by some detached tube-like cells (TLCs); **(b)** PEM II, showing a defined polarization with one pole formed by several ECs, linked to TLCs. Scattered vacuolated cells (SCs) can also be observed; **(c)** cluster of embryogenic cells without clear polarization, with the presence of starch grains (arrow); **(d)** detail of starch grains (arrow) that could be detected on samples from all induction treatments; **(e)** PEM clusters induced at 60 ℃ for 5 min, without defined polarization, containing phenolic compounds (arrow).

Finally, a large number of starch grains (S) on ECs on samples from all treatments (Figure 3c,d) and some phenolic compounds (PCs) were found only in one sample from an embryogenic culture induced at 60 ℃ for 5 min (Figure 5e).

TEM observation of samples from the same embryogenic cultures analyzed by light microscopy confirmed the presence of three different types of cells, ECs, TLCs and SCs (Figure 6a–i).

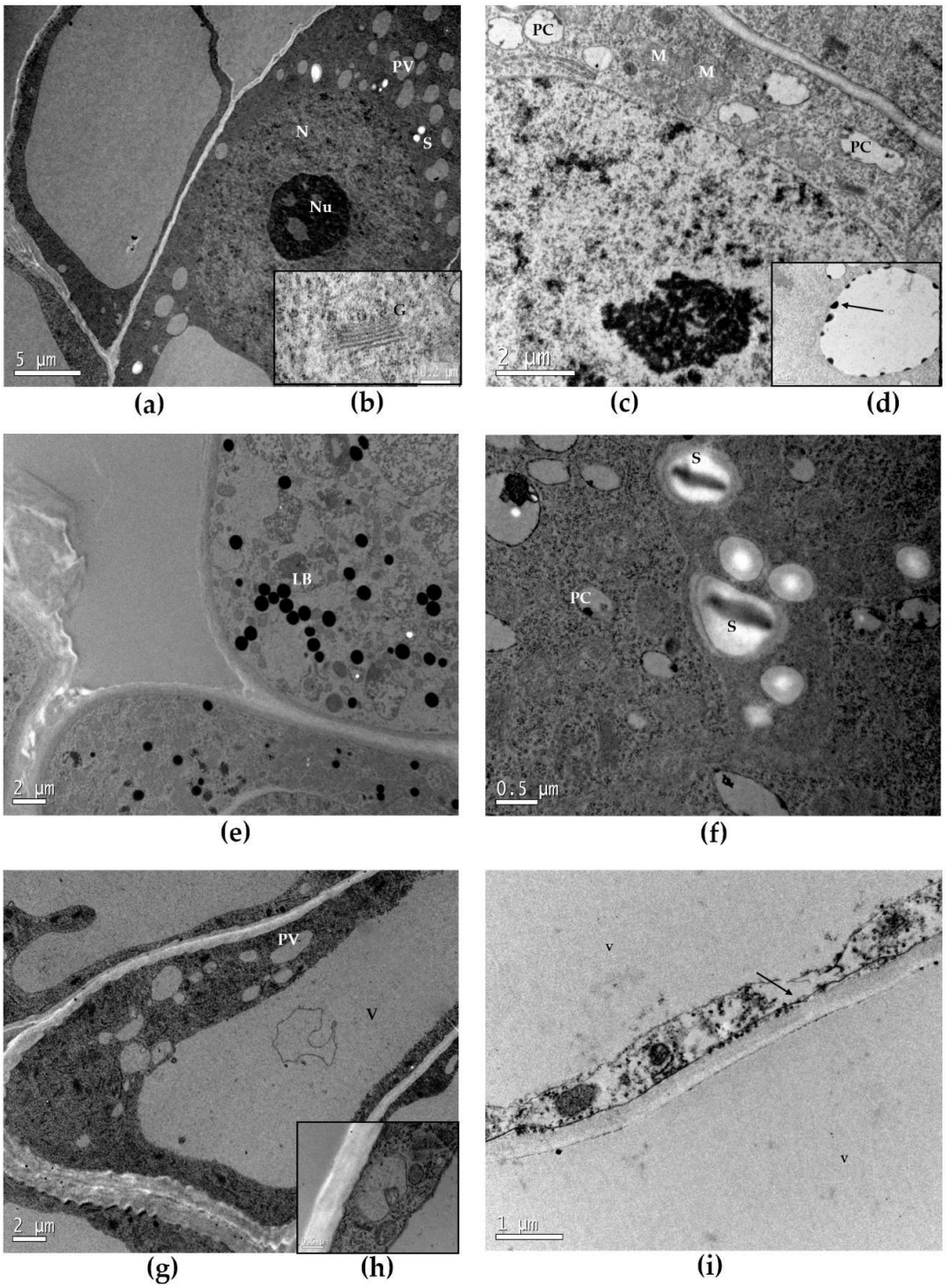

Figure 6. TEM analysis of embryogenic cultures **(a)** densely cytoplasmatic EC from control treatment (23 ℃), with a large central nucleus (N) and a prominent nucleolus (Nu), cytoplasmatic provacuoles (PV) and starch grains (S) inside amyloplasts; **(b)** detail of the cytoplasm of an embryogenic cell showing a Golgi apparatus (G); **(c)** EC from 50 ℃ treatment where some mitochondria (M) and vacuoles containing phenolic compounds (PCs) can be seen; **(d)** detail of PCs (arrow) inside a vacuole; **(e)** EC from cultures at 23 ℃ with high amount of lipid bodies (LB); **(f)** TLC from 40 ℃ treatment with the presence of S and PCs; **(g)** TLC from 60 ℃ treatment showing a large vacuole (V) and the regression of the cytoplasm where organelles are scarce and presents smaller provacuoles (PV); **(h)** detail of the degenerating cytoplasm pressed between the cell membrane and the tonoplast; **(i)** section of two SCs with a large central V and few degenerated organelles in a thin layer of cytoplasm (arrow).

ECs were characterized by a dense cytoplasm and a large central nucleus containing one or more nucleolus. Many cytoplasmic organelles, indicatory of intense metabolic activity such as mitochondria, Golgi complex, and PVs were found around the nucleus (Figure 6a–c). Quite common was the presence of vacuoles containing phenolic compounds in ECs (Figure 6d,e) in samples from different temperatures. These polyphenolic-containing vacuoles were particularly abundant in samples induced at 50 ℃ for 30 min. On the contrary, PCs could not be found in explants cultured under control temperatures. These observations confirm those obtained with light microscopy where PCs were only found in cultures kept at 60 ℃ for 5 min.

Concerning the starch found by light microscopy in samples from all treatments, TEM analysis displayed the same results. A great amount of starch was found in all treatments in ECs (Figure 6a,f) and some could also be found in TLCs (Figure 6f). It can also be noted that, contrary to light microscopy where no evident differences were clear between treatments, TEM allowed the identification of a higher number of starch in samples from cultures initiated at the control temperature (23 ℃). A great amount of lipid bodies (LB) was also detected on samples from all treatments (Figure 6e) particularly in samples cultured under the lowest temperature (control).

Regarding TLCs, that seem to be in transition between ECs and SCs, cells were more elongated and had a higher number of PVs when compared to ECs (Figure 6g). It appeared that by progressive destruction of the cytosol and organelles, PVs were formed on the cytoplasm and together started to form a large central vacuole (V). SCs appeared as PVs started rising in number toward the cell periphery and converged to the formation of a large central V that occupied the majority of cell volume, restraining the cytoplasm to a narrow layer confined between tonoplast and plasma membrane (Figure 6i). No clear differences among treatments were found for TLCs or PVs.

Endogenous Cytokinins Quantification

Statistically significant differences with a very defined pattern were found concerning the concentrations of total isoprenoids CKs, CKs bases, CKs ribosides, and CKs nucleotides (Table 5), Figure 7). Samples coming from control conditions showed the lowest values in all the CKs groups analyzed. On the contrary, tissues coming from EMs induced at 50 ℃ for 30 min contained significantly higher concentration compared to the control. The other treatments presented intermediate values (Figure 7a). The same results were obtained for CKs ribosides (Figure 7b). Samples coming from EMs initiated at 50 ℃ for 30 min showed significantly higher concentration of CKs bases when compared to all treatments (Figure 7c). In the same way, CKs nucleotides concentrations were significantly higher in samples coming from 50 ℃ treatment (Figure 7d). It should also be noted that this was the functional group that presented the highest concentration of isoprenoid endogenous CKs.

Table 5. One-way analysis of variance for concentration of endogenous isoprenoid cytokinins (pmol g^{-1} FW) detected in *P. halepensis* embryonal masses induced under different temperatures (23 °C, 9 weeks; 40 °C, 4 h; 50 °C, 30 min; 60 °C, 5 min).

Temperature (T)			
ANOVA	**D*f***	**F Value**	***p* Value**
CKs bases	3	6.454	0.0027
CKs nucleotides	3	16.83	< 0.0001
Total *c*Z types	3	36.85	< 0.0001
*c*ZR	3	2.609	n.s. [1]
Total *t*Z types	3	14.31	< 0.0001
*t*Z	3	6.953	0.0018
*t*ZR	3	0.7032	n.s.
*t*ZRMP	3	10.33	0.0002
Total DHZ types	3	7.731	0.001
DHZ	3	2.199	n.s.
DHZR	3	5.376	0.0063
DHZRMP	3	15.80	< 0.0001
Total iP types	3	3.347	0.0376
iP	3	5.450	0.0059
iPR	3	2.484	n.s.
iPMP	3	2.829	n.s.
Bases ribosides $^{-1}$	3	0.622	n.s.
Bases nucleotides $^{-1}$	3	4.283	0.0159
iP Z types $^{-1}$	3	1.054	n.s.
Kruskal-Wallis	**D*f***	**X^2 Test**	***p* Value**
Total CKs	3	16.15	0.0011
CKs ribosides	3	8.92	0.0303
*c*Z	3	14.87	0.0019
*c*ZRMP	3	20.40	0.0001
*c*Z *t*Z $^{-1}$	3	16.30	0.0010
*t*Z DHZ $^{-1}$	3	0.10	n.s.
DHZ *c*Z $^{-1}$	3	17.91	0.0005
[bases + ribosides] nucleotides $^{-1}$	3	10.02	0.0184

[1] not statistically significant.

When the total contents of different isoprenoids CKs types were analyzed, the results showed the same pattern observed for isoprenoids functional groups (Figure 8a–d).

*c*Z types showed significant differences between samples from all treatments and the control (Figure 8a). EMs induced at 50 ℃ for 30 min contained significantly higher amounts of *t*Z, DHZ, and iP types than the other treatments assayed (Figure 8b–d).

Examining the content of each isoprenoid CKs individually, *c*Z and iP concentrations in samples from 50 ℃ showed statistically significant differences from other treatments, apart from 40 ℃ that presented intermediate values (Figure 9a,b). In *t*Z and DHZRMP mean values of samples from 50 ℃ treatment resulted in the highest values of cytokinins (Figure 9c,d). *c*ZRMP and *t*ZRMP presented higher concentrations in samples cultured at highest temperatures (50 and 60 ℃) and DHZR showed the same pattern as *c*Z and iP (Figure 9e–g).

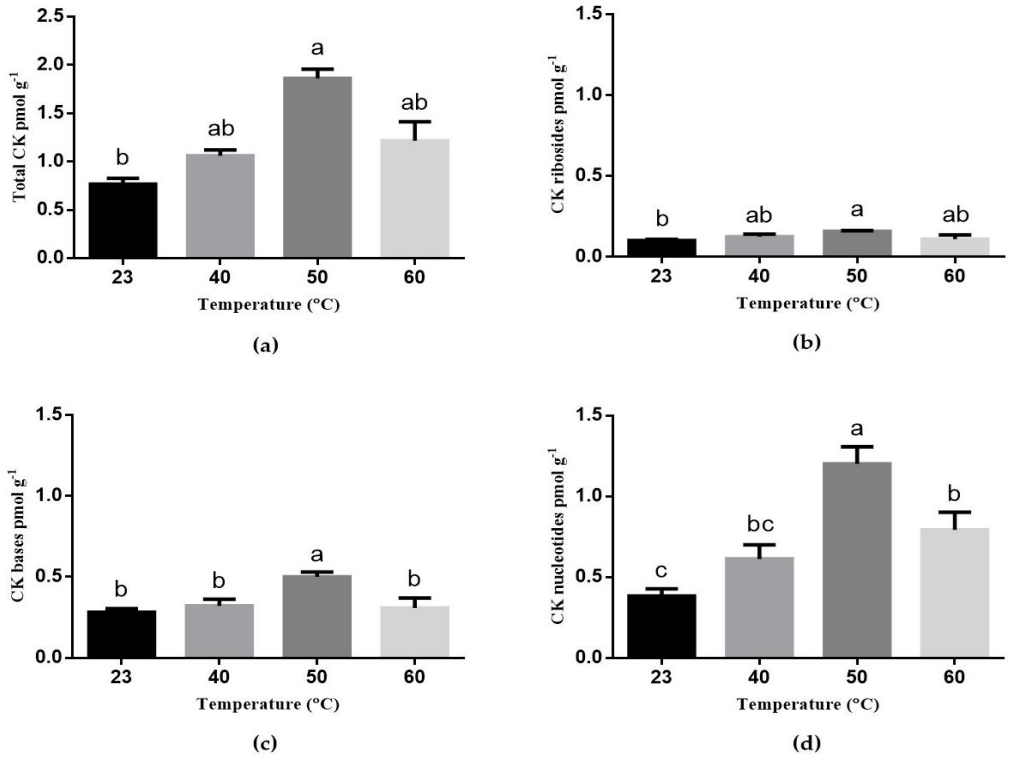

Figure 7. Effect of different temperatures (23 ºC, 9 weeks; 40 °C, 4 h; 50 °C, 30 min; 60 °C, 5 min) at endogenous concentration (pmol g^{-1} FW± SE) of isoprenoids CKs **(a)** Total CKs; **(b)** CK ribosides; **(c)** CK bases; **(d)** CK nucleotides.

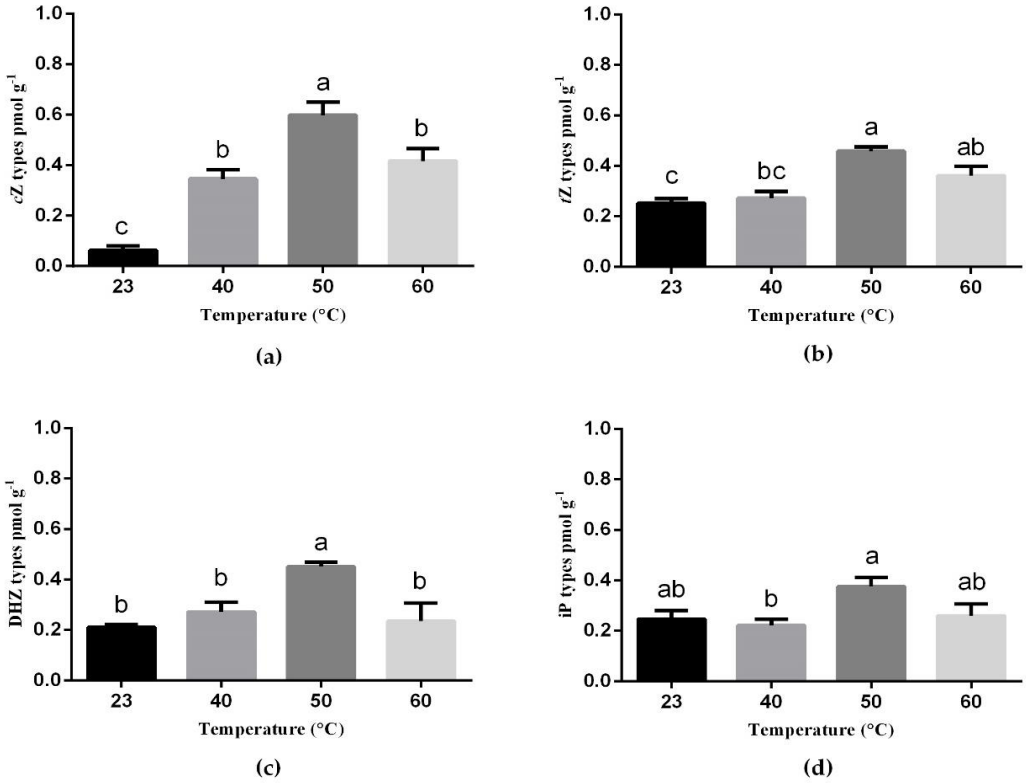

Figure 8. Effect of different temperatures (23 °C, 9 weeks; 40 °C, 4 h; 50 °C, 30 min; 60 °C, 5 min) on the endogenous concentration (pmol g^{-1} FW± SE) of **(a)** total *c*Z types; **(b)** total *t*Z types; **(c)** total DHZ types; **(d)** total iP types cytokinins.

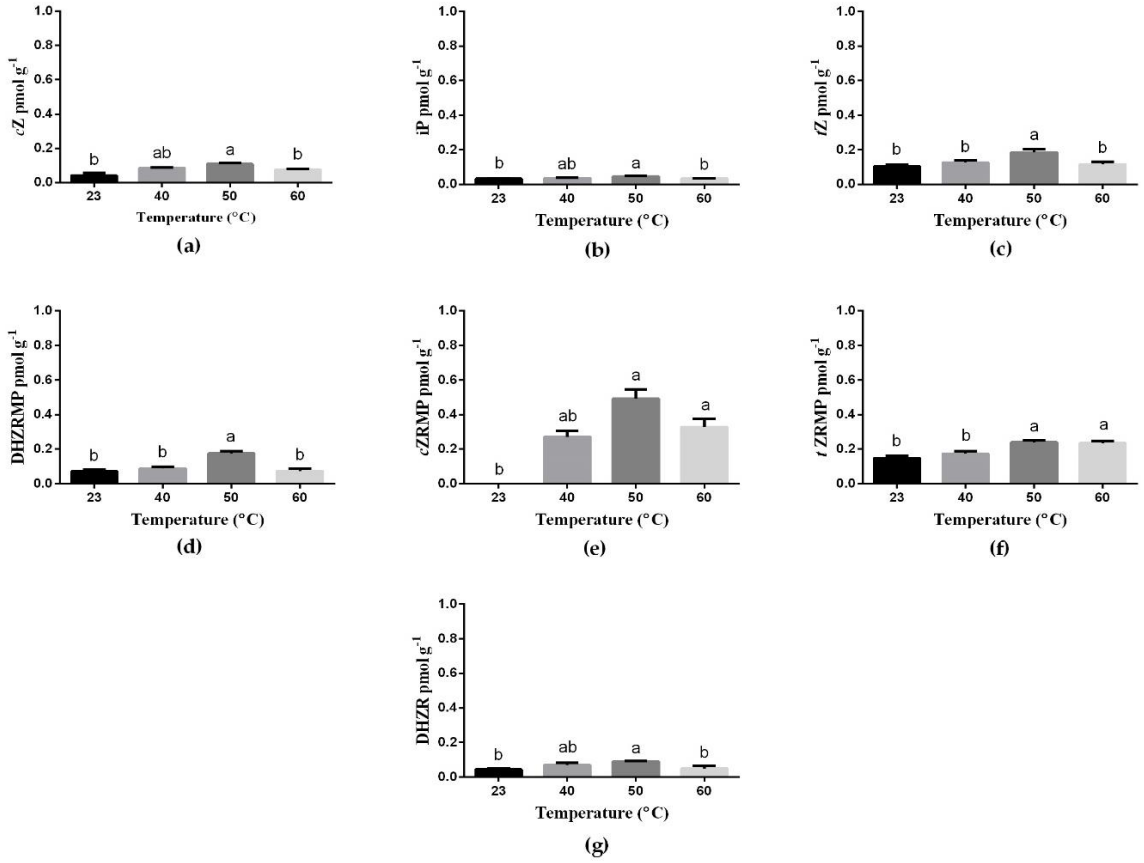

Figure 9. Effect of different temperatures (23 °C, 9 weeks; 40 °C, 4 h; 50 °C, 30 min; 60 °C, 5 min) at endogenous concentration (pmol g^{-1} FW± SE) of **(a)** *c*Z; **(b)** iP; **(c)** *t*Z; **(d)** DHZRMP; **(e)** *c*ZRMP; **(f)** *t*ZRMP; **(g)** DHZR.

The ratios between CK bases and CK nucleotides (Figure 10a), between total DHZ and *c*Z types (Figure 10b) and between [bases + ribosides] and nucleotides (Figure 10c) presented a decreasing pattern as the temperature increased, with samples from the control presenting a statistically significant higher ratio than the ones from 60 °C treatment. Contrary, the ratio between *c*Z and *t*Z types showed to be statistically significantly higher in samples from higher temperatures compared to the control (Figure 10d).

The majority of CKs N-glucosides (7-G/9-G) and *O*-glucosides were under the limit of detection in samples from all treatments applied. No statistically significant differences were found neither for *c*ZR, *t*ZR, DHZ, DHZR, iPR, and iPMP, nor for the ratios between CK bases and ribosides, iP, and Z types and *t*Z and DHZ (Table 6).

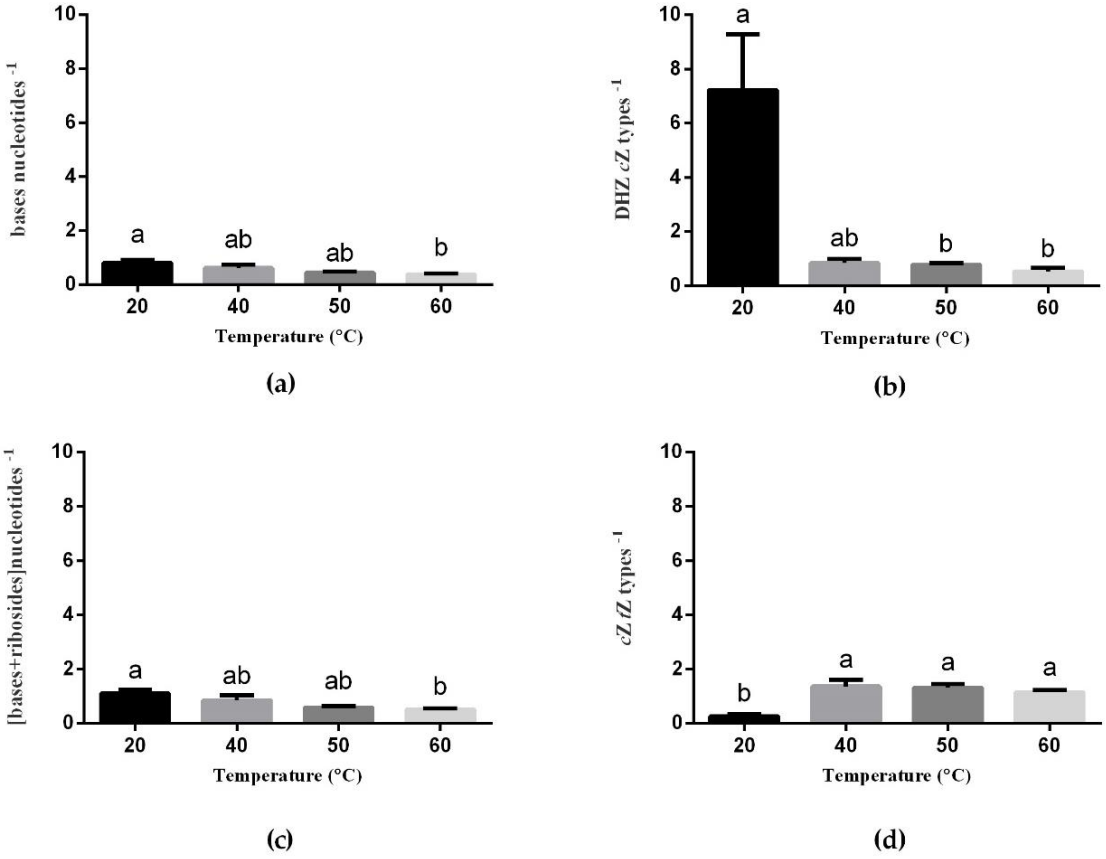

Figure 10. Effect of different temperatures (23 °C, 9 weeks; 40 °C, 4 h; 50 °C, 30 min; 60 °C, 5 min) at the ratios between endogenous concentrations (pmol g-1 FW± SE) of **(a)** CK bases and CK nucleotides; **(b)** DHZ and *c*Z types; **(c)** [bases + ribosides] and nucleotides; **(d)** *c*Z and *t*Z types.

Table 6. Concentration of endogenous isoprenoid cytokinins (pmol g^{-1} FW) of *P. halepensis* embryogenic masses collected at the end of initiation phase and induced under different temperatures.

Treatment	23 °C (9 weeks)	40 °C (4 h)	50 °C (30 min)	60 °C (5 min)
*c*ZR	0.02 ± 0.00 [a]	0.01 ± 0.00 [a]	0.02 ± 0.00 [a]	0.01 ± 0.00 [a]
*t*ZR	0.02 ± 0.01 [a]	0.03 ± 0.01 [a]	0.03 ± 0.00 [a]	0.03 ± 0.02 [a]
DHZ	0.11 ± 0.01 [a]	0.12 ± 0.01 [a]	0.18 ± 0.01 [a]	0.12 ± 0.04 [a]
DHZR	0.04 ± 0.00 [a]	0.07 ± 0.01 [a]	0.09 ± 0.00 [a]	0.05 ± 0.01 [a]
iPR	0.01 ± 0.00 [a]	0.01 ± 0.00 [a]	0.02 ± 0.00 [a]	0.02 ± 0.00 [a]
iPRMP	0.20 ± 0.03 [a]	0.17 ± 0.02 [a]	0.31 ± 0.03 [a]	0.21 ± 0.04 [a]
bases ribosides^{-1}	2.83 ± 0.26 [a]	2.70 ± 0.30 [a]	3.17 ± 0.21 [a]	2.87 ± 0.15 [a]
iP Z types^{-1}	0.96 ± 0.09 [a]	0.87 ± 0.17 [a]	0.83 ± 0.08 [a]	0.70 ± 0.08 [a]
*t*Z DHZ $^{-1}$	1.20 ± 0.06 [a]	1.08 ± 0.17 [a]	1.02 ± 0.05 [a]	2.13 ± 0.42 [a]

Data are presented as mean values ± SE. Significant differences at $p < 0.05$ are indicated by different letters

When the effect of different induction temperatures in the endogenous concentrations of aromatic CKs was analyzed, statistically significant differences were found concerning the concentrations of BA and K types, as well as BA, Kn, K9G, and *o*T (Table 7). Concentrations of BA types in samples coming from 40 ℃ treatment were significantly lower than samples from the control (Figure 11a). BA concentrations showed the same pattern, and samples coming from 50 and 60 ℃ treatment presented intermediate values (Figure 11b). K types and Kn mean values obtained in samples cultured under 50 ℃ were significantly higher when compared to the other

treatments. It should be noted that the Kn presented, by far, the higher concentration for all treatments (Figure 11c,d). K9G concentration was the highest in samples coming from 60 ºC initiation treatment (Figure 11e). *o*T concentrations in samples cultured at the control treatment were significantly lower when compared to higher temperatures (Figure 11f).

Table 7. One-way analysis of variance for concentration of endogenous aromatic cytokinins (pmol g^{-1} FW) detected in *P. halepensis* embryonal masses induced under different temperatures (23 °C, 9 weeks; 40 °C, 4h; 50 °C, 30min; 60 °C, 5min).

Temperature (T)			
ANOVA	***df***	**F Value**	***p* Value**
Total BA types	3	3.961	0.0212
BA	3	3.531	0.0316
BAR	3	2.395	n.s. [1]
*o*T	3	0.4331	0.0021
Total *m*T types	3	0.4012	n.s.
mT	3	0.3003	n.s.
*m*TR	3	0.8331	n.s.
Total K types	3	11.01	0.0001
Kn	3	10.81	0.0001
KR	3	2.749	n.s.
Kruskal-Wallis	***df***	**X^2 Test**	***p* Value**
K9G	3	15.06	0.0018

[1] not statistically significant.

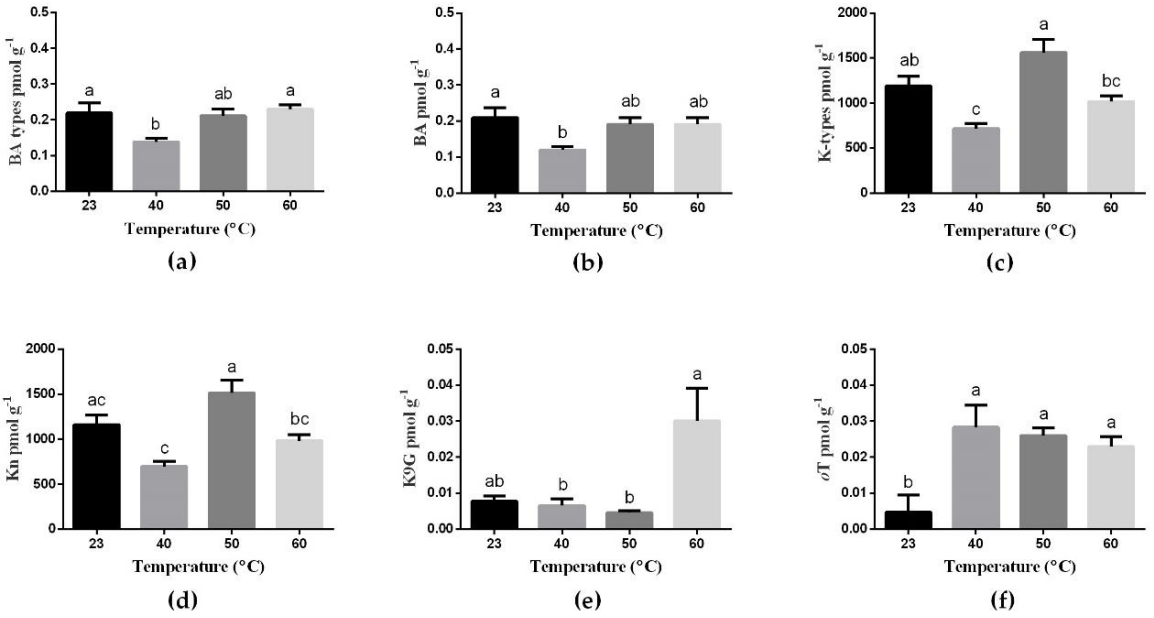

Figure 11. Effect of different temperatures (23 °C, 9 weeks; 40 °C, 4h; 50 °C, 30min; 60 °C, 5min) at endogenous concentration (pmol g^{-1} FW± SE) of **(a)** total BA types; **(b)** BA; **(c)** total K types; **(d)** Kn; **(e)** K9G; **(f)** *o*T

The majority of aromatic CKs N-glucosides (7-G/9-G) (apart from K9G), BARMP, *o*TR and all of *p*T types were under limit of detection in all samples from different treatments. Finally, it is worth to mention that statistically significant differences were not found for BAR, total *m*T types, *m*T, *m*TR or KR (Table 8).

Table 8. Concentration of endogenous aromatic cytokinins (pmol g^{-1} FW) of *P. halepensis* embryonal masses collected at the end of initiation phase and induced under different temperatures.

Treatment	23 °C (9 weeks)	40 °C (4h)	50 °C (30min)	60 °C (5min)
BAR	0.21 ± 0.03 [a]	0.12 ± 0.01 [a]	0.19 ± 0.02 [a]	0.19 ± 0.02 [a]
Total *m*T types	0.08 ± 0.02 [a]	0.12 ± 0.05 [a]	0.10 ± 0.02 [a]	0.12 ± 0.03 [a]
mT	0.06 ± 0.02 [a]	0.09 ± 0.05 [a]	0.08 ± 0.02 [a]	0.07 ± 0.02 [a]
*m*TR	0.02 ± 0.00 [a]	0.02 ± 0.00 [a]	0.02 ± 0.00 [a]	0.02 ± 0.00 [a]
KR	27.53 ± 4.19 [a]	20.87 ± 6.68 [a]	45.13 ± 6.91 [a]	34.81 ± 7.15 [a]

Data are presented as mean values ± SE. Significant differences at $p < 0.05$ are indicated by different letters

5. Discussion

Temperature Experiment

In the present study temperatures higher than used in standard routine were applied (40, 50, and 60 ℃) during the initiation stage of *P. halepensis* SE for different periods (4 h, 30 min, and 5 min, respectively). No statistically significant differences could be found between initiation, proliferation, maturation or germination rates obtained in the different treatments assayed during the induction of EMs. These results are in agreement with the ones obtained when the same temperatures and induction times were studied in *Pinus radiata* (Castander-Olarieta et al. 2019) where no significant differences were also found. Nonetheless, the control presented a lower initiation rate when compared to higher temperatures, in contrast with the results obtained in previous studies carried out in our laboratory (Pereira et al. 2016).

Also, the ECLs initiated under different temperatures did not show significant differences regarding their capacity to produce somatic embryos, corroborating the results found in *Pinus* spp. previous studies (Pereira et al. 2016; Castander-Olarieta et al. 2019). However, samples induced at 60 ℃ for 5 min showed a significantly higher number of somatic embryos, doubling the number of embryos produced in samples cultured at 40 or 50 ℃. Similar results have been obtained in *P. radiata*, where although not statistically significant differences were found, the highest embryo production was achieved at 60 ℃ (Castander-Olarieta et al. 2019). Similar experiments carried out in *P. pinaster* (Arrillaga et al. 2019) showed that an increase of temperature up to 28 ℃ resulted in initiation rates similar to those observed in standard conditions but a significantly higher number of somatic embryos were produced. This fact reinforces the idea that temperature exerts a selective pressure in the SE initial stages that can result in an initiation decrease but higher rates for the forthcoming steps (Fehér 2015; García-Mendiguren et al. 2016b).

It seems that the temperature treatment that triggered a deeper effect on the efficiency of *P. halepensis* SE, was 60 ℃ for 5 min. In spite of the association of stress with adaptation mechanisms and the induction of somatic embryos formation, cell responses to the applied stresses depend on its intensity (Zavattieri et al. 2010). The different induction times for each temperature could in a way affect samples´ response to the different high temperatures applied.

Regarding the morphological analysis of the somatic embryos obtained, more elongated embryos were obtained from samples induced at 60 ℃ for 5 min and from the control treatment,

while the ones obtained from 40 ℃ for 4 h or 50 ℃ for 30 min were smaller and more barrel-shaped. Barrel-shaped form has been described as a symptom of poor-quality embryos, which is usually accompanied by low germination rates in *P. taeda* (Pullman and Buchanan 2003), *P. Pinaster* (Ramarosandratana et al. 2001), and *P. radiata* (Castander-Olarieta et al. 2019). This is contrary to our results since no significant differences were found in the percentage of germinating somatic embryos, and, in fact, the highest percentage of germination was achieved in somatic embryos from ECLs initiated at 50 ℃ for 30 min. These results indicate that the shape of *P. halepensis* somatic embryos may not be related with their ability to germinate as long as they are well formed.

Cytological Characterization of Embryogenic Cultures

Previous work on *Picea abies* (Filonova et al. 2000) showed that embryogenic cultures appeared in three distinct levels or organization: PEM I, PEM II, and PEM III, formed by three different cell types (ECs, TLCs, and SCs) attached together in clusters in different proportions.

In Aleppo pine, three different types of cells (ECs, TLCs, and SCs) in embryogenic cultures from all different temperature treatments (23, 40, 50, and 60 ℃) were also found. Nonetheless, only two of the organizational structures described by Filonova et al. (2000) could be found, since no PEM III were present. In *Picea abies* (Filonova et al. 2000) PEM III were described as enlarged clumps of densely cytoplasmic cells loosely attached to each other that do not present polarity while in the case of *P. radiata* these cells formed compact clusters which showed a well-organized structure with a clear polarization in samples from the control and a higher disorganization at samples from higher temperatures treatments (Castander-Olarieta et al. 2019). Also, despite the fact that well organized and polarized PEMs could be observed from different treatments, the common scenario featured high cellular disorganization with a disproportionate number of TLCs and SCs and no apparent discrepancies in the analyzed samples could be found between treatments when it comes to these features. In *P. sylvestris* (Abrahamsson et al. 2017) a continuous loop of embryo degeneration and differentiation of new embryos during the initiation of embryogenic tissue was suggested. However, they could not find if the differentiation pattern during the initiation stage would give rise to differences in the embryos obtained. This can explain the higher number of TLCs and SCs found in our samples and the fact that all of the analyzed embryogenic cultures produced somatic embryos despite their disorganization.

A large number of starch was found both in light microscopy and TEM analysis from all treatments. In fact, TEM analysis showed that starch grains were present both in ECs and TLCs and in higher numbers in samples from the control. Some authors support the idea that, in ECs, the accumulation of starch around the nucleus is a signal of loss of embryogenic competence and it is also linked with the appearance of dead cells in meristematic centers, leading to low initiation and proliferation rates (Morel et al. 2014; Castander-Olarieta et al. 2019). This was not the case in *P. halepensis*, since no differences were found for initiation or proliferation rates between treatments. Other authors pointed out that starch, as a primary source of energy for cell proliferation, is

abundantly found in competent embryogenic cells that will later differentiate into PEMs. High metabolic activity of these cells will deplete this reserve in such a way that it will no longer be present when embryos start to organize (Borji et al. 2018; de Araújo Silva-Cardoso et al. 2020). In *Picea glauca* a precise pattern of storage compound accumulation during SE was identified with the first accumulation of starch further followed by the formation of lipid bodies and protein vacuoles (Joy IV et al. 1991). In *P. halepensis* lipid bodies were also found in all treatments, although more abundantly in the control. Numerous protein bodies of different sizes or lipid bodies were also observed in ECs of other species (Steiner et al. 2016; de Araújo Silva-Cardoso et al. 2020). In the case of *P. halepensis*, the presence of the above-mentioned storage compounds could not be directly correlated with the progress of SE and their function could probably be related with house-keeping functions of the cells more than with a control of the embryogenic process.

Finally, PCs were found in cultures induced at the higher temperatures. These compounds started to accumulate in the internal face of membrane vacuoles and were particularly notorious when cultures were initiated at 50 ℃. The accumulation of this type of secondary metabolites has been described as playing an essential role in preventing oxidative damage caused by different types of stresses (Eliášová et al. 2017; Falahi et al. 2018), explaining their appearance in samples coming from high temperature treatments and not in control ones. In *P. radiata* differences were also seen among different treatments with respect to PCs with larger accumulations at higher temperatures (Castander-Olarieta et al. 2019). Also, opposite to our results, a positive association between accumulation of phenolic compounds and somatic embryo formation has been indicated in *Acca sellowiana* (Reis et al. 2008).

Quantification of Endogenous Cytokinins

A significantly higher concentration of isoprenoid CKs is present at EMs induced at 50 ℃ when compared to the control. Samples from 40 and 60 ℃ treatments presented concentrations that could be similar to one or another, but were generally intermediate. This pattern was detected through the analysis of the endogenous content of total CKs, CK ribosides, CK nucleotides, *c*Z, *t*Z and DHZ types, and finally for *c*Z, *t*Z, iP, *c*ZRMP, *t*ZRMP, DHZRMP, and DHZR. The results obtained in *P. halepensis* are in line with the concept that short-term or mild stresses stimulate CKs accumulation, while prolonged or more severe stresses are generally associated with downregulation of active CKs levels (Havlová et al. 2008; Nishiyama et al. 2011; Liu et al. 2019a). Furthermore, the ribosylated form of the initial precursor of CKs biosynthesis, iPA, across the time of heat stress exposure in *P. radiata* showed an increase as another author pointed out (Escandón et al. 2015). Contrary, when the same temperatures and induction times were analyzed in *P. radiata*, the results showed a decreasing tendency when applying high temperatures for isoprenoid CKs, especially for those applied for the longest periods of time (40 and 50 ℃) (Castander-Olarieta et al. 2021a).

Although the physiological function of each individual CKs is not yet completely understood they can be classified into different functional groups: (1) Active forms (bases), (2) translocation

forms (ribosides), (3) precursors (nucleotides), and (4) storage and inactivated forms usually bound to glycosides (N-glucosides (7-G/9-G) and *O*-glucosides) (Sakakibara 2010; Spíchal 2012). Regarding the analysis of different isoprenoid functional groups, the results showed that the highest concentration was obtained for CK nucleotides. As reviewed by Frébort et al. (2011), it has been demonstrated that exogenously applied free cytokinin bases are rapidly metabolized into the corresponding ribosides and nucleotides and that, in general, high concentrations of these are found in developing organs. In this sense, when the same induction conditions were studied in *P. radiata* EMs a higher concentration of CKs bases was found (Castander-Olarieta et al. 2021a), while at mature SES of the same species CKs ribosides showed the highest concentration in general (Moncaleán et al. 2018).

The majority of N-glucosides (7-G/9-G) and *O*-glucosides, both for isoprenoids and aromatic CKs, were below the limit of detection. In terms of physiological activity, they exhibit little or no activity in CK bioassays (Letham 1984). These data are in agreement with those reported for *P. radiata* when high temperatures were analyzed (Castander-Olarieta et al. 2021a), and opposite to those obtained when different water availability and temperatures were tested at maturation stage of *P. radiata* SE, despite the low values obtained (Moncaleán et al. 2018), or when different CKs were examined on the induction of organogenesis (Montalbán et al. 2013a). The latter authors hypothesized that these types of forms are normally used by the plant as a form of detoxification in the face of excess hormone. Following this hypothesis, we can say that, in our case, the endogenous content of the hormone is not such that it needs this detoxification mechanism. Data obtained with Norway spruce showed that CKs *O*-glucosides are the most abundant group during all stages of the SE process, including at callus stage, whereas CKs N-glucosides were practically absent (Vondrakova et al. 2018). This can be explained by the difference in the tissues and species analyzed, and the fact that these metabolites have distinctive importance at different stages of SE in these species.

When endogenous concentrations of aromatic CKs were analyzed, a different pattern was obtained when compared to isoprenoid CKs. In K types, despite the fact that samples from 50 ℃ showed the higher concentrations, 40 ℃ showed a significantly lower concentration and, in BA types, samples from 40 ℃ showed significantly lower concentrations when compared with samples from the control. It seems that, when it comes to BA and K types, 40 ℃ for 4 h acted more as a severe stress, contrary to its effect on isoprenoids CKs (Havlová et al. 2008; Nishiyama et al. 2011; Liu et al. 2019a). Also, our results show that the different temperature treatments did not lead to a clear accumulation of these hormones. Reports in apple trees (Ghafari et al. 2020), where concentration of Kn tended to reduce with the intensity of water deficit, and in soybean (Hamayun et al. 2015), where its growth under salt stress was significantly promoted by elevated Kn levels that effectively improved the quantities of isoflavones, presented a clearer function of Kn in response to stress.

Kinetin showed to be the most abundant cytokinin in our samples which might be related to its exogenous application in the culture media. Despite the fact that the majority of naturally

occurring CKs in plants are the N^6-isopentenyl conjugated adenine derivatives, in addition to a small amount of N^6-aromatic CK species (Spíchal 2012; Liu et al. 2019b), exogenous addition of CKs to culture media is known to have an effect by altering and increasing the endogenous CKs pool (Montalbán et al. 2013a; Kumari et al. 2018). Similarly, reports in *Solanum tuberosum* (Baroja-Fernández et al. 2002), *Pinus pinea* (Cuesta et al. 2012), and *Pinus radiata* (Montalbán et al. 2013a) found that aromatic CKs accounted for more than 90% of the total endogenous CK pool although isoprenoid forms are generally the most abundant CKs in plant materials that have not been hormonally treated.

High temperatures application overlaps with higher endogenous concentrations of *o*T, *c*Z types and higher ratios between *c*Z types and *t*Z types. Within the CKs identified in response to mistletoe infestation in *P. sylvestris*, the levels of biologically highly active (*t*Z, iP) and less active (*c*Z, DHZ) CKs were also found to be generally enhanced (Hu et al. 2017). It should be noted that, despite the fact that there were no significant differences, the ratio between iP types and Z types also decreased as the temperatures applied rose. Z-type cytokinins are derived from iP-type compounds and not vice versa (Sakakibara 2010; Nishiyama et al. 2011; Spíchal 2012) and both cell fate and organ formation have been associated with local concentration gradients of these hormones (Frugis et al. 2001). Despite the fact that *o*T is present in inferior concentrations compared to *m*T (Figure 8; Table 7) it seems to have a stronger effect in stress response as well as in cellular activity since *m*T did not present significant variations. Contrary, the results found in *Pinus pinea* (Cuesta et al. 2012) suggest that a higher cellular activity that led to a stronger callogenesis response was related to higher concentrations of *m*T as well as BAR and KR that also did not present significant differences in our case.

Apart from their influence on stress response *per se*, differences obtained in CKs profiles can explain some of the behaviors seen throughout different SE stages between the different treatments applied. After all, CKs are known to be responsible for the regulation of a number of aspects of plant growth and development, such as cell differentiation and growth (Ciura and Kruk 2018).

Although there were also no statistically significant differences at proliferation and germination stages, high concentrations of *t*Z types, *t*ZRMP and iPR of samples from 50 and 60 ℃ treatments overlays with the highest germination rate achieved during SE, at the same time that the treatments with lower concentrations of these hormones presented lower proliferation rates. In coffee it was reported that the transition to the callus stage was accompanied by significant decrease of Z-type (*cis*- and *trans*-) (Awada et al. 2019). Experiments carried out in *P. pinea* (Alvarez et al. 2020) indicated that *t*ZR, *t*Z, and DHZ had a relevant role in the callogenic process. Also, in *P. radiata* (Escandón et al. 2015) ZR seems to be a key element to further acclimation and the recovery mechanism in plants while iPR and DHZR seems to be highly implied, across time, at the heat stress response.

It must be stressed out that samples from 60 ℃ and control treatment (23 ℃) had a similar endogenous low hormonal concentration of *c*Z, iP and DHZR, and these are the treatments that were able to induce a significantly higher number of somatic embryos. It was observed in (Fraga et

al. 2016) that high concentrations of Z and active CKs in general are important during the initial cell division phase of somatic embryogenesis, but not for the later stages of embryo development and maturation. However, as reported in *P. radiata*, low levels of iP types leads to higher success in the SE process (Moncaleán et al. 2018; Castander-Olarieta et al. 2021a). Additionally, the only CK N-glucoside found in our samples, K9G, presented a significantly higher concentration at 60 °C, the treatment that produced more somatic embryos. In *Cocos nucifera* (Sáenz et al. 2003) the isoprenoid cytokinin profiles showed a predominant pattern of 9-conjugation as a major metabolism route and the detection of high levels of inactive metabolic products has been cited as evidence of high CK turnover.

6. Conclusions

As far as we know, this is the first study developed in Aleppo pine that focus on the initiation of EMs under high temperatures analyzing both the phytohormones involved in the success of the SE process as well as the cytological characterization of embryogenic cultures.

We found that it is possible to improve the efficiency of the SE process, under high temperatures, strengthening its productivity through the significant increase of somatic embryos obtained at samples induced at 60 °C for 5 min. Different hormonal profiles overlap with the application of temperature stress as lower endogenous concentrations of *o*T and *c*Z types cytokinins were found at control. Also, a correlation between high rates at specific steps of the process and higher concentrations of *t*Z types, *t*ZRMP, and iPR led to higher germination rates.

Further investigations on the effect of temperature stress during the induction phase of *P. halepensis* SE should focus on complementary molecular pathways, as well as the epigenetics involved along the process. Also, the analysis of physiological parameters in somatic embryogenesis-derived plants should be developed in order to confirm if the application of these different treatments allows the production of plants better adapted to the present scenario of climate change.

CHAPTER II: Heat Stress in *Pinus halepensis* Somatic Embryogenesis Induction: Effect in DNA Methylation and Differential Expression of Stress-Related Genes

(Pereira C, Castander-Olarieta A, Sales E, Montalbán I.A, Canhoto J, Moncaleán P (2021) Heat stress in *Pinus halepensis* somatic embryogenesis induction: Effect in DNA methylation and differential expression of stress-related genes. *Plants* 10:2333.)

1. Abstract

In the current context of climate change, plants need to develop different mechanisms of stress tolerance and adaptation to cope with changing environmental conditions. Temperature is one of the most important abiotic stresses that forest trees have to overcome. Recent research developed in our laboratory demonstrated that high temperatures during different stages of conifer somatic embryogenesis modify subsequent phases of the process and the behavior of the resulting *ex vitro* somatic plants. For this reason, Aleppo pine somatic embryogenesis was induced under different heat stress treatments (40 ℃ for 4 h, 50 ℃ for 30 min, and 60 ℃ for 5 min) in order to analyze its effect on the global DNA methylation rates and the differential expression of four stress-related genes at different stages of the somatic embryogenesis process. Results showed that a slight decrease of DNA methylation at proliferating embryonal masses can correlate with the final efficiency of the process. Additionally, different expression patterns for stress-related genes were found in embryonal masses and needles from the *in vitro* somatic plants obtained; the *DEHYDRATION INDUCED PROTEIN 19* gene was up-regulated in response to heat at proliferating embryonal masses, whereas *HSP20 FAMILY PROTEIN* and *SUPEROXIDE DISMUTASE [Cu–Zn]* were down-regulated in needles.

Keywords: Aleppo pine; conifers; *DEHYDRATION INDUCED PROTEIN 19*; epigenetics; priming; *SUPEROXIDE DISMUTASE [Cu–Zn]*; 5-hydroxymethylcytosine; 5-methylcytosine

2. Introduction

As long-lived sessile organisms with complex life cycles, plants need to develop different mechanisms of protection and adaptation for a broad range of biotic and abiotic stresses in order to maximize growth, reproduction, and survival (Edreva et al. 2008; Baránek et al. 2010). As well as genetics, epigenetics has become an emerging and promising research field to understand tree phenotypic plasticity and adaptive responses (Arnholdt-Schmitt 2004; Ribeiro et al. 2009; Lira-Medeiros et al. 2010; Correia et al. 2013; Lee and Seo 2018).

Alterations in epigenetic marks are reversible enzyme-mediated modifications of DNA and/or associated histones that regulate transcriptional activity of genes as well as their sequences (Smulders and Klerk 2010; Hauser et al. 2011; Us-Camas et al. 2014). The most studied epigenetic mark is DNA methylation because of its stability, its incidence in both plants and mammals, and its influence on gene expression and genome structure regulation (Amaral et al. 2020).

Most epigenetics marks are reverted when the environmental constraints that triggered them are no longer present. However, higher plants appear to be able to retain some "stress memory" or "stress imprinting", since a first stress exposure often leads to an enhanced resistance to a later stress (Bruce et al. 2007; Conrath 2011). What is also known as "priming" or "hardening", prior exposure to the eliciting factors leads to a faster and stronger induction of basal resistance mechanisms (or greater tolerance) against them. In some cases, crosstalk among different stimuli can happen, leading to multiple stress memory attainments (cross-priming) (Blödner et al. 2005). Heat is sometimes accompanied by other stresses, such as drought, and recent studies showed that both stresses have overlapping roles (Pereira et al. 2016; García-Mendiguren et al. 2016b; Moncaleán et al. 2018).

Variations in epigenetic marks were revealed to be involved in morphological and physiological changes in trees in a large number of processes, including embryogenesis, organ maturation, phase change, and bud set or burst (Johnsen et al. 2005b; Valledor et al. 2010; Yakovlev et al. 2016; Castander-Olarieta et al. 2019). Moreover, epigenetic regulation plays a critical role in modulation of multiple aspects of plant development through the adjustment of gene expression in response to environmental factors factors (Hauser et al. 2011).

Somatic embryogenesis (SE) is a worldwide studied biotechnology tool that allows large-scale propagation for many conifers (von Arnold et al. 2019). The first report of SE in Aleppo pine was carried out in our laboratory (Montalbán et al. 2013b). Later, a subsequently developed experiment showed that changes in temperature and water availability at the induction phase of SE affects the success of the process in this species (Pereira et al. 2016). Considering those results, we focused on the application of higher temperatures (40 ℃ (4 h), 50 ℃ (30 min), and 60 ℃ (5 min)) at the initial stage of SE to see if a "priming" effect could be obtained. It was already found that this stress application during SE induction can modulate the morphology and hormonal profiles of embryonal masses (EMs) as well as the efficiency of the process itself (Pereira et al. 2020)(Chapter I).

Notwithstanding that stress affects plants at different levels and several defense mechanisms are activated, it leads to the accumulation of reactive oxygen species (ROS) that can reach toxic

levels and cause cell damage and death (Feher et al. 2008). To avoid this, plants have evolved antioxidant machinery consisting of enzymatic components, such as superoxide dismutase (Almeselmani et al. 2006). Additionally, as previously mentioned, heat is sometimes accompanied with drought, and the dehydration-induced 19 family of proteins appears to be involved in the response to both stresses (Liu et al. 2013; Alvarez et al. 2016). Finally, the induction of heat shock proteins (HSPs) seems to be essential to facilitate continued homeostasis and survival against heat stress (Neilson et al. 2010; Ling et al. 2018).

In this sense, in the present study, the effects of different temperature treatments applied during the initial stage of Aleppo pine SE on the epigenetic patterns were evaluated. For this reason, levels of cytosine residues 5-methylcytosine (5mC) and 5-hydroxymethylcytosine (5hmC), both at proliferating EMs and at needles from the *in vitro* somatic plants produced, were measured. At the same time, the expression of stress-related genes involved in the defense mechanisms mentioned above was analyzed to assess if the initial heat stress triggered long-lasting modifications at the transcriptome along the different stages of the process.

3. Material and Methods

SE temperature Experiment and Plant Material Collection

Induction of *Pinus halepensis* EMs under different temperatures was performed as described in Pereira et al. (2020) (Chapter I). Briefly, one-year-old green female cones, enclosing immature seeds of *P. halepensis* from five open pollinated trees were used; storage and preparation of plant material was the same as described in Montalbán et al. (2015). Whole megagametophytes were placed horizontally on DCR initiation medium (Gupta and Durzan 1986). For temperature treatments, closed Petri dishes containing initiation medium were preheated for 30 min, and immature megagametophytes were cultured at 40, 50, and 60 ℃ for 4 h, 30 min, and 5 min, respectively. As control, 23 ℃ was used, and, after the application of the different treatments, all explants were kept at standard conditions in darkness.

After nine weeks on the initiation medium, proliferating EMs were detached from the megagametophyte and transferred to the proliferation medium. This medium had the same composition to that used in the initiation stage, but a higher gellan gum concentration (4.5 g L^{-1}). EMs were subcultured every two weeks and kept in the dark.

Following 4 subcultures, fresh tissue from twenty proliferating embryogenic cell lines (ECLs) were immersed in liquid nitrogen and immediately stored at −80 ℃ until further analysis. Eight/nine ECLs per treatment were selected to maturation at DCR medium supplemented with 60 g L^{-1} sucrose, 75.0 µM abscisic acid, the EDM amino acid mixture (Walter et al. 2005), and 9 g L^{-1} Gelrite®.

For germination, somatic embryos were transferred to Petri dishes containing half-strength macronutrient LP medium (Quoirin and Lepoivre 1977; Aitken-Christie et al. 1988) supplemented with 2 g L^{-1} of activated charcoal and 9.5 g L^{-1} Difco® granulated agar (Becton Dickinson, Franklin

Lakes, NJ, USA). Cultures were cultured under dim light for 7 days and afterwards were kept under a 16:8 h photoperiod at 100 µmol m^{-2} s^{-1} provided by cool white fluorescent tubes (TFL 58 W/33, Philips, France). The obtained plantlets were transferred onto fresh medium of the same composition every 4 weeks. During the first 8 weeks, plantlets were cultured in Petri dishes and then transferred to glass culture vessels. After 6 months, needles from *in vitro* somatic plants from eleven ECLs were immersed in liquid nitrogen and immediately stored at −80 °C until further analysis.

Global DNA Methylation / Hydroxymethylation Analysis

Genomic DNA extraction and subsequent methylation analysis were performed both on samples from twenty proliferating EMs and needles from *in vitro* somatic plants from eleven ECLs (comprising five samples of EMs and three samples of needles, per treatment). Previously collected samples were lyophilized, and 15 mg of homogenized lyophilized tissue were used.

DNA extraction and its hydrolyzation were performed as described in Castander-Olarieta et al. (2020b).

Methylation and hydroxymethylation levels of cytosine were analyzed on a 1200 Series HPLC system coupled to a 6410 Triple Quad mass spectrometer (Agilent Technologies, Santa Clara, CA, USA). The chromatographic separation was performed on a Zorbax SBC18 column (2.1 × 100 mm, 3.5 µm, Agilent Technologies). The mobile phase was 11% methanol and 0.1% formic acid in water, and 5 µL of samples were injected in the column at a flow rate of 0.1 mL min^{-1}. The electrospray ionization source (ESI) was operated in the positive ion multiple reaction monitoring mode (MRM) set to an ion spray voltage of 3500 V, 40 psi for nebulizer, and source temperature at 350 °C. The intensities of specific $MH^+ \rightarrow$ fragment ion transitions were recorded (5mC *m*/*z* 242→126, 5hmC *m*/*z* 258→142, and C *m*/*z* 228→112). Identification of cytosine, 5mC, and 5hmC was assessed by injection of commercial standards (5-Methylcytosine and 5-Hydroxymethylcytosine DNA Standard Set, Zymo Research, Irvine, CA, USA) under the same LC-ESI-MS/MS-MRM conditions. The percentage of 5mC and 5hmC at each sample was calculated from the MRM peak area divided by the combined peak areas for 5mC, 5hmC, and cytosine.

Relative Expression of Stress-Related Genes

RNA extraction and further analysis of expression patterns from stress-related genes were performed on samples from sixteen proliferating EMs and needles from *in vitro* somatic plants from eleven embryogenic lines (comprising four samples of EMs and three samples of needles, per treatment). As initial material, 10 mg of lyophilized tissue, previously grinded for homogenization in a TissueLyser II (Qiajen, Hilden, Germany), were used. The analysis was performed based on the protocol described in Castander-Olarieta et al. (2020b).

Total RNA extraction was carried out using a plant/fungi total RNA purification kit (Norgen Biotek Corp., Thorold, ON, Canada), and genomic DNA was degraded by using recombinant

DNase I (RNase-free, Takara Bio Inc., Shiga, Japan), following manufacturer's instructions. A NanodropTM 2000 was used for RNA quantification, and its integrity was assessed by agar gel electrophoresis.

cDNA was synthesized from 1000 ng of RNA using the PrimeScript RT Reagent Kit (Takara) and random hexamers as primers following the manufacturer's instructions. Real time PCR amplifications were performed in StepOne Plus (Applied Biosystems, Carlsbad, CA, USA), using a final volume of 20 µL containing 0.8 µM of each primer and 10 µL of SYBR Green I Master mix (Takara Bio Inc., Shiga, Japan) in triplicate for each sample. The PCR conditions were an initial denaturation at 95 ℃ for 20 s, followed by 40 cycles of 95 ℃ for 3 s and 60 ℃ for 30 s.

Primers previously described (Alvarez et al. 2016; Escandón et al. 2017) were used and their efficiencies estimated using the qPCR Efficiency Calculator available at Thermofisher.com, based on the standard curve previously developed with four dilution points for each primer. Analyzed genes as well as primers details are summarized in Table 9.

Table 9. List of primers used in quantitative real time PCR (qRT-PCR) for relative expression analysis. Names of the genes, forward and reverse primer sequences and melting temperatures of primers are described.

ID	Name	Forward (5' → 3')	Reverse (5' → 3')	Tm (℃)
ACT	*ACTIN*	CACTGCACTTGCTCCCAGTA	AACCTCCGATCCAAACACTG	60
P439	*CHLOROPLAST SMALL HEAT PROTEIN*	AAGTTGTCGGTTCGAACCCC	CAGAACACCGTCCTCCACAG	62
P444	*HSP20 FAMILY PROTEIN*	TTTCCGACTTCTTCACGGGG	TTTGACAGTCCCGGCATGTC	62
DI19	*DEHIDRATION INDUCED PROTEIN 19*	ATAGATGCCCATGCTGTGTAG	CTTCCCTCTGTTCCCACTTG	54
SOD	*SUPEROXIDE DISMUTASE [Cu-Zn]*	ACAAAACGGGTGCATGTCAAC	CCCATCCGCTCCTACAGTTAC	66

The relative transcript levels were normalized using *ACTIN (ACT)*, and the relative expression of each gene (R) was calculated on the basis of DCt values using the following formula: $R = 2^{-\Delta Ct}$ (Livak and Schmittgen 2001). Finally, the fold changes between expression values obtained at control treatment (23 ℃) and different temperature treatments were calculated in logarithmic scale.

Statistical Analysis

A one-way analysis of variance, through the application of the non-parametric Kruskal– Wallis test, was carried out to assess the effect of different temperature treatments both for total DNA methylation rates (%) and for genes' relative expression values. When significant differences were found ($p < 0.05$), Dunn's multiple comparison test was carried out to find out which treatments were statistically different.

4. Results

Global DNA Methylation / Hydroxymethylation Analysis

No statistically significant differences were found regarding global DNA methylation rates (%) between samples from the different induction temperature treatments applied at the initiation stage of *P. halepensis* SE (Table 10).

Regarding the results obtained for EMs, the treatment that presented the lowest levels of 5mC was 60 ºC (5 min) (37.52%), followed by the control (23 ºC) (38.01%), and the highest methylation rate was obtained at 50 ºC (30 min) with a difference of 3.3% with respect to the lowest (40.82%) (Table 11). The values obtained in needles were very similar between treatments (Table 11). All samples presented high rates of global DNA methylation (between 37.52 and 41.56%) (Table 11).

Table 10. One-way analysis of variance for methylation rates (%) detected in *P. halepensis* embryonal masses (EMs) and needles from *in vitro* somatic plants induced under different temperature treatments (23 ºC, 9 weeks; 40 ºC, 4 h; 50 ºC, 30 min; 60 ºC, 5 min).

Kruskal-Wallis	d*f*	X^2 test	*p* Value
EMs	3	5.960	n.s.[1]
Needles	3	5.359	n.s.

[1] not statistically significant.

Table 11. Total methylation rates (%) detected in *P. halepensis* proliferating embryonal masses (EMs) and needles from *in vitro* somatic plants induced under different temperature treatments (23 ºC (control); 40 ºC, 4 h; 50 ºC, 30 min; 60 ºC, 5 min). Data are presented as mean values ± SE and significant differences at $p < 0.05$ are indicated by different letters.

Methylation (%)	23 ºC (control)	40 ºC (4 h)	50 ºC (30 min)	60 ºC (5 min)
EMs	38.01 ± 0.72 [a]	39.48 ± 1.94 [a]	40.82 ± 0.84 [a]	37.52 ± 0.45 [a]
Needles	40.00 ± 0.21[a]	40.25 ± 1.21 [a]	41.47 ± 0.43 [a]	41.56 ± 0.41[a]

The detection of 5hmC was not possible in proliferating EMs, and it was only achieved, at very low levels, in five out of twelve analyzed samples of needles from *in vitro* somatic plants. Thus, no further analysis was carried out concerning hydroxymethylation data. Even so, it should be noticed that three of the five detected values at needles corresponded to the samples from the control (23 ºC).

Relative Expression of Stress-Related Genes

The different induction temperature treatments applied during the initial stage of *P. halepensis* SE led to changes in the relative expression patterns of the stress-related genes with respect to the control (23 ºC).

The results found in proliferating EMs showed that statistically significant differences were found for the relative expression of *DEHYDRATION INDUCED PROTEIN 19* (*DI19*) (Table 12); in both 50 ºC (30 min) and 60 ºC (5 min) treatments, despite the lower fold change obtained (Figure

12a), the relative expression of this gene was considerably higher than in the control treatment (23 ℃). *CHLOROPLAST SMALL HEAT PROTEIN* (*P439*), *HSP20 FAMILY PROTEIN* (*P444*), and *SUPEROXIDE DISMUTASE [Cu–Zn]* (*SOD*) were slightly higher expressed in samples induced at higher temperatures when compared to the control, except for *SOD* at the 50 ℃ treatment (Figure 12a), but these differences were not significant.

Table 12. One-way analysis of variance for expression of different genes detected in *P. halepensis* embryonal masses (EMs) and needles from *in vitro* somatic plants induced under different temperature treatments (23 ℃, 9 weeks; 40 ℃, 4 h; 50 ℃, 30 min; 60 ℃, 5 min).

Kruskal-Wallis	d*f*	X^2 test	*p* Value
EMs			
P439	3	5.286	n.s.[1]
P444	3	6.795	n.s.
DI19	3	35.23	< 0.0001
SOD	3	7.057	n.s.
Needles			
P439	3	3.983	n.s.
P444	3	15.75	0.0013
DI19	3	3.297	n.s.
SOD	3	15.42	0.0015

[1] not statistically significant.

In contrast, in needles from *in vitro* somatic plants, statistically significant differences were found for the relative expression of *P444* and *SOD* genes. A gradual decrease of *P444* relative expression was observed when priming temperature increased, being significantly repressed compared to control (23 ℃) for the 60 ℃ treatment. Expression of the *SOD* gene was lower in relation to the control (23 ℃), but significant differences were only detected in samples coming from the 50 ℃ treatment, which attained the highest fold change (Figure 12b). *P439* and *DI19* were slightly down-regulated at samples induced at higher temperatures when compared to the control (23 ℃), but these differences were not significant. In conclusion, induction of SE at higher temperatures resulted in different relative expression patterns of these stress-related genes in proliferating EMs and in needles from *in vitro* somatic plants. At proliferating EMs, the stress-related genes studied were generally overexpressed in primed plant material, whilst in the *in vitro* somatic plants obtained, their expression was lower in primed than in control.

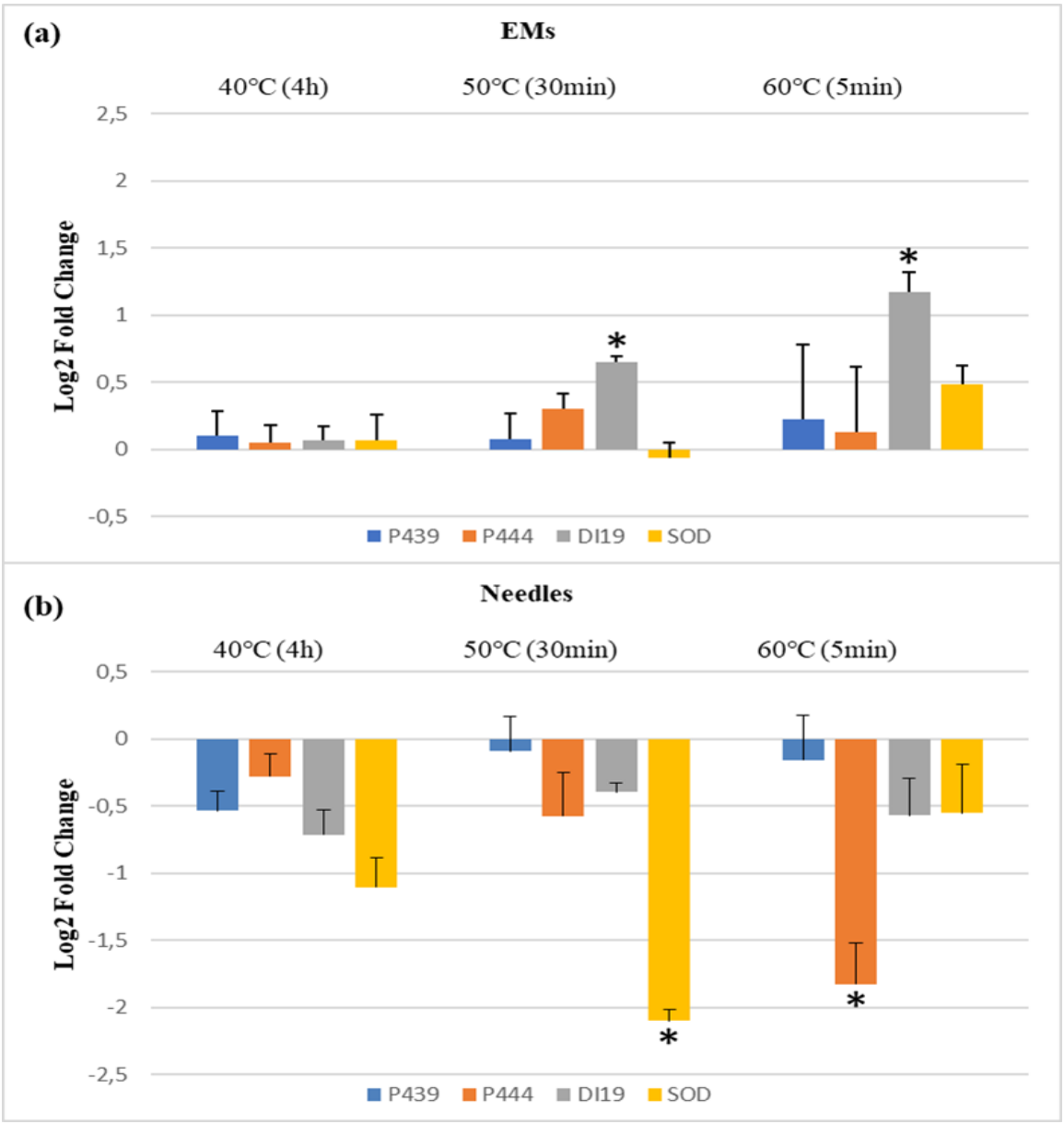

Figure 12. Fold-relative gene expression of four stress-related genes (P439, P444, DI19, and SOD) between *P. halepensis* samples induced under different temperature treatments (40 ℃, 4 h; 50 ℃, 30 min; 60 ℃, 5 min) from **(a)** proliferating embryonal masses (EMs); **(b)** needles from *in vitro* somatic plants. Data are presented as mean values ± SE, and * represents statistically significant differences at $p < 0.05$ of different temperature treatments with respect to the control (23 ℃).

5. Discussion

Accumulating data have shown that epigenetics changes are involved in many physiological processes, and the understanding of these mechanisms is crucial for forest tree management and breeding in the context of climate change (Boyko and Kovalchuk 2008; Lämke and Bäurle 2017; Sow et al. 2018). One of the most important epigenetic marks is DNA methylation. It occurs through the addition of a methyl group at position 5 of the pyrimidine ring of cytosine in the CG, CHG, and CHH (where H = A, T, or C) contexts (Viejo et al. 2012; Kumar et al. 2013), and understanding how its levels change under stressful conditions can lead to a better knowledge of

the plant response to environmental changes (Amaral et al. 2020; Korotko et al. 2021). Considering the use of epigenetic variations for breeding applications relies on their transmission features, and since 5mC patterns can be transmitted through mitosis as well as meiosis, this DNA methylation mark could be valuable in all crops regardless of their propagation method (Gallusci et al. 2017). In this sense, the concentrations of 5mC and 5hmC were assessed in order to perform a global DNA methylation study in samples from proliferating EMs and needles from *in vitro* somatic plants of Aleppo pine induced under high temperatures.

No statistically significant differences in methylation status were found between the induction treatments applied. Nonetheless, at proliferating EMs, a difference of 3.3% was found between the 60 ℃ (5 min) treatment that presented the lowest concentrations of 5mC with respect to the highest methylation rate obtained at 50 ℃ (30 min). In *Pinus nigra*, specific DNA methylation levels were analyzed in tissues with different embryogenic potentials, and the lowest levels were found in those with higher embryogenic capacity (Noceda et al. 2009). In *Coffea canephora* indirect SE, 5mC rates were stable during cell differentiation, and a significant increase occurred during somatic embryos regeneration (Amaral-Silva et al. 2021). Several studies suggest that DNA methylation is critical for SE success, and it is common to find lower values in embryogenic tissues with respect to the non-embryogenic tissues (De-la-Peña et al. 2015; Bravo et al. 2017; Lee and Seo 2018). Taking this into account and correlating the results presented here with the ones obtained in a previous study, where the effect of *Pinus halepensis* SE induction under high temperatures on the efficiency of the process was assessed, we can reaffirm this plausible hypothesis. The highest number of somatic embryos produced was obtained in EMs from the 60 ℃ (5 min) treatment (a mean of 317.4 somatic embryos per gram) followed by those from the control; the lowest number was gained when a priming treatment of 50 ℃ (30 min) was applied (a mean of 135.2 somatic embryos per gram) (Pereira et al. 2020) (Chapter I).

Considering the effect of heat stress on the variation of DNA methylation levels, different species and cell types display different responses. In a similar study, performed with *P. radiata*, the same decrease in samples induced at the highest temperature of 60 ℃ (5 min) compared to the control temperature and the 40 ℃ (4 h) treatment was found (Castander-Olarieta et al. 2020b). On the contrary, in Norway spruce, seedlings originating from a warm embryonic environment (Johnsen et al. 2005a) and the exposure of *Arabidopsis* plants to heat (Boyko et al. 2010) resulted in an increase of global DNA methylation. Interestingly, also in *Arabidopsis*, DNA methylation increased during heat stress, followed by the reduction of DNA methylation levels after transfer to the control conditions (Korotko et al. 2021).

Needles presented slightly higher concentrations of 5mC relative to EMs, and the global DNA methylation values were stabilized between treatments at this stage. This is in accordance with the fact that a gradual increase in DNA methylation throughout ageing was previously reported for several forest trees (Valledor et al. 2007; Bräutigam et al. 2013). In *P. radiata* needles from field trees, DNA methylation increased with both ageing and phase change (Fraga et al. 2002). In

contrast, 5mC levels in proliferating EMs and needles from one-year-old somatic plants of *P. radiata* were similar (Castander-Olarieta et al. 2020b).

The 5hmC was detected in needles from *in vitro* somatic plants of Aleppo pine. As reviewed in Shi et al. (2017), numerous studies indicate that 5hmC acts not only as an intermediate during 5mC demethylation but also plays important roles during maintenance of pluripotency in animal embryonic stem cells; however, in plants the roles of 5hmC during development are still unknown. The first discovery of its presence in conifers was in Norway spruce (Yakovlev et al. 2019), and it was found that its concentration can fluctuate not only at different tissues but also at different temperatures in *P. radiata* (Castander-Olarieta et al. 2020b).

The differential expression of stress-related genes (*P439*, *P444*, *SOD*, and *DI19*) in primed plant material was also assessed in this study. To respond and adapt to different stresses, plants have developed a complex of molecular mechanisms by modulating the expression of a specific set of genes (Mittler et al. 2012; Escandón et al. 2015; Lämke and Bäurle 2017; Amaral et al. 2020), and we found that differential expression patterns changed between the two stages of the propagation process analyzed.

Regarding the relative expression of the stress-related genes in proliferating EMs, statistically significant differences were only found for *DI19*. A gradual increase at the relative expression of this gene along the higher temperature treatments was found and in EMs initiated at 50 ℃ (30 min) and 60 ℃ (5 min) was considerably higher than in the control (23 ℃). The *DI19* family of proteins is a novel type of Cys2/His2 zinc-finger proteins involved in the response to several abiotic stresses, especially drought (Milla et al. 2006). In *Populus simonii*, it was found that there is an overlapping heat–drought response (Jia et al. 2017), and our results suggest that *DI19* overexpression is involved in the abiotic stress response in *P. halepensis*. In accordance, in rice, the overexpression of the DI19-4 resulted in significantly increased tolerance to drought stress (Wang et al. 2014), and in *Arabidopsis*, DI19-1 overexpressing lines presented higher tolerance to drought stress than the wild-type lines (Qin et al. 2014). On the other hand, in *P. radiata* emerging EMs induced at higher temperatures, *DI19* initially presented similar levels to control; however, after 4 weeks, actively proliferating EMs induced at 40 ℃ (4 h) were significantly underexpressed (Castander-Olarieta et al. 2020b). In another study in *Arabidopsis*, transgenic lines with DI19–3 overexpression were more sensitive to salinity and drought than wildtypes (Milla et al. 2006). It appears that different protein members of this family, despite being clearly involved in stress response mechanisms, may have different functions unknown yet.

No differences were obtained in proliferating EMs for *P439*, *P444*, and *SOD*. However, needles from *in vitro* grown somatic plants showed statistically significant differences in transcript abundance for both *P444* and *SOD* genes. The relative expression of these genes was lower in plants coming from EMs initiated at high temperatures when compared to the control plants. Heat stress severely affects the stability of various cellular components, causing a state of metabolic imbalance and a cascade of cellular reactions. This disruption of the steady-state flux of cellular metabolites usually leads to the accumulation of toxic products, such as ROS (Mittler et al. 2012;

Jia et al. 2017). Furthermore, HSPs are closely involved in cellular protection, its structures and responses to heat stress being highly conserved amongst several organisms (Efeoğlu 2009; Neilson et al. 2010). According to this, in maritime pine, when heat priming was performed at immature megagametophytes through SE, similar levels of expression were observed in primed and control EMs for *HSP70* and *SOD*, but the expression of *HSP70* at the derived *in vitro* somatic plants was higher in control plants (Pérez-Oliver et al. 2021). In *P. radiata*, the gene coding for a heat shock protein (*HSP20*) was down-regulated in proliferating EMs and somatic plants coming from EMs initiated at high temperatures (Castander-Olarieta et al. 2020b). In contrast, *P. radiata* one-year-old seedlings subjected to heat treatments showed significantly higher short-term expression of *P439* and *P444* (Escandón et al. 2017). Different sampling times, as well as different tissues, seem to lead to different relative expressions of stress-related genes. Taking this into account, we suggest that in *P. halepensis* stress-related gene overexpression may happen during and/or shortly after the heat stress occurs. With time and at different tissues, the priming effect leads to their stabilization and their lower expression relative to controls.

Finally, it is important to note that different patterns of stress-related genes relative expression have been observed. In this sense, *DI19* presented a gradual increase along the higher temperatures at EMs and *P444* a gradual decrease in the needles from *in vitro* somatic plants. In its turn, *SOD* was significantly repressed in needles sampled in plants derived from priming at 50 ℃ (30 min), while those from plants primed at 60 ℃ (5 min) showed expression rates similar to non-primed plants. When the effect of these temperature treatments in EMs endogenous cytokinin (CK) profiles was assessed in a previous work on this species, diverse patterns were also found for different CKs (Pereira et al. 2020) (Chapter I). Those results were related to the different induction times between treatments and the concept that for some CKs, temperature treatments acted as short or mild stress, while for others they were sensed as a prolonged or more severe stress. In *Arabidopsis*, heat stress has been connected with fluctuations in the endogenous levels of CKs and ABA that seem to be involved in HSPs regulation (Dobrá et al. 2015). It is possible that an interaction between CKs and the regulation of other stress-related genes, in response to heat stress, also occurs in *P. halepensis*.

6. Conclusions

As far as it is known, this is the first report concerning the effect in DNA methylation and expression of stress-related genes in response to heat stress application during SE induction in Aleppo pine. Regarding the DNA methylation results, the temperatures treatments applied were not enough to provoke significantly different levels of DNA methylations at the analyzed samples. Nonetheless, it is important to note that the treatment that presented the lowest methylation level was also the one that produced the highest number of somatic embryos (60 ℃, 5 min) (Pereira et al. 2020) (Chapter I). It appears that lower levels of DNA methylation/DNA hypomethylation are associated with higher embryogenic capacity and, therefore, with a higher number of somatic embryos produced.

Concerning the application of high temperatures at the early stage of *P. halepensis* SE at the expression of stress-related genes, long-term changes in the differential expression of stress-related genes, specifically *DI19*, *P444*, and *SOD*, at different stages of SE were found. Despite the fact that the pattern of overexpression of primed EMs and lower expression of primed needles were consistent, it appears that different induction times between treatments had an effect on the relative expression of the stress-related genes studied.

Further analysis concerning the effect of heat stress application during the induction phase of *P. halepensis* SE regarding its effect on metabolomics and protein profiles will be performed. This data can lead to a better understanding of all the mechanisms involved in the heat stress response in this species.

CHAPTER III: Proteomic and Metabolic Analysis of *Pinus halepensis* Mill. Embryonal Masses Induced under Heat Stress

(Pereira C, Castander-Olarieta A, Montalbán IA, Mendes VM, Correia S, Pedrosa A, Manadas B, Moncaleán P, Canhoto J (2023) Proteomic and metabolic analysis of *Pinus halepensis* Mill. embryonal masses induced under heat stress. *International Journal of Molecular Sciences* 24:721.)

1. Abstract

Understanding the physiological and molecular adjustments occurring during tree stress response is of great importance for forest management and breeding programs. Somatic embryogenesis has been used as a model system to analyze various processes occurring during embryo development, including stress response mechanisms. In addition, "priming" plants with heat stress during somatic embryogenesis seems to favor the acquisition of plant resilience to extreme temperature conditions. In this sense, *Pinus halepensis* somatic embryogenesis was induced under different heat stress treatments (40 ℃ for 4 h, 50 ℃ for 30 min, and 60 ℃ for 5 min) and its effects on the proteome and the relative concentration of soluble sugars, sugar alcohols and amino acids of the embryonal masses obtained were assessed. Heat severely affected the production of proteins, and 27 proteins related to heat stress response were identified; the majority of the proteins with increased amounts in embryonal masses induced at higher temperatures consisted of enzymes involved in the regulation of metabolism (glycolysis, the tricarboxylic acid cycle, amino acid biosynthesis and flavonoids formation), DNA binding, cell division, transcription regulation and the life-cycle of proteins. Finally, significant differences in the concentrations of sucrose and amino acids, such as glutamine, glycine and cysteine, were found.

Keywords: Aleppo pine; conifers; metabolism; proteins; stress-response

2. Introduction

Forest ecosystems present an uncountable environmental and economic value; notwithstanding, breeding forest trees for abiotic stress tolerance by conservative techniques is difficult (Trontin et al. 2016). The efficiency of modern forest management and breeding programs highly depends on our understanding of the mechanisms involved in their adaptation to stress conditions.

Heat stress is frequently defined as a period in which temperatures are substantially high during a sufficient amount of time that causes permanent damage to functions or the correct development of plants (Hemantaranjan et al. 2014). Moreover, heat is usually accompanied by drought and both stresses present overlapping roles (García-Mendiguren et al. 2016b; Jia et al. 2017; Moncaleán et al. 2018). Nonetheless, the stimulation of induced defense and adaptation responses by "priming" plants with stressful temperatures during both zygotic (Johnsen et al. 2005b) and somatic embryogenesis (SE) (Castander-Olarieta et al. 2020b; Pérez-Oliver et al. 2021) seems to favor plants´ resilience to extreme temperature conditions through a "memory" formation.

In this sense, micropropagation of conifers through SE has been widely studied as a promising technique for improving the effectiveness of breeding programs (Hargreaves et al. 2017; Montalbán et al. 2021). This biotechnological tool, which allows the formation of somatic embryos from somatic cells (Von Arnold et al. 2002; von Arnold et al. 2019), brings the opportunity for large-scale propagation of "elite" plants (Park 2002) and is an effective model system to analyze the physiological and biochemical events occurring during embryo induction and development as well as responses to abiotic stresses (Montalbán et al. 2011a; Eliášová et al. 2017; do Nascimento et al. 2021).

In plants, all abiotic stresses induce a cascade of physiological and molecular events that may lead to similar final responses that impact metabolic pathways (alterations in the levels of crucial metabolites, proteins or transcriptions factors) and / or epigenetic memory (Bruce et al. 2007; Crisp et al. 2016). Metabolic memory might appear as a possible consequence of epigenetic regulations and is related to changes in metabolites, enzymes, and proteins that could result in phenotypic changes (Auler et al. 2021).

Since the first results on SE in *Pinus halepensis* achieved in our laboratory (Montalbán et al. 2013b), SE has been used to better understand how this species behaves under abiotic stresses. Initial experiments showed that changes in temperature and water availability in the early stages of the process determine not only the success of its different stages but also the final outcome of the process (Pereira et al. 2016, 2017). Considering those results, extreme temperature treatments, 40 ℃ (4 h), 50 ℃ (30 min), and 60 ℃ (5 min), were applied during the induction of embryonal masses (EMs) to realize if a "priming" effect could be obtained. Those heat stress treatments modulated, again, the efficiency of the process itself, as well as the morphology and endogenous hormonal profiles of the resultant EMs (Pereira et al. 2020) (Chapter I). Then, the effect of the same treatments on the global DNA methylation rates and the differential expression of stress-related genes at EMs and needles from in vitro somatic plants was evaluated: even though no significantly

different levels of DNA methylations were found, small fluctuations were presumably related with the success of different stages of SE and long-lasting variations in the differential expression of stress-related genes were found (Pereira et al. 2021) (Chapter II). The study of stress-responsive genes is crucial for the understanding of plant adaptation (Zang et al. 2021); nevertheless, the characterization of how the expression of those genes is regulated through posttranscriptional and post-translational modifications offers a deeper level of knowledge of the molecular mechanisms governing plant adaptation and stress tolerance (Mazzucotelli et al. 2008; Castander-Olarieta et al. 2021b).

In the present work, in order to complement our understanding of the stress mechanisms triggered by temperature stress during the induction of SE in Aleppo pine, the study of the proteome of EMs produced under the high temperatures referred above was conducted. Proteomics is a powerful tool to determine the identity, abundance and post-translational modifications of proteins in association with stress responses (Juarez-Escobar et al. 2021). The accumulation of heat shock proteins (HSPs) under the control of heat shock transcription factors is known to play a central role in the heat stress response and in acquired thermotolerance in plants (Kotak et al. 2007). Moreover, the mechanism involved in the scavenging of stress, which produces reactive oxygen species (ROS) and can provoke severe cellular damage, primarily involves an enzymatic regulated system (Yadav et al. 2022). In turn, metabolites reflect the integration of gene expression, protein interaction as well as other different regulatory processes, and metabolomics has been widely used as a research tool to elucidate how plants respond to abiotic stress (Arbona et al. 2013; Nakabayashi and Saito 2015). In this sense, we also analyzed the different concentrations of soluble sugars, sugar alcohols and amino acids between induction treatments

3. Material and Methods

SE temperature Experiment and Plant Material Collection

SE induction of *Pinus halepensis* EMs under different temperatures was performed as described in (Pereira et al. 2020) (Chapter I). One-year-old green female cones gathered from Manzanos (Spain; latitude: 42º44´29” N, longitude: 2º52´35” W), and enclosing immature seeds of *P. halepensis* from five open pollinated trees were stored and prepared according to (Montalbán et al. 2012). Whole megagametophytes containing immature embryos were used as initial explants and placed horizontally on modified DCR (Gupta and Durzan 1986) initiation medium supplemented with 30 g L^{-1} sucrose, 3.5 g L^{-1} gellan gum (Gelrite®, Duchefa Biochemie, Amsterdam, Netherlands), a combination of 9.0 µM 2,4-dichlorophenoxyacetic acid and 2.7 µM kinetin and a EDM amino acid mixture (Walter et al. 2005). For temperature treatments, Petri dishes containing initiation medium were preheated for 30 min, and immature megagametophytes were cultured at 40, 50 and 60 ℃ for 4 h, 30 min and 5 min, respectively. As control conditions, 23 ℃ were used and, after the application of the different treatments, all explants were kept at 23 ℃ in darkness.

After nine weeks on the initiation medium, initiation percentages were recorded and proliferating EMs were detached from the megagametophyte and transferred to the proliferation medium. This medium had the same composition to that used in the initiation stage, but a higher gellan gum concentration (4.5 g L^{-1}). EMs were subcultured every two weeks and kept in the dark.

Following 4 proliferation subcultures, fresh tissue from five embryogenic cell lines (ECLs) per treatment were immersed in liquid nitrogen and immediately stored at −80 ℃ until further analysis.

Metabolites, RNA and protein extraction

Metabolites, RNA and protein extraction, from five proliferating EMs (previously selected for maturation) per SE induction treatment, was performed following a modified protocol described by (Valledor et al. 2014).

Two milliliters of cold (4 ℃) metabolite extraction buffer (methanol:chloroform:water 2.5:1:0.5) was added to 500 mg FW of proliferation tissue (liquid nitrogen grinded) and mixed on a vortex. Samples were centrifuged (4700× *g*, 10 min, 4 ℃) and the supernatant, containing metabolites, was transferred to 15 mL falcon tubes that contained 2 mL of phase separation mix (chloroform:water 1:1). Tubes were then centrifuged (4700× *g*, 10 min at room temperature) and two phases were clearly defined with a sharp interface. The upper and lower layers of polar and nonpolar metabolites were transferred to new falcons. These two layers were rewashed with 600 µL of phase separation buffer for a second fractionation and the upper layers, containing polar metabolites, were saved to new tubes and stored at -80 ℃ for further HPLC analysis.

Pellets containing proteins and nucleic acids were washed immediately with 2 mL of 0.75% (*v*/*v*) β-mercaptoethanol in 100% methanol, centrifuged (4700× *g*, 10 min, 4 ℃) (×2) and air-dried. Pellets were dissolved in 1 mL of pellet solubilization buffer (PSB) (7 M guanidine HCl, 2% (*v*/*v*) Tween-20, 4% (*v*/*v*) Triton X - 100, 50 mM Tris, pH 7.5, 1% (*v*/*v*) β-mercaptoethanol) and incubated at 37 ℃ for 30 min. Samples were then centrifuged (4700× *g*, 6 min) and supernatants were transferred to new silica columns to bind DNA (Zymo Research, Irvin, CA, USA). After 1 min of incubation, columns were centrifuged (10,000× *g*, 1 min), and the flowthrough that contained RNA and proteins was immediately mixed with 600 µL of acetonitrile for total RNA extraction. The mix was transferred to a new silica column, incubated for 1 min and centrifuged (10,000× *g*, 1 min). The flowthrough was transferred to a new falcon tube and kept at 4 ℃ until protein isolation. Columns with bound RNA were washed with 750 µL of WB1 (2 mM Tris pH 7.5, 20 mM NaCl, 0.1 mM EDTA, 90% ethanol) and centrifuged (12,000× *g*, 2 min), and 50 µL of DNase I was added to each column and incubated for 15 min at room temperature. After nuclease treatment, the WB1 step was repeated, and then columns were washed with 750 µL of WB2 (2 mM Tris pH 7.5, 20 mM NaCl, 70% ethanol) and centrifuged (12,000× *g*, 2 min). Flowthrough was discarded, and columns were centrifuged again (14,000× *g*, 1 min) to dry the membrane

completely. RNA was eluted from the column in 50 µL of RNase-free water. RNA samples were kept at -80 ℃ until further analysis.

Proteins were purified from the flowthrough using phenolic extraction: 1100 µL phenol (Tris-buffered, pH 8) and 1200 µL of water were added to each falcon. Samples were mixed on a vortex for 2 min and then centrifuged (4700× *g*, 8 min, room temperature). The supernatant, containing the phenolic phase, was transferred to a new falcon that contained 1200 µL of PWB (0.7 M sucrose, 50 mM Tris–HCl pH 7.5, 50 mM EDTA, 0.5% β-mercaptoethanol, 0.5% (*v*/*v*) Plant Protease Inhibitor Cocktail) and mixed thoroughly by vortex. After centrifugation (4700× *g*, 8 min, room temperature), upper phenolic phase was transferred to a new falcon, and proteins were precipitated by adding 3 mL of 0.1 M ammonium acetate and 0.5% β-mercaptoethanol in methanol in an overnight incubation at -20 ℃. Samples were then centrifuged (4700× *g*, 20 min, 4 ℃), and protein pellets were washed with acetone in an ultrasound bath until complete disaggregation of the pellet. Proteins were precipitated by centrifugation (4700× *g* for 20 min at 4 ℃), and acetone was removed (2×). Protein pellets were allowed to air dry and resuspended in 80 µL of elution buffer (7M urea, 2M thiourea, 2% (*w*/*v*) CHAPS, 1% (*w*/*v*) DTT). Protein samples were stored at -20 ℃ until further analysis.

Protein LC-MS analysis

Protein extracts (70 µL) were precipitated with 4 volumes of cold acetone (280 µL) for 30 minutes at -80 ℃. Samples were centrifuged (20,000× *g*, 4 ℃, 20 min) and the pellet was resuspended in 50 µL of 1× Laemmli Sample Buffer. The total protein concentration was measured for each sample using the Pierce 660 nm Protein Assay kit (Thermo Scientific™, Waltham, MA, USA). For data-dependent acquisition (DDA) experiments, replicates from each condition were pooled into four different samples (Cond1: 23 ℃, Cond2: 40 ℃ for 4h, Cond3: 50 ℃ for 30 min, and Cond4: 60 ℃ for 5 min) to create a library for each condition before sample processing, and for data-independent acquisition (DIA), each sample was processed individually for quantification purposes, as described by Anjo et al. (2015). Protein content from each sample, adjusted based on the protein quantification values obtained previously, was separated by SDS-PAGE for about 17 minutes at 110 V (Short-GeLC Approach) and stained with Coomassie Brilliant Blue G-250. For DDA experiments, each lane was divided into 5 gel pieces, in order to increase the depth of the analysis and to acquire more fragmentation spectra to correlate with the database, and, for DIA experiments, they were divided into 3 gel pieces for further individual processing. After the discoloration step with a 50 mM ammonium bicarbonate and 30 % acetonitrile solution, gel bands were incubated overnight with trypsin for protein digestion and peptides were extracted from the gel using 3 solutions containing different percentages of acetonitrile (30, 50, and 98 %) with 1% formic acid. The organic solvent was evaporated using a vacuum-concentrator and peptides were re-suspended in 30 µL of a solution containing 2 % acetonitrile and 0.1 % formic acid. Each sample was sonicated using a cup-horn (Ultrasonic processor, 750W) for about 2 min, 40 % amplitude, and

pulses of 1 sec ON/OFF. Ten microliters of each sample were analyzed by LC-MS/MS, either for DIA or DDA experiments.

Samples were analyzed on a NanoLC™ 425 System (Eksigent, Framingham, MA, USA) coupled to a Triple TOF™ 6600 mass spectrometer (Sciex, Framingham, MA, USA). The ionization source was the OptiFlow® Turbo V Ion Source equipped with the SteadySpray™ Low Micro Electrode (1-10 µL). The chromatographic separation was performed on a Triart C18 Capillary Column 1/32" (12 nm, S-3 µm, 150 x 0.3 mm, YMC) and using a Triart C18 Capillary Guard Column (0.5 × 5 mm, 3 µm, 12 nm, YMC) at 50 °C. The flow rate was set to 5 µl min^{-1} and mobile phases A and B were 5% DMSO plus 0.1 % formic acid in water and 5% DMSO plus 0.1 % formic acid in acetonitrile, respectively. The LC program was performed as follows: 5-35 % of B (0-40 min), 35-90 % of B (40-41 min), 90 % of B (41-45 min), 90-5 % of B (45-46 min), and 5 % of B (46-50 min). The ionization source was operated in the positive mode set to an ion spray voltage of 4500 V, 10 psi for nebulizer gas 1 (GS1), 15 psi for nebulizer gas 2 (GS2), 25 psi for the curtain gas (CUR), and source temperature (TEM) at 100 °C. For DDA experiments, the mass spectrometer was set to scanning full spectra (m/z 350-1250) for 250 ms, followed by up to 100 MS/MS scans (m/z 100-1500). Candidate ions with a charge state between +1 and +5 and counts above a minimum threshold of 10 counts per second were isolated for fragmentation and one MS/MS spectrum was collected before adding those ions to the exclusion list for 15 seconds (mass spectrometer operated by Analyst® TF 1.7, Sciex®). The rolling collision was used with a collision energy spread of 5. For SWATH experiments, the mass spectrometer was operated in a looped product ion mode and specifically tuned to a set of 90 overlapping windows, covering the precursor mass range of 350-1250 m/z. A 50 ms survey scan (350-1250 m/z) was acquired at the beginning of each cycle, and SWATH-MS/MS spectra were collected from 100-1800 m/z for 35 ms resulting in a cycle time of 3.2 s.

Relative expression of stress-related transcripts

RNA quality and concentration were assessed using a spectrophotometer (NanoDrop™, Thermo Scientific, Waltham, Massachusetts, USA) and samples with good quantity and integrity criteria were used for cDNA synthesis. An equal RNA quantity (1000 ng/sample) was reverse transcribed into cDNA, using NZY First-Strand cDNA Synthesis kit according to the instructions provided by the manufacturer. Three biological replicates were obtained for each treatment, e.g., cycle of temperature. Primer pairs were designed for transcripts of nine proteins previously identified as differentially accumulated between treatments, using the available NCBI Primer Design Tool, (amplicon length < 200 bp) and its specificity was validated through the amplification of a PCR product of the predicted size, using NZYTaq II 2x Green Master Mix kit, and visualization in a 1.5 % (w/v) agarose gel electrophoresis. The melting curves evaluation corroborated the primer specificity as well.

Quantitative reverse transcription PCR (RT-qPCR) amplifications were performed in 96-well plates and in a CFX Connect™ Real-Time System (Bio-Rad, Kaki Bukit, Republic of Singapore). PCR conditions were conducted under an initial denaturation at 95 °C for 2 min and 40 cycles of 5

s at 95 °C and 25 s at 55 °C. All the reactions were evaluated with two technical replicates and non-template controls were incorporated as well. Analyzed transcripts as well as primer pairs details are summarized in Table 13. The relative transcript levels were normalized using *ACTIN* and α-*TUBULIN*, and the relative expression of each gene (R) was calculated on the basis of ΔCt values using the following formula: $R = 2^{-\Delta Ct}$ (Livak and Schmittgen 2001). Finally, the fold changes between expression values obtained at the control treatment (23 ℃) and different temperature treatments were calculated on logarithmic scale.

Table 13. List of primers used in quantitative reverse transcription PCR (RT-qPCR) for relative expression analysis. Name of transcript, accession number of the correspondent transcript, forward and reverse primer sequences, product length and melting temperatures of primers are described.

Name	Forward (5' → 3')	Reverse (5' → 3')	Product Lenght	Tm (℃)
ACTIN (ACT)	CACTGCACTTGCTCCCAGTA	AACCTCCGATCCAAACACTG	130	56
α-TUBULIN	ATCTGGAGCCGATGTCA	TGATAAGCTGTTAGGATGGAA	75	55
PYRUVATE DEHYDROGENASE E1 COMPONENT SUBUNIT BETA-4	TGCGCATGTACCAGGATTGA	AACTTCCGCAGAAACAGGGA	151	57
CHAPERONIN CPN60 (CPN60)	CAAACAGGTTGCTAACCGCC	TTGCATTCATTCCAGCAGCG	128	57
NADPH--CYTOCHROME P450 REDUCTASE 1(ATR1)	GAGCCTACTGACAATGCTGCC	GGCGATTACCAAGAGCAAACAC	109	58
TRIFUNTIONAL UDP-GLUCOSE 4,6-DEHYDRATASE	TATCGCTAGTGCTGACTTGGT	CCGAAGGAATTGTCGACGTC	99	56
PYRUVATE DEHYDROGENASE E1 COMPONENT SUBUNIT BETA-1	CATAAGGAGCGAGAACCCCG	CGCGAGTATGTGAGGATGGT	150	57
6-PHOSPHOGLUCONATE DEHYDROGENASE DECARBOXYLATING 1 (G6PGH1)	ATGGGAGTTTCGGGTGGAGA	AAGCAACACACGGTCCACTAT	142	58
20 kDa CHAPERONIN (CPN20)	AACAGCTGGAGGGTTGTTGTT	CCTTCCTCGTCTAGGGAACC	96	57
PROBABLE FRUCTOKINASE-7	CTGACCGGTGGTGATGATCC	TCTCCTGCACCGGTTGTATC	179	57
CITRATE SYNTHASE (PDHB)	TGGACATGGTGTTCTGCGTAA	ACCCCACTATGGGCATCAAC	186	57

Quantification of sugars and sugars alcohols

For sugars (sucrose, glucose, fructose and raffinose) and sugar alcohols (mannitol and sorbitol) quantification, 500 µL of the obtained polar metabolites were totally dried on a Speedvac and pellets were re-suspended in 100 µL ultrapure water. Sugars were analyzed by HPLC using an Agilent 1260 Infinity II coupled to a refractive index detector (RID) (Agilent Technologies, Santa Clara, USA). A Hi-Plex Ca column (7.7 x 300 mm, 8 µm) was used for sugar and sugar alcohols separation. The mobile phase was ultrapure water and the samples were injected in the column at a flow rate of 0.2 mL min^{-1} at 80 °C for 40 min. Sugar concentrations were determined from internal calibration curves constructed with the corresponding commercial standards. Concentrations obtained from the HPLC analysis (g L^{-1}) were conveniently adjusted, taking into account the initial concentration step (5 times), to express the results as µmol g FW^{-1}.

Quantification of amino acids

For amino acids quantification, 500 µL of the obtained polar metabolites were totally dried on a Speedvac and pellets were resuspended in 250 µL ultrapure water. Amino acid analysis was performed by HPLC using an Agilent 1260 Infinity II coupled to a fluorescence detector (FLD) (Agilent Technologies). An AdvancedBio Amino Acid Analysis (AAA) column, 100 mm, 2.7 µm Superficially Porous Particle (SPP), was used for separation of 21 amino acids. The mobile phase A was 10mM Na_2HPO_4 + 10mM $Na_2B_4O_7$, pH 8.2, and the mobile phase B was acetonitrile:methanol:water (45:45:10). The gradient program was the following: min 0-13.40, solvent A 98 % and solvent B 2 %, min 13.40–13.50, solvent A 43 % and solvent B 57 %, min 13.50–15.80, solvent B 100 %, and min 15.80–18, solvent A 98 % and solvent B 2 %. The primary amino acids: aspartic acid, glutamic acid, asparagine, serine, glutamine, histidine, glycine, threonine, arginine, alanine, tyrosine, cysteine, valine, methionine, tryptophan, phenylalanine, isoleucine, leucine and lysine were derivatized with OPA and monitored at 338nm. Hydroxyproline and proline were derivatized with FMOC and monitored at 262 nm. 1 µL of sample was injected in the column at a flow rate of 1.5 mL min^{-1} for 18 min. Amino acid concentrations were determined from internal calibration curves constructed with the corresponding commercial standards. Concentrations obtained from the HPLC analysis (pmol $µl^{-1}$) were conveniently adjusted, taking into account the initial concentration step (2 times), to express the results as µmol g FW^{-1}.

Data analysis

Ion-Library construction (DDA information)

A specific ion-library of the precursor masses and fragment ions was created by combining all files from the DDA experiments in one protein identification search using the ProteinPilot™ software (v5.0, Sciex®). The paragon method parameters were the following: searched against the reviewed Viridiplantae database (Swissprot) downloaded on 1st April from UniProtKB (The UniProt Consortium, 2019), cysteine alkylation by acrylamide, digestion by trypsin, and gel-based ID. An independent False Discovery Rate (FDR) analysis, using the target-decoy approach provided by Protein Pilot™, was used to assess the quality of identifications.

Relative quantification of proteins (SWATH-MS)

SWATH data processing was performed using the SWATH™ processing plug-in for PeakView™ (v2.0.01, Sciex®). Protein relative quantification was performed in all samples using the information from the protein identification search. Quantification results were obtained for peptides with less than 1% of FDR and by the sum of up to 5 fragments/peptides. Each peptide was normalized for the total sum of areas for the respective sample. Protein relative quantities were obtained by the sum of the normalized values for up to 15 peptides/protein. A correlation analysis between samples was performed using the Spearman Rank Correlation method and considering the relative quantification values determined for all the samples to ensure that those from the same condition showed the same behavior.

Statistical analysis

A one-way analysis of variance was carried out to assess the effect of different induction treatments at concentrations of sugars, sugar alcohols, stress-related transcripts expression, and amino acids. An ANOVA was made after confirmation of the homogeneity of variances and normality of the samples. Whenever the analysis of variance did not fulfill the normality hypothesis, the corresponding non-parametric test, Kruskal–Wallis test, was applied. When significant differences were found ($p < 0.05$), the Tukey HSD post hoc test or Dunn's multiple comparison test, respectively, were conducted to determine which treatments were statistically different.

Two different approaches were employed to analyze the proteins´ results, combining multivariate and univariate analyses. First, a partial least square-discriminant analysis (PLS-DA) using the MetaboAnalyst web-based platform (Pang et al. 2020) was performed to find out the separation between the four conditions and simultaneously identify the most significant top protein features able to classify the four groups based on variable influence on projections (VIP) values. Those proteins were then clustered based on their biological function according to FunRich and the Plants database from UniProt database. A correlation analysis between samples was performed showing that sample #04 is less correlated with the others of the same group. Nonetheless, the statistical analysis was performed including that sample. For the univariate analysis, as cross validation, a Kruskal-Wallis test was performed to select the proteins which were statistically different between the 4 conditions. Dunn's test of Multiple Comparisons, with Benjamini-Hochberg *p*-value adjustment, was performed to determine which statistical differences were observed. Finally, the 27 proteins overlapping on both approaches were selected and a cluster analysis was performed. The MetaboAnalyst web-based platform was used in order to investigate their relation and relative abundance by generating heatmap and correlation matrix plots. The Euclidean distance and the Complete algorithm were used for the heatmap hierarchical clustering, whereas for the correlation matrix, the Pearson's correlation test was applied.

4. Results

Relative quantification of proteins

The search performed against the 4256 protein sequences reviewed at the *Viridiplantae* database allowed the identification of 1315 proteins, and relative protein quantification was attained for 858 proteins. The primary application of PLS-DA multivariate analysis of these 858 proteins allowed for the reduction of the complexity of the results and for the sample groups' visualization. As shown in Figure 13a, the differences between the four induction treatments, analyzed by the bi-dimensional representation of their score's plots, did not completely separate the loading plots. Nevertheless, it appears that the first component of PLS-DA pairwise comparison models assembled the variability related to heat stress response; as the induction temperature applied increased, so did the corresponding values along this component. The complexity of the results obtained at the second component may be associated with the variability between samples.

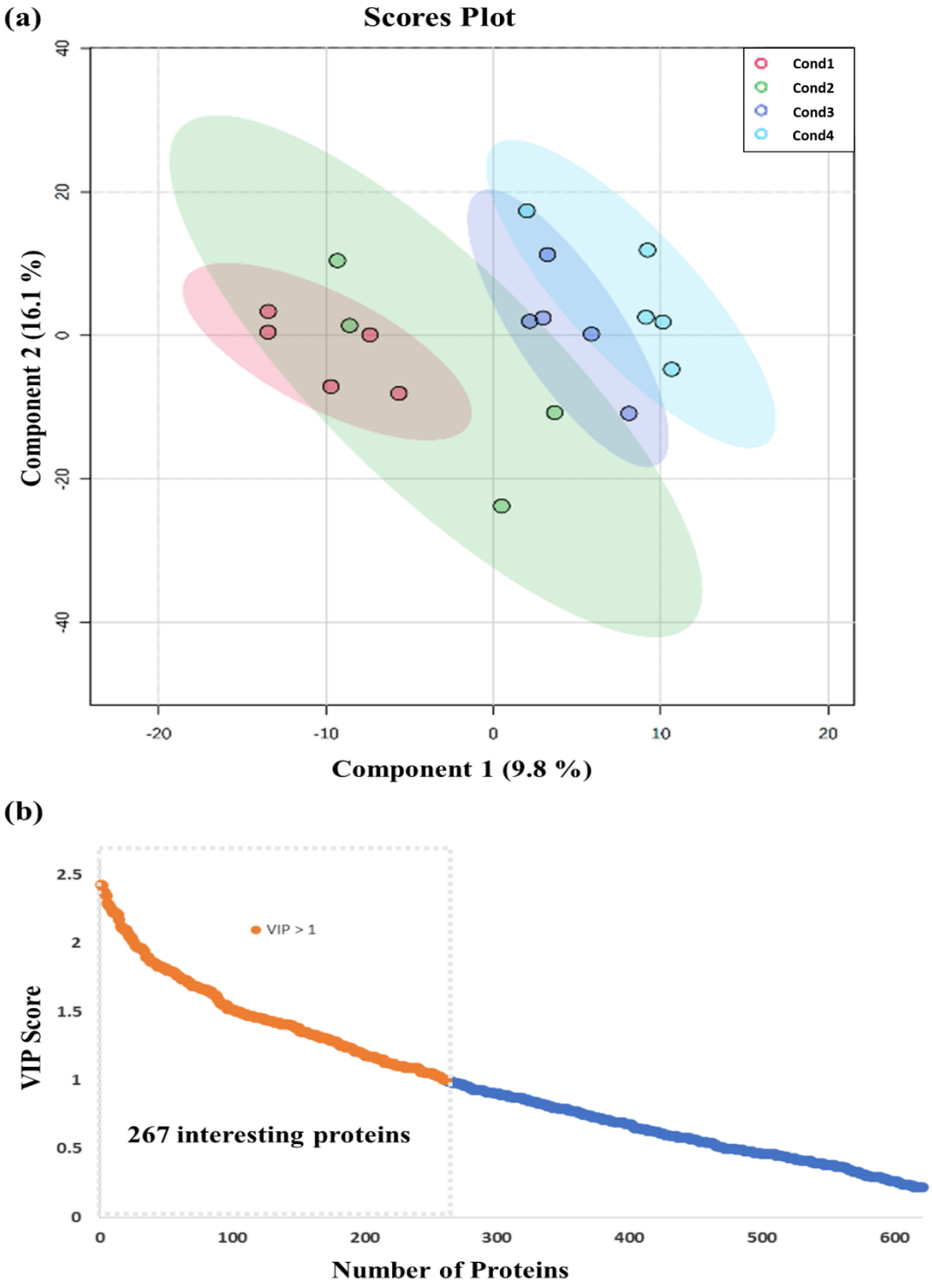

Figure 13. PLS-DA multivariate analysis of the detected 858 proteins from embryonal masses induced under four different temperature treatments (Cond1: 23 ℃; Cond2: 40 ℃ (4 h); Cond3: 50 ℃ (30 min); Cond4: 60 ℃ (5 min)): **(a)** bi-dimensional representation of the scores. Data normalization was performed using the AutoScale method, and the scores of the two first components are represented, showing the ovals at 95% confidence interval; **(b)** variable importance in projection (VIP) scores. From the 858 quantified proteins, 267 were selected as interesting variables for the group separation observed in the scores plot. A cut-off of 1 was considered to select the important variables.

At the same time, this multivariate analysis allowed for the identification of the most significant proteins able to classify the four conditions based on the variable influence on projections (VIP) values (Figure 13b). A cut-off of 1 was defined to select the important variables, considered the best classifiers for the group separation observed in the scores plot of the four conditions. In this sense, 267 proteins were selected and considered the ones to be involved in heat stress responses.

As a preliminary step to interpret the data and to categorize these proteins, a gene ontology (GO) enrichment analysis was performed using FunRich and the Plants database from UniProt database. It allowed us to extract information about the cellular components in which these 267 proteins are associated (Figure 14a), as well as the molecular functions (Figure 14b) and the biological processes (Figure 14c) that they are involved in. Cytosol (32.5%), cytoplasm (26.4%) and mitochondrial (15.5%) proteins were the ones with the highest representation concerning cellular location (Figure 14a). Regarding their molecular function, two functional major groups appeared: proteins involved in metabolism (ATP binding, endopeptidase activity, threonine-type endopeptidase activity, phosphoglocunate (decarboxylating) activity and fructose-bisphosphate aldolase activity) that account for 30.2%, and signaling involved proteins (GTP binding, GTPase activity and mRNA binding) that accounted for 18% (Figure 14b). Finally, concerning the biological processes, response to cadmium ion (7.2%), proteasome-mediated ubiquitin-dependent protein catabolic process (4.2%), the tricarboxylic acid cycle (3.8 %) and the glycolytic process (3.8 %) presented the highest representativeness.

The parallel univariate analysis performed with the Kruskal-Wallis test identified 34 proteins with significant differences ($p < 0.05$) between the four induction treatments (Supplementary Table 1). These results, in combination with the ones previously obtained by PLS-DA analysis, allowed the identification of the 27 proteins with higher interest concerning heat stress response (Figure 15). The detailed list of these proteins, including their accession number, identified species, the fold-change obtained between conditions, and the results from both statistical analyses, are presented in Table 14.

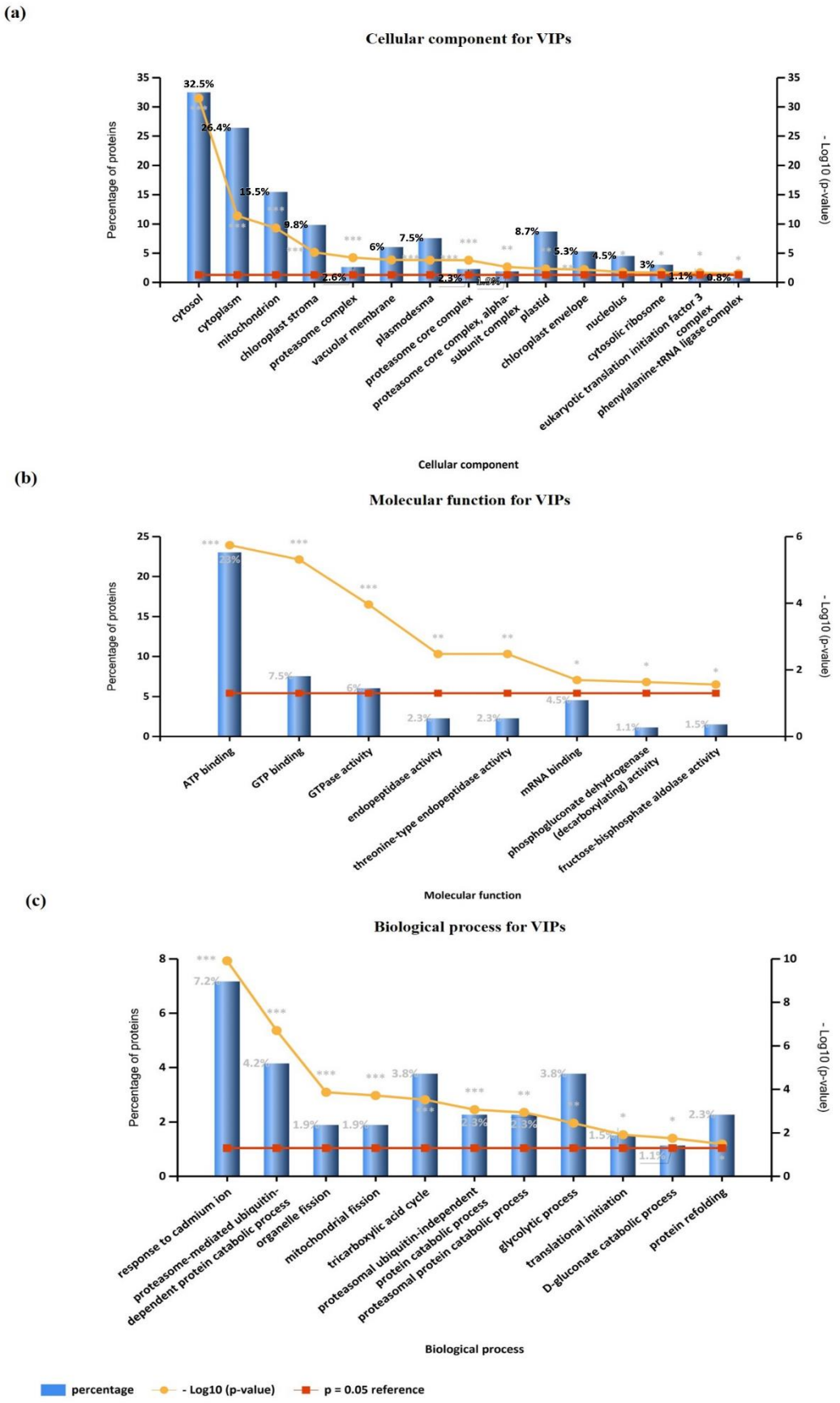

Figure 14. Gene ontology enrichment analysis of the 267 VIP proteins, selected by PLS-DA analysis, performed using FunRich and the Plants database from UniProt database: **(a)** cellular component; **(b)** molecular function and **(c)** biological process. *: $p < 0.05$; **: $p < 0.01$; ***: $p < 0.001$.

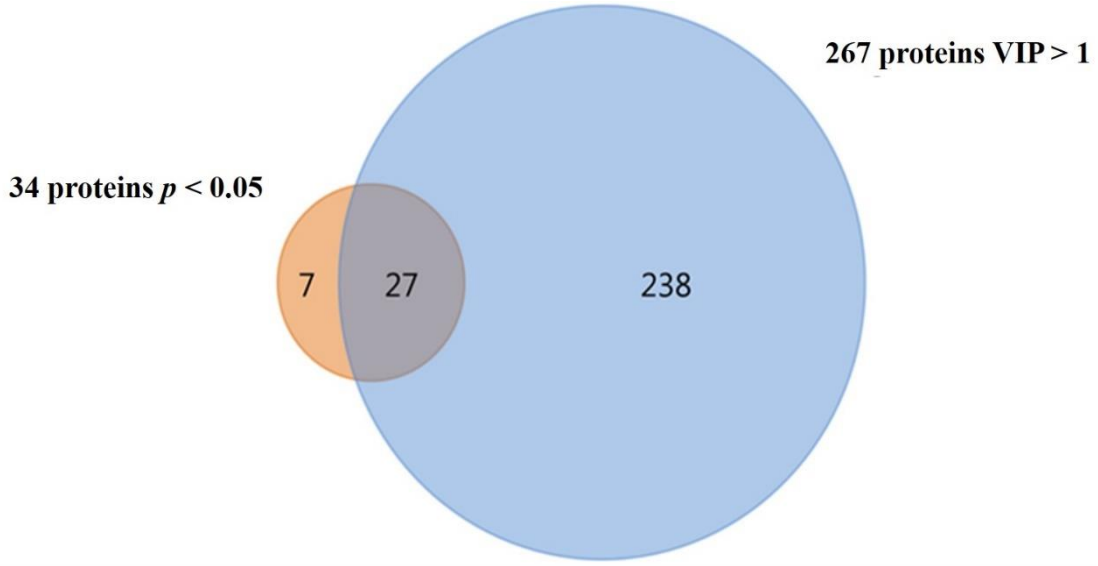

Figure 15. Venn-diagram showing that 27 proteins were common between the significant proteins from the univariate analysis (Kruskal-Wallis, $p < 0.05$) and the multivariate analysis (PLS-DA, VIP >1).

Table 14. Details of the twenty-seven proteins with higher interest, selected from the combination of the multivariate (PLS-DA) and the univariate statistical analysis (Kruskal–Wallis), detected in *P. halepensis* EMs induced under different temperatures treatments: Cond1: 23 ℃; Cond2: 40 ℃ (4 h); Cond3: 50 ℃ (30 min); Cond4: 60 ℃ 5 (min).

Protein	**Uniprot Accession**	**Species**	Fold change			Kruskal-Wallis	PLS-DA
			Cond2 / Cond1	**Cond3 / Cond1**	**Cond4 / Cond1**	***p* - value**	**VIP**
NADP-dependent malic enzyme 3	Q9XGZ0	*Arabidopsis thaliana*	2.25	0.96	0.44	0.006	1.26
20 kDa chaperonin, chloroplastic	O65282	*Arabidopsis thaliana*	0.08	0.16	0.13	0.018	2.08
Alcohol dehydrogenase	P17648	*Fragaria ananassa*	0.79	0.34	0.21	0.041	2.00
Polyadenylate-binding protein RBP47	Q9LEB3	*Nicotiana plumbaginifolia*	0.47	0.49	0.67	0.015	1.45
Aconitate hydratase, cytoplasmic	P49608	*Cucurbita maxima*	0.39	0.26	0.51	0.006	2.30
Probable fructokinase-7	Q9FLH8	*Arabidopsis thaliana*	0.30	0.20	0.23	0.024	2.74
Agglutinin	P06750	*Ricinus communis*	0.23	0.22	0.18	0.011	2.80
25.3 kDa vesicle transport protein	Q94AU2	*Arabidopsis thaliana*	0.44	0.20	0.20	0.036	2.59
Protein kinase G11A	Q0DCT8	*Oryza sativa* subsp. *japonica*	0.38	0.17	0.15	0.014	3.05
Molybdenum cofactor sulfurase	Q8LGM7	*Solanum lycopersicum*	0.16	0.11	0.13	0.016	2.65

Table 14 cont.

Chaperonin CPN60, mitochondrial	P35480	*Brassica napus*	2.84	2.13	2.01	0.025	1.08
Pyruvate dehydrogenase E1 component subunit beta-1, mitochondrial	Q6Z1G7	*Oryza sativa* subsp. *japonica*	1.21	1.18	1.28	0.034	2.47
Chalcone synthase	P30079	*Pinus sylvestris*	2.02	1.60	3.19	0.031	1.95
Glutamyl-tRNA(Gln) amidotransferase subunit B, chloroplastic/mitochondrial	Q2R2Z0	*Oryza sativa* subsp. *japonica*	1.18	1.64	1.79	0.036	2.14
Dynamin-related protein 12A	Q39821	*Glycine max*	2.55	3.92	3.58	0.023	2.02
Citrate synthase, mitochondrial	O80433	*Daucus carota*	1.12	1.55	2.39	0.0040	3.08
6-phosphogluconate dehydrogenase, decarboxylating 1	Q9LI00	*Oryza sativa* subsp. *japonica*	1.00	1.17	1.28	0.026	2.71
Carbamoyl-phosphate synthase large chain, chloroplastic	B9EXM2	*Oryza sativa* subsp. *japonica*	1.02	1.18	1.29	0.042	2.57
Pyruvate dehydrogenase E1 component subunit beta-4, chloroplastic	Q10G39	*Oryza sativa* subsp. *japonica*	0.80	1.48	1.63	0.025	2.13
3-isopropylmalate dehydrogenase, chloroplastic	P29696	*Solanum tuberosum*	0.82	1.32	1.46	0.038	2.35
Trifunctional UDP-glucose 4.6-dehydratase/UDP-4-keto-6-deoxy-D-glucose 3.5-epimerase/UDP-4-keto-L-rhamnose-reductase RHM1	Q9SYM5	*Arabidopsis thaliana*	0.68	1.49	1.60	0.009	2.39
NADPH--cytochrome P450 reductase 1	Q9SB48	*Arabidopsis thaliana*	1.07	1.58	1.34	0.019	1.79
Actin-depolymerizing factor 10	Q9LQ81	*Arabidopsis thaliana*	1.24	1.53	1.56	0.017	3.03
Histone H2A.2.2	P02277	*Triticum aestivum*	2.34	4.10	4.50	0.023	2.53
40S ribosomal protein S15a-1	P42798	*Arabidopsis thaliana*	0.59	1.26	1.26	0.018	1.62
60S ribosomal protein L18-3	Q940B0	*Arabidopsis thaliana*	0.96	1.35	1.25	0.028	2.08
Histone H4 variant TH091	P62786	*Triticum aestivum*	0.78	1.50	1.50	0.023	2.15

Finally, a hierarchical clustering heatmap (Figure 16) was generated to better visualize the differences between treatments regarding the top 27 proteins´ relative accumulation. Two main groups were clearly defined. The first main group corresponds to proteins with decreased amounts at samples induced under higher temperatures relative to the control (condition 1). Within this main group, different patterns were found (Table 14, Figure 16). Thus, polyadenylate-binding protein RBP47 (a protein involved in RNA binding and its aggregation in the cytoplasm) and aconitate hydratase (involved at the biosynthesis of carbohydrates) presented significantly decreased

amounts in samples from 40 ℃ (4 h) (condition 2) and 50 ℃ (30 min) (condition 3). On the other hand, it was found that a 25.3 kDa vesicle transport protein, protein kinase G11A and molybdenum cofactor sulfurase, three proteins with catalytic activity enrolled in metabolism regulation and signal transduction processes, had significantly decreased amounts in samples from 50 ℃ (30 min) and 60℃ (5 min) (condition 4). It should also be noted that the amounts of 20 kDa chaperonin, probable fructokinase-7, and agglutinin were decreased at all heat-stress treatments applied.

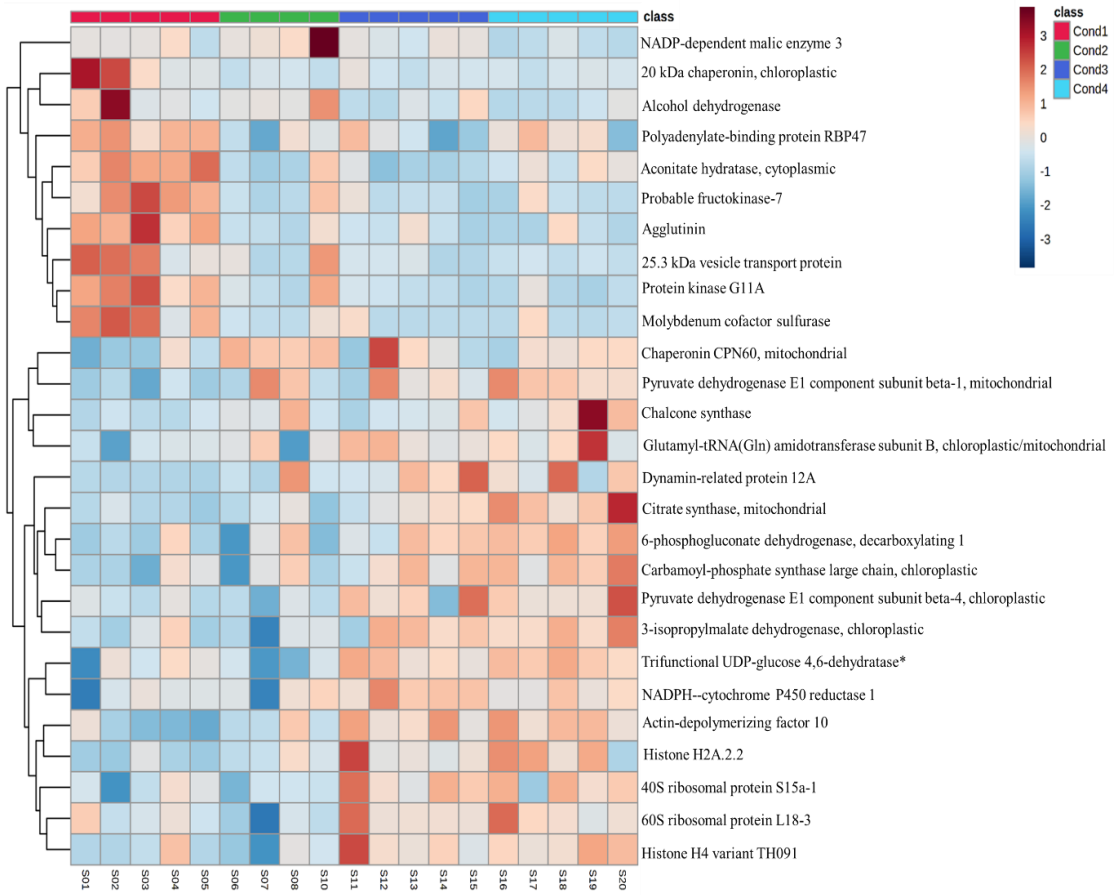

Figure 16. Hierarchical clustering heatmap using the 27 proteins selected, with the combination of univariate and multivariate analysis, from EMs induced under four different temperatures treatments (Cond1: 23 ℃; Cond2: 40 ℃ (4 h); Cond3: 50 ℃ (30 min); Cond4: 60 ℃ 5 (min)). S01-S20: sample1 to tample20. Hierarchical clustering was performed only at the protein (rows) level using Euclidean distance and Complete for the clustering algorithm. *: Trifunctional UDP-glucose 4.6-dehydratase/UDP-4-keto-6-deoxy-D-glucose 3.5-epimerase/UDP-4-keto-L-rhamnose-reductase RHM1

The second main group gathers the proteins with increased amounts at samples from heat-stress treatments. Apart from the heat-shock protein chaperonin CPN60, which presented the highest fold change between 40 ℃ (4 h) and the control (Table 14), proteins presented higher concentrations at 50 ℃ (30 min) and 60 ℃ (5 min). It seems important to mention that the majority of the proteins with increased amounts at samples induced at higher temperatures include enzymes directly involved at the regulation of metabolism: a high number of proteins with increased concentrations under heat stress conditions implicated at glycolysis and the tricarboxylic acid cycle (pyruvate dehydrogenase E1 component subunit beta-4, citrate synthase, pyruvate dehydrogenase

E1 component subunit beta-1, trifunctional UDP-glucose 4.6-dehydratase/UDP-4-keto-6-deoxy-D-glucose 3.5-epimerase/UDP-4-keto-L-rhamnose-reductase RHM1, 6-phosphogluconate dehydrogenase decarboxylating 1), a membrane-bound enzyme required for electron transfer from NADPH to cytochrome P450 (NADPH-cytochrome P450 reductase 1), as well as amino acid biosynthesis (3-isopropylmalate dehydrogenase, carbamoyl-phosphate synthase large chain) and flavonoids formation (chalcone synthase), were identified. Also, proteins involved in DNA binding and cellular division (dynamin-related protein 12A, actin-depolymerizing factor 10), transcription regulation (histone H4 variant TH091, histone H2A.2.2) and the life-cycle of proteins, such as those directly related with nuclear (40S ribosomal protein S15a-1, 60S ribosomal protein L18-3) and mitochondrial (glutamyl-tRNA (Gln) amidotransferase subunit B) translation were present in this group. NADP-dependent malic enzyme 3 and alcohol dehydrogenase presented significantly lower amounts at 60 ℃ (5 min) compared to 40 ℃ (4 h).

Relative expression of stress-related transcripts

Nine top proteins were selected, and the primers for their respective transcripts were designed. Afterwards, the relative expression patterns of the selected stress-related transcripts with respect to the control (23 °C) for the different induction temperature treatments were quantified using an RT-qPCR approach.

The stress-related transcripts analyzed did not present statistically significant differences between treatments (Figure 17, Supplementary Table 2). Nonetheless, *20 kDa CHAPERONIN (CPN20)*, *CHAPERONIN CPN60 (CPN60)*, *CITRATE SYNTHASE (PDHB)*, *PYRUVATE DEHYDROGENASE E1 COMPONENT SUBUNIT BETA-1* and *6-PHOSPHOGLUCONATE DEHYDROGENASE, DECARBOXYLATING 1 (G6PGH1)* presented a similar expression pattern: a lower expression in samples from 40 ℃ (4h), a higher expression in samples from 60℃ (5 min), and a similar response in samples from 50 ℃ (30 min) when compared to the control (23 ℃). In its turn, regarding the expression patterns of *PYRUVATE DEHYDROGENASE E1 COMPONENT SUBUNIT BETA-4*, *TRIFUNCTIONAL UDP-GLUCOSE A,6-DEHYDRATASE/UDP-4-KETO-6DEOXY-D-GLUCOSE 3,5-EPIMERASE/UDP-4-KETO-L-RHAMNOSE-REDUCTASE RHM1 (RHM1)*, *NADPH-CYTOCHROME P450 REDUCTASE 1 (ATR1)* and *PROBABLE FRUCTOKINASE-7*, samples generally presented lower expression in samples from high temperatures relative to the control samples.

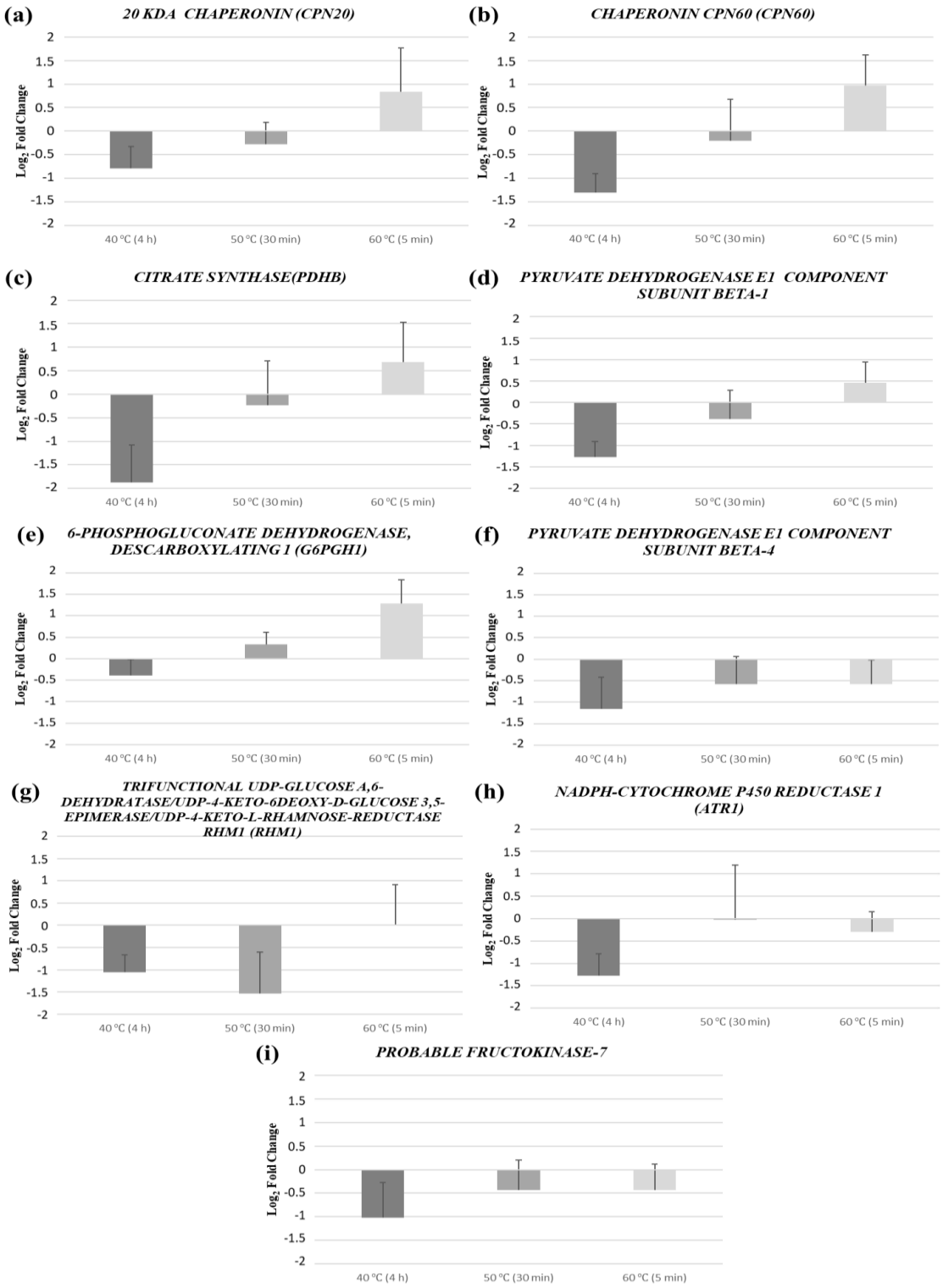

Figure 17. Relative expression fold change, with respect to the control (23 °C), of the nine transcripts from *P. halepensis* EMs induced under different temperature treatments (40 °C (4 h), 50 °C (30 min) and 60 °C (5 min)) **(a)** *20 KDA CHAPERONIN (CPN20)*; **(b)** *CHAPERONIN CPN60 (CPN60)*; **(c)** *CITRATE SYNTHASE (PDHB)*; **(d)** *PYRUVATE DEHYDROGENASE E1 COMPONENT SUBUNIT BETA-1*; **(e)** *6-PHOSPHOGLUCONATE DEHYDROGENASE, DECARBOXYLATING 1 (G6PGH1)*; **(f)** *PYRUVATE DEHYDROGENASE E1 COMPONENT SUBUNIT BETA-4*; **(g)** *TRIFUNCTIONAL UDP-GLUCOSE A,6-DEHYDRATASE/UDP-4-KETO-6DEOXY-D-GLUCOSE 3,5-EPIMERASE/UDP-4-KETO-L-RHAMNOSE-REDUCTASE RHM1 (RHM1)*; **(h)** *NADPH-CYTOCHROME P450 REDUCTASE 1 (ATR1);* **(i)** *PROBABLE FRUCTOKINASE-7*. Data are presented as mean values + SE.

Quantification analysis of sugars and sugars alcohols

All sugars (sucrose, glucose, fructose, raffinose) and sugar alcohols (mannitol and sorbitol) analyzed were detected at EMs from different induction treatments. Nonetheless, raffinose was only detected in half of the analyzed samples, and no statistical analysis was performed regarding this data.

Significant differences between treatments were only found for sucrose concentrations (Supplementary Table 3). Samples from the control (23 ℃) presented a significantly higher concentration of sucrose when compared to samples from 50 ℃ (30 min), with the other two treatments presenting an intermediate response (Table 15). The same pattern was found for glucose, the sugar that presented the highest concentration levels, despite the fact that no significant differences were found. Respecting the concentrations of fructose, mannitol and sorbitol, each presented different individual responses without substantial differences (Table 15).

Table 15. Concentration of sugars (µmol g^{-1} FW) detected in *P. halepensis* EMs, collected at proliferation phase, induced under different temperatures.

Sugars (µmol g $^{-1}$ FW)	**Cond1 23 ℃**	**Cond2 40 ℃ (4 h)**	**Cond3 50 ℃ (30 min)**	**Cond4 60 ℃ (5 min)**
Sucrose	5.39 ± 0.75 ^{a}	3.35 ± 0.94 ^{ab}	2.26 ± 0.53 ^{b}	2.77 ± 0.55 ^{ab}
Glucose	40.90 ± 1.86 ^{a}	40.81 ± 4.29 ^{a}	32.24 ± 5.68 ^{a}	35.28 ± 2.71 ^{a}
Fructose	24.48 ± 1.11 ^{a}	29.53 ± 2.60 ^{a}	21.21 ± 4.52 ^{a}	21.57 ± 1.69 ^{a}
Mannitol	0.18 ± 0.06 ^{a}	0.32 ± 0.10 ^{a}	0.34 ± 0.06 ^{a}	0.41 ± 0.14 ^{a}
Sorbitol	0.14 ± 0.04 ^{a}	0.16 ± 0.06 ^{a}	0.13 ± 0.04 ^{a}	0.13 ± 0.03 ^{a}

Data are presented as mean values ± SE. Significant differences at $p < 0.05$ within a line are indicated by different letters.

Quantification analysis of amino acids

Except for hydroxyproline, all other amino acids under study were detected in EMs from different induction treatments. The amino acids that presented higher concentrations were alanine and asparagine, but no significant differences were detected. In fact, statistically, significant differences between treatments were only found for the concentrations of glutamine, glycine and cysteine (Supplementary Table 4). Glutamine presented a significantly higher concentration in samples from 40 ℃ (4 h) compared to samples from the control (23 ℃) and 50 ℃ (30 min). In turn, glycine and cysteine presented a significantly higher concentration at samples from the control (23 ℃) when compared to samples from 50 ℃ (30 min) (Table 16). As previously observed for the concentrations of sugars, different amino acids presented individual patterns as result of the induction treatments applied (Table 16).

Table 16. Concentration of amino acids (µmol g^{-1} FW) detected in *P. halepensis* EMs, collected at proliferation phase, induced under different temperatures.

Amino acids (µmol g^{-1} FW)	Cond1 23 ºC	Cond2 40 ºC (4 h)	Cond3 50 ºC (30 min)	Cond4 60 ºC (5 min)
Aspartic acid	0.135 ± 0.004 [a]	0.126 ± 0.019 [a]	0.109 ± 0.026 [a]	0.137 ± 0.019 [a]
Glutamic acid	0.428 ± 0.011 [a]	0.465 ± 0.061 [a]	0.375 ± 0.073 [a]	0.445 ± 0.043 [a]
Asparagine	0.725 ± 0.111 [a]	0.994 ± 0.038 [a]	0.760 ± 0.116 [a]	0.849 ± 0.094 [a]
Serine	0.315 ± 0.023 [a]	0.288 ± 0.029 [a]	0.253 ± 0.035 [a]	0.289 ± 0.027 [a]
Glutamine	0.449 ± 0.032 [b]	0.734 ± 0.102 [a]	0.430 ± 0.009 [b]	0.564 ± 0.076 [ab]
Histidine	0.057 ± 0.006 [a]	0.069 ± 0.015 [a]	0.059 ± 0.009 [a]	0.053 ± 0.005 [a]
Glycine	0.331 ± 0.027 [a]	0.256 ± 0.023 [ab]	0.230 ± 0.020 [b]	0.292 ± 0.019 [ab]
Threonine	0.102 ± 0.009 [a]	0.110 ± 0.012 [a]	0.086 ± 0.012 [a]	0.098 ± 0.011 [a]
Arginine	0.266 ± 0.036 [a]	0.349 ± 0.078 [a]	0.353 ± 0.062 [a]	0.356 ± 0.105 [a]
Alanine	0.891 ± 0.029 [a]	0.851 ± 0.002 [a]	0.824 ± 0.028 [a]	0.867 ± 0.011 [a]
Tyrosine	0.055 ± 0.004 [a]	0.063 ± 0.009 [a]	0.052 ± 0.005 [a]	0.056 ± 0.005 [a]
Cysteine	0.369 ± 0.028 [a]	0.277 ± 0.028 [ab]	0.254 ± 0.023 [b]	0.322 ± 0.017 [ab]
Valine	0.159 ± 0.012 [a]	0.157 ± 0.019 [a]	0.136 ± 0.018 [a]	0.154 ± 0.020 [a]
Methionine	0.020 ± 0.001 [a]	0.021 ± 0.001 [a]	0.019 ± 0.001 [a]	0.020 ± 0.001 [a]
Tryptophan	0.068 ± 0.004 [a]	0.068 ± 0.009 [a]	0.061 ± 0.006 [a]	0.061 ± 0.009 [a]
Phenylalanine	0.071 ± 0.004 [a]	0.068 ± 0.007 [a]	0.071 ± 0.008 [a]	0.068 ± 0.007 [a]
Isoleucine	0.082 ± 0.006 [a]	0.090 ± 0.012 [a]	0.079 ± 0.012 [a]	0.080 ± 0.011[a]
Leucine	0.063 ± 0.006 [a]	0.072 ± 0.015 [a]	0.067 ± 0.008 [a]	0.061 ± 0.006 [a]
Lysine	0.092 ± 0.006 [a]	0.113 ± 0.025 [a]	0.085 ± 0.013 [a]	0.098 ± 0.010 [a]
Proline	0.105 ± 0.018 [a]	0.141 ± 0.036 [a]	0.104 ± 0.032 [a]	0.098 ± 0.032 [a]

Data are presented as mean values ± SE. Significant differences at $p < 0.05$ within a line are indicated by different letters

5. Discussion

In this report, in order to extend our knowledge of the stress mechanisms triggered by heat stress during the induction of SE of P. halepensis, we studied its effect on the proteome and the relative concentration of soluble sugars, sugar alcohols and amino acids. For protein identification, a short gel liquid-chromatography coupled to tandem mass spectrometry (Short-GeLCMS/MS) approach, using DDA and DIA acquisition methods, was performed in EMs induced under different temperature treatments. Notwithstanding that the genome of *P. halepensis* is yet to be fully sequenced and may have negatively influenced the identification numbers, we were able to identify 1315 proteins and determine the relative concentration for 858. This is in agreement with the average number found in other proteomic studies in *Pinus* species (Morel et al. 2014; Escandón et al. 2017; Castander-Olarieta et al. 2021b, 2022).

The PLS-DA multivariate analysis permitted the selection of the 267 most significant proteins regarding the heat stress response, and the GO enrichment analysis disclosed that proteins involved in cellular metabolism and signaling were the most abundant. Accordingly, the 27 proteins identified with higher interest concerning heat stress response presented the same molecular

functions. As reviewed by Pinheiro et al. (2014), several proteome studies developed in Mediterranean woody species for the identification of stress-responsive proteins and tolerance/adaptation mechanisms under stress revealed high metabolic adjustment. Furthermore, in agreement with the data presented here, the rearrangement of various basal and secondary metabolic pathways such as glycolysis, the tricarboxylic acid cycle, and secondary metabolites production has been found in different pine species as a general stress-response (Morel et al. 2014; Escandón et al. 2017; Castander-Olarieta et al. 2019, 2021b, 2022; do Nascimento et al. 2021; Ghazghazi et al. 2022).

Transcriptomics and proteomics have been used to identify heat stress-responsive genes and proteins, including signaling components, such as protein kinases and transcription factors, and functional genes, such as heat shock proteins (HSPs) and catalase (Qu et al. 2013). In control temperature conditions HSPs bind to heat shock factors, maintaining them in an inactive state. During stress, they are released and facilitate the repairing or removing of damaged proteins. The consequential release of the heat shock factors leads to an activation boost to produce more HSPs to protect the cells and restore the cellular balance between these components, diminishing the stress response (Perrella et al. 2022). HSPs allow other proteins to preserve their stability under heat stress by assisting in protein folding and processing (Hasanuzzaman et al. 2013), and its relation with heat stress response has been widely studied (Haider et al. 2022).

Accordingly, the HSP chaperonin CPN60 was at higher amounts in samples under temperature stress. However, 20 kDa chaperonin, a HSP that functions as a co-chaperone along with CPN60, was down- accumulated in samples under heat stress conditions. This can be related to the fact that it has been proved that this co-chaperone, alone, has other functions, such as the upregulation of superoxide dismutase genes in *A. thaliana* chloroplasts (Kuo et al. 2012) and a negative regulation of the abscisic acid signaling in the same species (Zhang et al. 2013). In this regard, in a previous study conducted in *P. halepensis* concerning the effect of heat stress in the relative expression of stress-related genes (Pereira et al. 2021), no significant differences could be found regarding *SUPEROXIDE DISMUTASE [Cu–Zn]* concentrations at EMs, but a down-regulation was found at the *in vitro* somatic plants obtained from stressful conditions (Chapter II).

RNA-binding proteins interact with mRNA via RNA-binding domains affecting RNA stability and accessibility for translation, regulating both RNA and protein expression (Marondedze et al. 2019). In this report, the concentration of polyadenylate-binding protein RBP47 was lower at samples under heat stress treatments. In accordance with our results, in *A. thaliana*, this protein was reported to be located at the nucleus at control conditions while, under stress conditions, it was relocated to cytoplasmic granules (Weber et al. 2008). The authors suggest that, under stress conditions, the concentration of these molecules can diminish rapidly due to their aggregation to mRNA polysomes to maintain cellular homeostasis. Agglutinin amounts were also decreased under stressful conditions. *Ricinus communis* agglutinin is one of the most important applied lectins and has been widely used as a tool to study cell surfaces and to purify glycans (Wu et al. 2022). Lectins are proteins with diverse molecular structures able to recognize and bind specifically and reversibly

to carbohydrate structures and have been proven to be involved in stress response (Van Damme et al. 2004; Coninck and Van Damme 2021).

NADP-dependent malic enzyme 3 is a protein expressed by the *NADP-ME3* gene. According to Wheeler et al. (2008), there are four NADP-dependent malic enzymes genes (*NADP-ME1-4*) at the *A. thaliana* genome, and the different isoforms of this enzyme are responsible to catalyze the reversible oxidative decarboxylation of L-malate to pyruvate, CO_2 and NADPH in the presence of a divalent cation. However, they lead to the creation of proteins with unique regulatory mechanisms, and *NADP-ME3* is inhibited by fumarate with no modification of the enzymatic activity in the presence of aspartate and succinate (Wheeler et al. 2009). Concerning its role in stress response, it appears that NADP-dependent malic enzyme plays an important role in different biotic and abiotic stresses. As reviewed by Chen et al. (2019), and in accordance with our results, in tobacco, chloroplastic NADP- malic enzyme increased after polyethylene glycol and drought treatments, whereas the transcription of cytosolic *NADP-ME* remained similar or decreased. In *A. thaliana*, *NADP-ME2* appears to be involved in plant basal defense following pathogen recognition through the production of ROS (Voll et al. 2012). In its turn, alcohol dehydrogenase, a protein that presented the exact same pattern as the previous, is responsible for converting alcohols to aldehydes in plants and is important for NAD metabolism during anaerobic respiration (Wolyn and Jelenkovic 1990). A proteomic study developed in *A. thaliana* ecotypes that developed contrasting but efficient methods of adaptations to phosphate deficiency revealed that aconitate hydratase 2, alcohol dehydrogenase and malic enzyme consistently presented a reverse response between the two ecotypes (Chevalier and Rossignol 2011). Grapevine leaves overexpressing alcohol dehydrogenase suffered a drastic reduction of 90 % of sucrose levels (Tesniere et al. 2006). This is in contrast with our results since the concentration of sucrose was significantly higher in samples from the control, the same treatment where we found a higher concentration of alcohol dehydrogenase.

Proteins involved in DNA binding and cellular division, namely dynamin-related protein 12A and actin-depolymerizing factor 10, presented higher amounts at EMs from heat stress conditions. Actin depolymerization has been shown to induce programmed cell death (Thomas et al. 2006). The application of high doses of an actin-depolymerizing drug at the proliferation stage of Norway spruce SE induced cell death of suspensor cells followed by disintegration of the meristematic centers and their subsequent death, while at the maturation stage, low doses led to suspensors cell death which accelerated and synchronized the development of high-quality embryos (Schwarzerová et al. 2010). In this sense, it appears that the reorganization of cytoskeletal structures has an important role in programmed cell death as well as in the embryogenesis process.

The histone H4 variant TH091 and histone H2A.2.2 (core components of nucleosomes), and the 40S ribosomal protein S15a-1 and 60S ribosomal protein L18-3 (structural components of ribosomes) had increased amounts at samples from heat stress conditions. This agrees with previous studies on temperature stress response, where ribosomal proteins, translation regulator factors, and translation regulatory proteins played a significant role (Neilson et al. 2010; Schlaen et al. 2015; Liu et al. 2019b; Castander-Olarieta et al. 2022). This data, combined with the fact that proteins´

abundance variations are not always correlated with changes in the corresponding transcriptome (Correia et al. 2012), can explain the lack of significant differences found at the transcription assay performed here. The protein-coding genes transcribe to pre-messenger ribonucleic acid, being further processed to messenger ribonucleic acid, and finally translated into proteins, which in turn can be further processed and modified post-translationally (Ludvigsen and Honoré 2018). Most differences found at the proteomic profiles may result from posttranscriptional regulation rather than transcription.

A parallel analysis of the proteome of EMs induced under heat stress (40 ℃ for 4 h and 60 ℃ for 5 min) of radiata pine was developed by our group (Castander-Olarieta et al. 2022). The results found from the GO analysis showed the same over-representation of proteins regarding their biological processes (response to cadmium ion, proteasome mediated ubiquitin-dependent protein catabolic process, the glycolytic process and the tricarboxylic acid cycle); likewise, a deep reorganization of the machinery involved in protein synthesis, folding, transport and degradation was found. Notwithstanding, despite the fact that the proteins found as top-significant being involved in the same processes, the results regarding the effect of heat stress on their accumulation generally contrast; the few HSPs and chaperones, a variety of proteins related to oxidative stress response, and most of the enzymes directly involved in central metabolism (the glycolytic process and the tricarboxylic acid cycle) were present at significantly lower amounts in samples from the higher temperatures in *P. radiata*. Additionally, in somatic embryos produced under the same conditions in that species (Castander-Olarieta et al. 2021b), the same pattern was found for central metabolism enzymes and proteins related to oxidative stress, while HSPs and chaperones had a contrary response. The hypothesis postulated by the results in *P. radiata* that HSPs and chaperones are important during long-term heat stress response, while proteins and metabolites involved in oxidative stress defense are required during earlier response stages, do not apply in *P. halepensis*.

As reviewed by Lamelas et al. (2020), a great variety of metabolites of low molecular mass can avoid the damaging change in cellular components and restore homeostasis under stress. These include soluble carbohydrates such as glucose and fructose, amino acids and a variety of sugar alcohols. In this sense, regarding the quantification analysis of sugars, we found a significantly higher concentration of sucrose in control samples than those from the 50 ℃ (30 min) treatment. In this line, a study developed in *P. halepensis* seeds showed different concentrations of glucose, fructose and sucrose under drought stress, with the latest showing an enhanced accumulation in drought-tolerant seeds (Taïbi et al. 2017). Furthermore, we found significant differences at the concentrations of glutamine, glycine, and cysteine between samples from different induction treatments. Glycine betaine seems to be important at abiotic stress tolerance; genes associated with glycine betaine synthesis have been transferred into plants such as maize, which do not accumulate glycine betaine, and enhance the level of synthesis upon stress (Quan et al. 2004). Also in maze, the exogenous application of glycine and L-arginine to crops in order to analyze its effects on temperature stress showed that, while L-arginine led to more vigorous plants under stress, glycine presented none or negative effects (Matysiak et al. 2020). Furthermore, in EMs of *P. radiata*, heat

stress affected the abundance of phenolic compounds and several amino acids; tyrosine and isoleucine presented significantly lower concentrations in samples from the control, while leucine and histidine presented significant differences between the higher concentration at 50 ℃ (30 min) and the lower at 40 ℃ (4 h) (Castander-Olarieta et al. 2019). Furthermore, while no effect was found in the concentration of soluble sugars in *P. radiata* somatic embryos, sucrose levels were on the verge of statistical significance and decreased at higher temperatures (Castander-Olarieta et al. 2021b). In *P. radiata* EMs, significantly higher concentrations of fructose and glucose were found in samples from 40 ℃ (4 h), compared to the control and 60 ℃ (5 min) (Castander-Olarieta et al. 2022). Altogether, it is clear that all these metabolites are highly involved in the heat stress response pathway, but it seems that the clear mechanisms are not fully defined yet.

6. Conclusions

As far as it is known, this is the first report studying the effect of heat stress on the proteome and the concentration of soluble sugars, sugar alcohols and amino acids of *P. halepensis* EMs.

Heat stress during the induction phase of SE led to proteomic and metabolomic reorganization; several enzymes directly involved in metabolic pathways as well as proteins previously found to be involved in temperature stress response such as histones (histone H4 variant TH091 and histone H2A.2.2) and ribosomal proteins (40S ribosomal protein S15a-1 and 60S ribosomal protein L18-3) presented higher amounts at higher temperatures. In addition, sucrose, glycine and cysteine presented lower concentrations at higher temperatures, while the concentrations of glutamine were higher, emphasizing the direct involvement of these primary metabolites in stress response.

The results of this work reinforce the idea that a temperature priming effect during the initial stages of somatic embryogenesis can trigger long-lasting effects in the mechanisms involved in heat stress response.

7. Supplementary Material

Supplementary Table 1. Proteins differentially accumulated in *P. halepensis* EMs induced under different temperatures treatments, according to the Kruskal-Wallis test ($p < 0.05$) and Dunn´s test of multiple comparisons (Benjamini-Hochberg *p*-value adjustment): Cond1: 23 ℃; Cond2: 40 ℃ (4 h); Cond3: 50 ℃ (30 min); Cond4: 60 ℃ 5 (min).

Protein	Uniprot Accession	Species	Dunn's Test of Multiple Comparisons			Kruskal-Wallis
			Cond2/ Cond1	**Cond3/ Cond1**	**Cond4/ Cond1**	***p* - value**
Citrate synthase. mitochondrial	O80433	*Daucus carota*	0.350	0.056	0.003	0.004
Aconitate hydratase. cytoplasmic	P49608	*Cucurbita maxima*	0.017	0.002	0.081	0.006
NADP-dependent malic enzyme 3	Q9XGZ0	*Arabidopsis thaliana*	0.069	0.478	0.056	0.006
Trifunctional UDP-glucose 4.6-dehydratase/UDP-4-keto-6-deoxy-D-glucose 3.5-epimerase/UDP-4-keto-L-rhamnose-reductase RHM1	Q9SYM5	*Arabidopsis thaliana*	0.275	0.061	0.021	0.009
Agglutinin	P06750	*Ricinus communis*	0.026	0.018	0.006	0.011
Protein kinase G11A	Q0DCT8	*Oryza sativa* subsp. *japonica*	0.080	0.017	0.007	0.014
Polyadenylate-binding protein RBP47	Q9LEB3	*Nicotiana plumbaginifolia*	0.009	0.015	0.056	0.015
Molybdenum cofactor sulfurase	Q8LGM7	*Solanum lycopersicum*	0.116	0.010	0.014	0.016
Actin-depolymerizing factor 10	Q9LQ81	*Arabidopsis thaliana*	0.188	0.017	0.015	0.017
40S ribosomal protein S15a-1	P42798	*Arabidopsis thaliana*	0.129	0.118	0.116	0.018
20 kDa chaperonin. chloroplastic	O65282	*Arabidopsis thaliana*	0.011	0.025	0.028	0.018
NADPH--cytochrome P450 reductase 1	Q9SB48	*Arabidopsis thaliana*	0.181	0.006	0.072	0.019
Eukaryotic translation initiation factor 2 subunit beta	Q41969	*Arabidopsis thaliana*	0.016	0.015	0.144	0.019
Histone H4 variant TH091	P62786	*Triticum aestivum*	0.352	0.061	0.033	0.023
Histone H2A.2.2	P02277	*Triticum aestivum*	0.139	0.020	0.015	0.023
Dynamin-related protein 12A	Q39821	*Glycine max*	0.139	0.015	0.020	0.023
Probable fructokinase-7	Q9FLH8	*Arabidopsis thaliana*	0.027	0.025	0.017	0.024

Supplementary Table 1 cont.

Pyruvate dehydrogenase E1 component subunit beta-4. chloroplastic	Q10G39	*Oryza sativa* subsp. *japonica*	0.403	0.048	0.033	0.025
Chaperonin CPN60. mitochondrial	P35480	*Brassica napus*	0.007	0.130	0.097	0.025
6-phosphogluconate dehydrogenase. decarboxylating 1	Q9LI00	*Oryza sativa* subsp. *japonica*	0.401	0.129	0.018	0.026
60S ribosomal protein L18-3	Q940B0	*Arabidopsis thaliana*	0.380	0.049	0.069	0.028
Chalcone synthase	P30079	*Pinus sylvestris*	0.075	0.162	0.012	0.031
Diacylglycerol O-acyltransferase 1	Q9SLD2	*Arabidopsis thaliana*	0.021	0.038	0.037	0.032
Glutathione reductase. cytosolic	P48642	*Oryza sativa* subsp. *japonica*	0.071	0.043	0.455	0.032
Pyruvate dehydrogenase E1 component subunit beta-1. mitochondrial	Q6Z1G7	*Oryza sativa* subsp. *japonica*	0.060	0.064	0.015	0.034
Glutamyl-tRNA(Gln) amidotransferase subunit B. chloroplastic/mitochondrial	Q2R2Z0	*Oryza sativa* subsp. japonica	0.160	0.021	0.032	0.036
25.3 kDa vesicle transport protein	Q94AU2	*Arabidopsis thaliana*	0.056	0.024	0.029	0.036
Ubiquitin carboxyl-terminal hydrolase 13	Q84WU2	*Arabidopsis thaliana*	0.045	0.287	0.171	0.037
Serine/threonine-protein phosphatase 2A 65 kDa regulatory subunit A gamma isoform	Q38951	*Arabidopsis thaliana*	0.093	0.162	0.204	0.038
3-isopropylmalate dehydrogenase. chloroplastic	P29696	*Solanum tuberosum*	0.385	0.061	0.049	0.038
Alcohol dehydrogenase	P17648	*Fragaria ananassa*	0.321	0.097	0.056	0.041
Carbamoyl-phosphate synthase large chain. chloroplastic	B9EXM2	*Oryza sativa* subsp. *japonica*	0.401	0.072	0.040	0.042
Transcription factor TGA5	Q39163	*Arabidopsis thaliana*	0.058	0.098	0.520	0.042
40S ribosomal protein S12	Q9XHS0	*Hordeum vulgare*	0.031	0.049	0.162	0.049

Supplementary Table 2. One-way analysis of variance for expression of different genes detected in *P. halepensis* embryonal masses induced under different temperature conditions (23 ℃, 9 weeks; 40 ℃, 4 h; 50 ℃, 30 min; 60 ℃, 5 min).

Kruskal-Wallis	d*f*	X^2 test	*p* Value
20 KDA CHAPERONIN (CPN20)	3	0.5245	n.s.[1]
CHAPERONIN CPN60 (CPN60)	3	0.0745	n.s.
CITRATE SYNTHASE (PDHB)	3	0.2167	n.s.
PYRUVATE DEHYDROGENASE E1 COMPONENT SUBUNIT BETA- 1	3	0.1841	n.s.
6-PHOSPHOGLUCONATE DEHYDROGENASE, DECARBOXYLATING 1 (G6PGH1)	3	0.2401	n.s.
PYRUVATE DEHYDROGENASE E1 COMPONENT SUBUNIT BETA-4	3	0.8395	n.s.
TRIFUNCTIONAL UDP-GLUCOSE A,6-DEHYDRATASE/UDP-4-KETO-6DEOXY-D-GLUCOSE 3,5-EPIMERASE/UDP-4-KETO-L-RHAMNOSE-REDUCTASE RHM1 (RHM1)	3	0.5921	n.s.
NADPH-CYTOCHROME P450 REDUCTASE 1 (ATR1)	3	0.5959	n.s.
PROBABLE FRUCTOKINASE-7	3	0.6958	n.s.

[1] not statistically significant.

Supplementary Table 3. One-way analysis of variance for concentration of sugars (μmol g^{-1} FW) detected in *P. halepensis* embryonal masses induced under different temperature conditions (23 ℃, 9 weeks; 40 ℃, 4 h; 50 ℃, 30 min; 60 ℃, 5 min).

Sugars ANOVA	d*f*	F value	*p* value
Sucrose	3	3.7320	0.0330
Glucose	3	1.1930	n.s.[1]
Fructose	3	1.8890	n.s.
Mannitol	3	0.9782	n.s.
Sorbitol	3	0.1167	n.s.

[1] not statistically significant.

Supplementary Table 4. One-way analysis of variance for concentration of amino acids (µmol g^{-1} FW) detected in *P. halepensis* embryonal masses induced under different temperature treatments (23 ℃, 9 weeks; 40 ℃, 4 h; 50 ℃, 30 min; 60 ℃, 5 min).

Amino acids / **ANOVA**	**d*f***	**F value**	***p* value**
Aspartic A	3	0.4546	n.s.[1]
Glutamic A	3	0.5485	n.s.
Asparagine	3	1.6030	n.s.
Serine	3	0.8004	n.s.
Glutamine	3	4.4920	0.0181
Histidine	3	0.5378	n.s.
Glycine	3	3.9470	0.0277
Threonine	3	0.8126	n.s.
Arginine	3	0.3369	n.s.
Alanine	3	1.8050	n.s.
Tyrosine	3	0.5632	n.s.
Cysteine	3	4.2780	0.0213
Valine	3	0.3568	n.s.
Metionine	3	0.5148	n.s.
Tryptophan	3	0.2859	n.s.
Phenilalanine	3	0.0708	n.s.
Isoleucine	3	0.2505	n.s.
Leucine	3	0.3126	n.s.
Lysine	3	0.5958	n.s.
Proline	3	0.4094	n.s.

[1] not statistically significant.

CHAPTER IV: Regeneration of *Pinus halepensis* (Mill.) trough Organogenesis from Apical Shoot Buds

(Pereira C, Montalbán IA, Pedrosa A, Tavares J, Pestryakov A, Bogdanchikova N, Canhoto J, Moncaleán P (2021) Regeneration of *Pinus halepensis* (Mill) trough organogenesis from apical shoot buds. *Forests* 12:363.)

1. Abstract

Organogenesis and somatic embryogenesis have been widely applied as the two main regeneration pathways in plant tissue cultures. However, recalcitrance is still the main restriction in the clonal propagation of many woody species, especially in conifers. They undergo a "phase change" that leads to significant loss of vegetative propagation capacity, reducing the aptitude of tissues and organs to be regenerated in vitro beyond this point. In line with this, the *in vitro* regeneration of mature conifer trees has been a long-cherished goal in many laboratories worldwide. Based on previous works in *Pinus* species regeneration from adult trees, we now present data about the culture of apical shoot buds in an attempt to induce organogenesis and somatic embryogenesis to clone mature trees of Aleppo pine (*Pinus halepensis*). Reinvigorated axillary shoots were submitted to conditions usually applied to induce somatic embryogenesis through the manipulation of culture media, including the use of auxins such as 2,4-Dichlorophenoxyacetic acid and 1-Naphthaleneacetic acid, cytokinins (6-benzyladenine and kinetin), and phytosulfokine (50, 100, and 200 nM). Although somatic embryos could not be obtained, an embryogenic-like tissue was produced, followed by the emergence of actively proliferating non-embryogenic calli. Variations in the consistency, texture, and color of non-embryogenic calli were observed; especially those arising in the media containing phytosulfokine. Reinvigorated shoots, induced by 22 or 44 µM 6-benzyladenine, were obtained through organogenesis and acclimatized, and phenotypically normal plants were obtained.

Keywords: Aleppo pine; conifers; phytosulfokine; plant growth regulators; rooting

2. Introduction

Approximately 52% of land surface is occupied by forests (Boisvenue and Running 2006). Among trees, conifers are particularly important since they are by far the largest and most diverse gymnosperm group, covering approximately 60% of the forested areas of the world (von Arnold et al. 2019). I*n vitro* propagation techniques have been widely applied as a model system for plant regeneration analysis and as a large-scale propagation system for coniferous cloning (Klimaszewska et al. 2007; von Arnold et al. 2019). Aleppo Pine (*Pinus halepensis* Mill.) is native to the Mediterranean region, thriving in the driest and warmest areas due to its tolerance to high temperatures and drought stress (Ne'eman et al. 2004; Klein et al. 2011), which makes it a potential alternative for reforestation in the climate change scenarios predicted for large areas of the globe in the near future (Vennetier et al. 2010; Botella et al. 2010).

Multicellular organisms harbor multiple types of tissues, each consisting of cells with particular features and functions. However, in some cases, cell specificity can be totally or partially lost and the cells return to a juvenile proliferating state usually known as dedifferentiation (Sugiyama 2015). Cellular plasticity defines the competence of differentiated cells to switch their differentiation process and to acquire new fates. This loss of a specialized state previously acquired during development has been one of the central concepts in plant regeneration (Vasil 2008).

In vitro regeneration of plants can be accomplished through two different pathways: shoot organogenesis and somatic embryogenesis (SE) (Ramage and Williams 2002; Zhang and Lemaux 2004).]. Organogenesis relies on the *de novo* formation of a shoot that requires further rooting to develop into an entire plant. Somatic embryogenesis is a more direct pathway of regeneration since bipolar structures possessing a root and shoot meristem are formed. However, SE induction is mostly restricted to juvenile embryonary organs and, in most cases, immature zygotic embryos have been used to produce somatic embryos in coniferous and other trees (Bonga et al. 2010). Regeneration from embryonary explants is less valuable for cloning because the process rules out the selection of specific traits that can only be seen when trees have entered the mature phase. However, the switch of a developmental program in adult cells remains a difficult obstacle to overcome in many species, especially in forest trees (Díaz-Sala 2014). Thus, recalcitrance is still the main restriction for the clonal propagation of elite trees (Bonga et al. 2010; Bonga 2017).

The direct induction of axillary shoot buds and somatic embryo formation are both morphogenic pathways highly controlled by exogenous plant growth regulators added to the culture media and their interaction with endogenous phytohormones (de Almeida et al. 2012). The balance between auxin and cytokinin and changes to their composition and ratio in culture media have been found to determine the morphogenic competence of cultured explants (Skoog and Miller 1957). Variations in this ratio are frequently the primary empirical approach to the optimization of *in vitro* cultures. However, many species do not respond to this common approach and require additional physical or chemical stimuli (Ramage and Williams 2002). For example, it has been shown that the presence of phytosulfokine in the culture medium stimulates the initial steps of cellular dedifferentiation even at nanomolar concentrations, significantly increasing cell proliferation and

callus growth (Matsubayashi et al. 2006). Endogenous and environmental factors, such as genotype, excision tissue and timing, phenology, and tree maturation are other factors influencing *in vitro* regeneration (Bonga et al. 2010).

Several protocols for adult pine organogenesis have been established in our lab (De Diego et al. 2008, 2010; Cortizo et al. 2009; Montalbán et al. 2011b) and SE has been successfully reported in various *Pinus* species using juvenile material as the initial explant (Becwar et al. 1990; Carneros et al. 2009; Castander-Olarieta et al. 2020a). Despite all the progress that has been made in the practical applications of somatic embryogenesis induction, the results concerning adult cloning are still scarce. Moreover, cloning from adult trees would substantially reduce field testing and the time for breeding (Bonga 2017). Therefore, cloning of adult trees is still being attempted in numerous laboratories.

In Aleppo pine, the first record of organogenesis was reported using mature zygotic embryos as explants (Lambardi et al. 1993). More recently, our team successfully developed the first SE protocol using immature megagametophytes as explants for this species (Montalbán et al. 2013b).

Considering the reasons mentioned above, the main goal of this work was to successfully develop protocols for *in vitro* regeneration (organogenesis and SE), using apical shoot buds as explants, which could allow for the selection and cloning of mature trees of Aleppo pine.

3. Material and Methods

Plant Material

Induction of Organogenesis

Four 20-year-old adult zygotic trees (17.3, 17.4, 17.5 and 18.1) from Manzanos (Spain; 42º44´29´´ N, 2º52´35´´ W) and four 4-year-old juvenile somatic trees (H8, H29, H32, and H5) planted at Neiker, Arkaute (Spain; 42º51´08.5´´ N, 2º37´37.1´´ W) were selected in 2017, and apical shoot buds were collected between January and March. In 2018, the apical shoot buds from five 20-year-old adult trees (P1, P5, P6, P7, and P8) were collected between November and January near Figueira da Foz (Portugal; 40º09´02.5´´ N, 8º49´07.3´´ W).

The apical shoot buds were stored in polyethylene bags at 4 °C for a maximum of 10 days until their use. For superficial cleaning, buds were washed with a commercial detergent, rinsed under running water for 5 min, and then immersed in ethanol 96% for 1 min. Afterward, explants in the first sample collection (2017) underwent three different sterilization protocols: (A) surface sterilization in commercial bleach, 1:1 diluted with sterile water plus two drops of Tween 20® (Scharlab, Barcelona, Spain) for 15–20 min before being rinsed three times with sterile distilled H_2O; (B) surface sterilization in commercial bleach, 1:1 diluted with sterile water plus two drops of Tween 20® for 15 min, rinsed one time with sterile distilled H_2O before being immersed in a silver nanoparticle solution (Argovit®, Vector Vita LLC, Novosibirsk, Russia) (200 mg L^{-1}) for 10 min, and then rinsed three times with sterile distilled H_2O; (C) surface sterilization in a silver nanoparticle solution (Argovit®, Vector Vita LLC, Novosibirsk, Russia) (200 mg L^{-1}) for 15 min

before being rinsed three times with sterile distilled H_2O. All sterilization protocols were performed under sterile conditions in a laminar flow unit. Sterilization protocol (A) was used for all the explants in the second 2017 collection and thereafter in the 2018 collection.

Attempts to Induce Embryogenic Tissue

Six 4-year-old juvenile somatic trees (H29, H32, H13, H18, H5, and H42) planted at Neiker, Arkaute (Spain; 42º51´08.5´´ N, 2º37´37.1´´ W) and two 20-year-old adult zygotic trees (17.3 and 17.4) from Manzanos (Spain; 42º44´29´´ N, 2º52´35´´ W) were selected in 2017, and the apical shoot buds were collected between January and March. The storage, cleansing, and sterilization of the apical shoot buds were performed as described at the former section. Twelve reinvigorated axillary shoots (2.0–3.0 cm) from two genotypes previously obtained through organogenesis were also selected for embryogenic tissue induction.

Organogenesis

Axillary Shoot Induction, Growth and Elongation

Scales from apical shoot buds (0.5–3 cm length) (Figure 18a,b) were removed, and the buds were cut transversely with a surgical scalpel blade into slices 0.3–0.8 cm thick (Figure 18c). Four to five bud slices were cultured in 90 × 14 mm Petri dishes containing twenty milliliters of O1 induction medium (Table 17). Two different concentrations of 6-benzyladenine (BA; 11 and 22 µM), were tested in the first sample collection of 2017. Five to six Petri dishes per BA treatment and genotype were cultured. The explants were maintained at 23 ℃ under a 16 h photoperiod at 100 µmol m^{-2} s^{-1} provided by cool white fluorescent tubes (TFL 58 W/33; Philips, France).

After 35–50 days, the elongated needles were cut off and the explants were transferred to the same medium to promote axillary bud growth. At this point, since the explants cultured in the medium with 11 µM of BA did not show the expected response, they were transferred to a new O1 induction medium with 44 µM of BA. For the samples from the second and third collection in 2017 and all three collections in 2018, the initial BA concentrations tested were 22 and 44 µM of BA. Overall, a total of 1511 bud slices were cultured.

When the needle fascicles emerged, the explants with axillary buds were transferred to glass jars with the O2 elongation medium (Table 17; Figure 18d). Once axillary bud growth was evident and shoots were 0.5 cm long, they were separated and cultured individually in a fresh elongation medium (Figure 18e). The part of the explant that had secondary needles was separated, the secondary needles were cut, and the explants were returned to the O1 medium to promote re-induction.

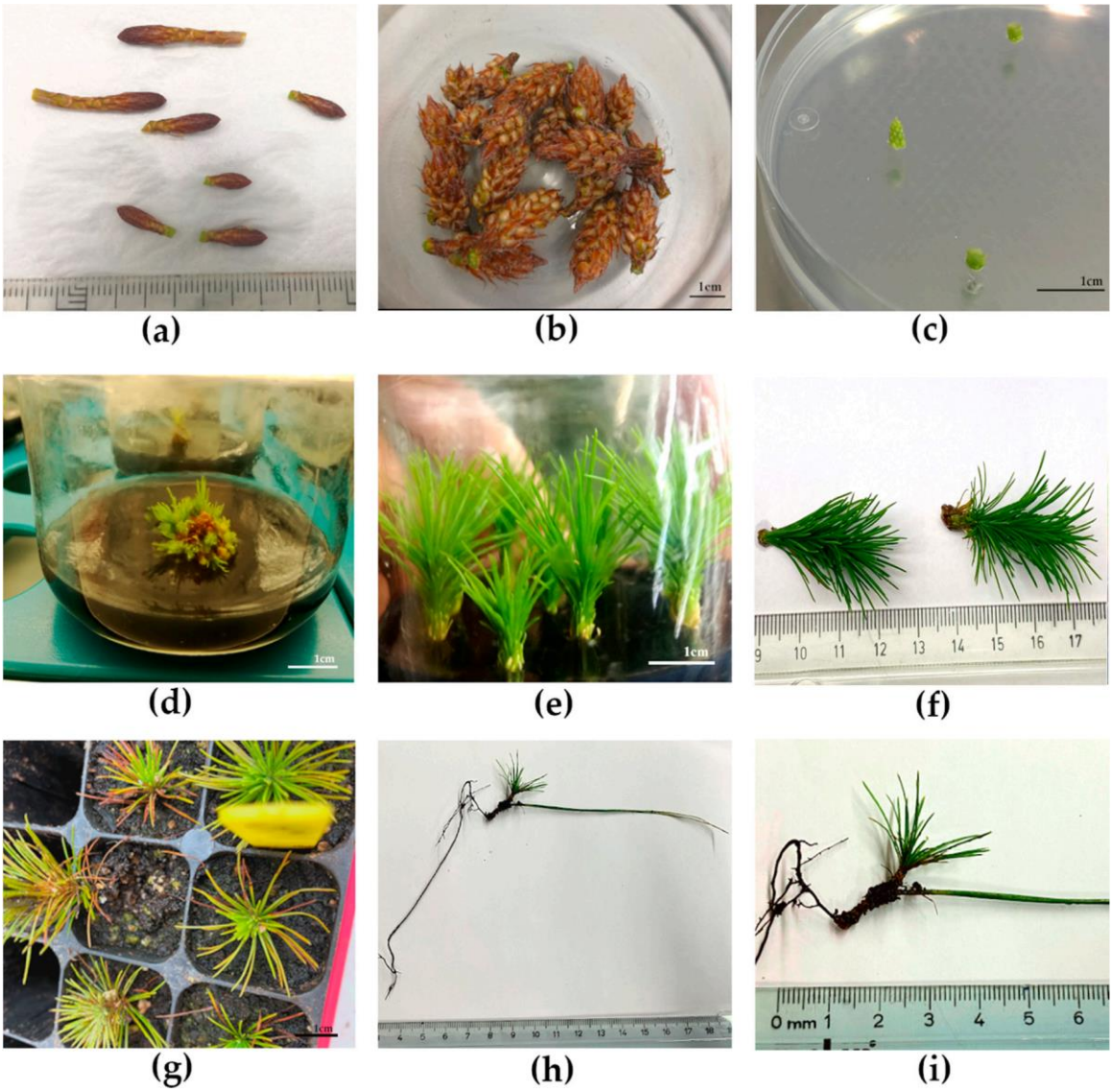

Figure 18. Plant material at different stages of the organogenic process **(a)** apical shoot buds with different sizes and totally closed scales; **(b)** apical shoot buds at an advanced developmental stage with open scales; **(c)** bud slices in the induction medium; **(d)** shoot organogenesis in a bud slice cultured in the elongation medium; **(e)** axillary shoots separately cultured in the elongation medium; **(f)** shoots with no roots immediately before acclimatization; **(g)** acclimatized shoots; **(h)** acclimatized shoot removed from the container to display the *ex vitro* developed roots; **(i)** closer view of the latter acclimatized shoot.

Root Induction

Shoots 2.0–3.0 cm long were transferred to the O3 root induction medium (Table 17). Three to four shoots per five replicates of five genotypes (H8, H32, 17.3, P1, and P8), comprising a total of 89 explants, were tested for root induction. After four weeks of culture, shoots were transferred into a fresh O2 medium to promote root growth. None of the shoots developed visible roots, so they were retransferred to the O3 medium for two weeks. After this time, no roots were developed in vitro (Figure 18f). Despite that fact, shoots were directly transferred *ex vitro* to sterile peat:perlite (3:1, v/v) and acclimatized under controlled conditions (Figure 18g). During *ex vitro* conditions, roots spontaneously developed, and four months later the percentage of acclimatized plantlets was recorded.

Table 17. Variations of basal DCR medium (Gupta and Durzan 1986) used along different stages of *P. halepensis* organogenesis (O1 - O3) and embryogenic tissue induction (S1 – S10).

Medium	PGRs (µM)	AC (g L^{-1})	Others (g L^{-1})	Agar (g L^{-1})	pH (1)	[*] EDM amino acid mixture (2)	Phytosulfokine (nM) (2)
O1	BA (11,22,44)	-	Sucrose (30)	Difco® granulated agar (9)	5.8	-	-
O2	-	(2)	Sucrose (30)	Difco® granulated agar (9.5)	5.8	-	-
O3	IBA (7)	-	Sucrose (30)	Difco® granulated agar (9.5)	5.8	-	-
S1 [**]	-	(3)	Maltose (32)	Gelrite® (2)	5.7	-	-
S2	BA (9) 2,4-D (20) NAA (25) (2)	-	Maltose (32)	Gelrite® (1.5)	5.7	yes	(50)
S3	-	-	Sucrose (30)	-	5.7	-	-
S4	BA (9) 2,4-D (20) NAA (25) (2)	-	Maltose (32)	Gelrite® (2.5)	5.7	yes	(50)
S5	BA (9) 2,4-D (20) NAA (25) (2)		Maltose (32)	Gelrite® (2.5)	5.7	yes	(100)
S6	-	(10)	Sucrose (60)	-	5.7	-	-
S7	BA (9) 2,4-D (20) NAA (25) (2)	-	Maltose (32) PVP (0.2)	Gelrite® (2.5)	5.7	yes	(100)
S8	ABA (80) (2)		Sucrose (68) Casein hydrolysate (1) Glutamine (0.5) (2)	Gelrite® (10)	5.7	yes	-
S9	ABA (120) (2)		Sucrose (68) Casein hydrolysate (1) Glutamine (0.5) (2)	Gelrite® (12)	5.7	yes	-
S10	BA (9) 2,4-D (20) NAA (25) (2)	-	Maltose (32)	Gelrite® (1.5)	5.7	yes	(200)
S11	2,4-D (9) Kinetin (2.7)		Sucrose (30)	Gelrite® (3.5)	5.7	yes	-

PGRs, plant growth regulators; AC, activated charcoal; BA, 6-benzyladenine; IBA, indole-3-butyric acid; 2,4-D, 2,4-dichlorophenoxyacetic acid; NAA, 1-naphthaleneacetic acid; PVP, polyvinylpyrrolidone; ABA, abscisic acid. (1) Adjusted before autoclaving at 121 ℃ for 20 min. (2) Filter-sterilized and added to the medium after autoclaving. [*] (Walter et al. 2005). [**] (Park et al. 2010).

Data Collection and Statistical Analysis

At the time that axillary shoots were isolated and cultured individually in the elongation medium, the percentage of explants forming shoots (EFS) (%) and the mean number of shoots formed per explant (NS/E) were calculated with respect to the non-contaminated explants. Following the confirmation of the homogeneity of variances and the normality of the samples, an

unpaired t-test analysis [GraphPad Prism 8.4.1 (676) (GraphPad Software Inc., California, CA, USA)] was performed in order to identify possible differences in these two variables regarding explant induction at 22 and 44 µM of BA. Each measurement was made by considering the mean data collected for each genotype from different sample collections (sample collections with 100% contamination were not considered), comprising a total of 20 replicates per BA treatment.

Regarding possible differences in acclimatization percentages between genotypes, since there was no homogeneity of variances between samples, a Kruskal–Wallis test was applied using the percentage of successfully acclimatized plants counted after four months.

Attempts to Induce Embryogenic Tissue

Apical Shoot Buds as Initial Explants

Scales from the apical shoot buds (0.5–3 cm length) were removed, and the buds were cut transversely with a surgical scalpel blade into 0.3–0.8 cm thick slices that were first cultured in the S1 medium (Table 17). Two to five Petri dishes per genotype and five bud slices per Petri dish, comprising a total of 490 bud slices, were cultured and maintained for three days, at dark conditions at 4 ℃. Afterward, the explants were cultured in the S2 induction medium (Table 17) and the cultures were maintained, at dark conditions at 23 ℃.

After 3–5 weeks in the S2 induction medium, half of the embryogenic-like proliferating calli were directly transferred to the proliferation medium, and half were detached from the bud slices. The detachment was performed by resuspending the explants in the S3 medium (Table 17), in 50 mL centrifuge tubes, and vigorously shaking them by hand for a few seconds. Thereafter, a 5 mL aliquot was poured onto a filter paper disc (Whatman no. 2.7 cm) in a Büchner funnel, and a vacuum pulse was applied for 10 s (Montalbán et al. 2010). Filters containing the tissue were then poured into the S4 and S5 proliferation media (Table 17). Cultures were subcultured every 3–5 weeks and cultured in the dark, half at 23 and the other half at 28 ℃. Embryogenic-like tissue that presented a similar morphology to an embryogenic callus was selected and stained with 2% (w/v) acetocarmine and observed using a Leica DMS1000 (Leica Microsystems, Wetzlar, German) and a Nikon ECLIPSE 80 i (Nikon Corporation, Tokyo, Japan).

After 2–3 subcultures in the S4 and S5 proliferation medium, all samples were resuspended, using the resuspension method described above, in the S6 medium (Table 17) before being transferred to the S7 pre-maturation medium (Table 17). Samples were cultured at 23 ℃, in the dark, for 5–7 weeks.

With the embryogenic-like tissue, an attempt at tissue maturation was made and induction was carried out in the S8 and S9 maturation media (Table 17). Eight Petri dishes per sample, containing 60 mg of tissue each, were cultured in the dark for 18 weeks.

In Vitro Axillary Shoots as Initial Explants

Needles of the axillary shoots reinvigorated from organogenesis were cut before culture without damage to the apical meristem, and seven to nine transversal shoot slices (0.2–0.5 cm) per explant were cultured in three different induction media: S2, S10, and S11 (Table 17). Two to six

Petri dishes per induction medium were cultured and maintained, in the dark, at 23 ºC. The calli were subcultured in the same induction medium two times, after 5 and 10 weeks from the beginning of induction.

4. Results

Organogenic process

A total of 1010 bud slices were cultured at different induction media in 2017. The contamination rates obtained in the first sample collection of 2017 were 48.2% for protocol (A), 49.1% for (B), and 89.0% for (C). Protocol (A) was selected for the rest of the experiment, and a total contamination rate of 43.9% was obtained during this experiment, with 567 living explants remaining. In 2018, 501 bud slices were cultured, and a total of 242 explants remained after contamination.

The reinvigorated shoots were obtained from both of the BA treatments (22 and 44 µM), from adult zygotic trees, and juvenile somatic trees. Higher numbers of EFS (%) and the NS/E were obtained from explants cultured in the induction medium supplemented with 44 µM BA. No statistically significant differences were found for EFS (%) (Table 18). However, significant differences were obtained for the NS/E, since treatment at 44 µM BA (5.79) led to more than double the NS/E than treatment with 22 µM BA (2.87) (Tables 18,19). A total of 683 shoots were obtained from the 159 explants induced (4.3 shoots per explant).

Table 18. *T*-test analysis of variance for explants forming shoots (EFS) (%) and NS/E (number of shoots formed per explant) of *P. halepensis* apical shoot buds induced under two different concentrations of BA (22 and 44 µM L^{-1}) and Kruskal-Wallis analyses for *ex vitro* rooting of five different genotypes (H8, H32, 17-3, P1, P8).

Source			
***t*-Test**	**d*f***	***t***	***p* Value**
EFS	36	1.28	n.s. [1]
NS/E	34	2.12	0.0411
Kruskal-Wallis	**d*f***	**X^2 Test**	***p* Value**
Ex-vitro Rooting	4	2.613	n.s.

[1] not statistically different.

Table 19. Values for EFS (%) (explants forming shoots) and NS/E (number of shoots formed per explant) for *P. halepensis* apical shoot buds induced under two different concentrations of BA (22 and 44 µM).

Treatment	**EFS (%)**	**NS/E**
22 µM L^{-1} BA	21.47 ± 4.70 [a]	2.87 ± 0.51 [b]
44 µM L^{-1} BA	30.90 ± 5.58 [a]	5.79 ± 1.2 [a]

Data are presented as mean values ± SE. Significant differences at $p < 0.05$ within a column are indicated by different letters

No data could be obtained from families 17.5, H29, H5, or P7 since 100% of the cultured explants were contaminated. The rates of contamination were noticed to be related not only to the condition of the initial explant but, also, to its development stage. When explants consisted of apical shoot buds at an advanced developmental stage with open scales (Figure 18b), higher contamination

rates were observed, as in the third collection of both P5 and P6, when a 100% rate of contamination was recorded.

A representation of the mean results obtained for each genotype per BA treatment for EFS (%) and NS/E can be found in Table 20.

Table 20. Values for EFS (%) (explants forming shoots) and NS/E (number of shoots formed per explant) for *P. halepensis* apical shoot buds from different genotypes, induced under two different concentrations of BA (22 and 44 µM).

Genotype	EFS (%)		NS/E	
	22 µM	44 µM	22 µM	44 µM
H32	25 ± 0	33.3 ± 0	4.5 ± 0	8 ± 0
H8	0[1]	11.1 ± 0	0[1]	22 ± 0
17.3	41.2 ± 10.0	59.2 ± 8.3	3.85 ± 1.0	5.2 ± 1.1
17.4	14.3 ± 5,4	33.3 ± 7.2	2.5 ± 0.9	3 ± 1.1
18.1	13.66 ± 3.8	29.7 ± 9.8	1.7 ± 0.5	2.4 ± 0.5
P1	0[1]	39.9 ± 16.4	0[1]	9.8 ± 2.2
P5	14.8 ± 0.4	19.54 ± 1.3	3 ± 0	3.7 ± 0.24
P6	12.0 ± 4.2	11.1 ± 3.93	1.67± 0	11.33 ± 0
P8	38.5 ± 0	25.0 ± 0	6.8 ± 0	5.3 ± 0

Data are presented as mean values ± SE. [1]: Contaminated

None of the shoots cultured in the root-induction medium developed roots in vitro. Nevertheless, acclimatized ex vitro true-to-type plants from five different genotypes (H8, H32, 17.3, P1, and P8) were successfully obtained (Figure 18g), since *ex vitro* roots developed (Figure 19h,i). Regarding the acclimatization percentages, no statistically significant differences were found between the different genotypes (Table 18). However, the mean percentage was 65% for genotype H8, while in the other four genotypes the mean percentages were between 20 and 25% (Figure 19).

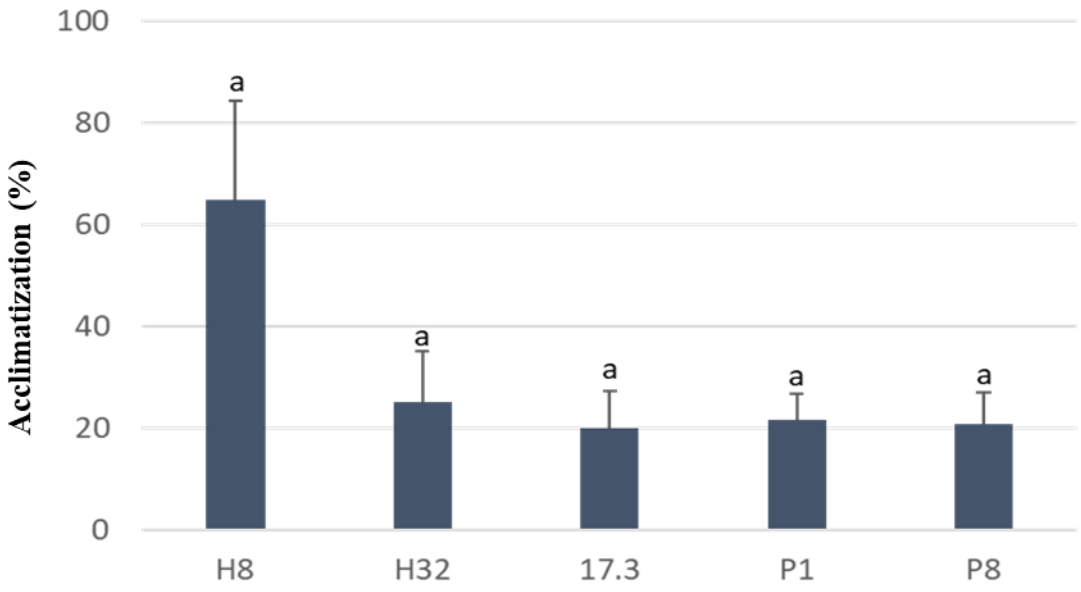

Figure 19. Acclimatization percentages of five different genotypes (H8, H32, 17.3, P1, and P8). The letter "a" indicates that there are no statistical differences between genotypes.

Attempts to Induce Embryogenic Tissue

A total of 490 bud slices from apical shoot buds were submitted to SE induction and a contamination rate of 61% was obtained. Of the 191 non-contaminated explants, 94.2% were induced and able to produce embryogenic-like tissue.

Bud slices from the juvenile somatic trees were cultured in their growth position in the S2 induction medium (Figure 20a) and approximately one week after culture, white-green soft embryogenic-like tissue began to appear, first at the wounded areas and then throughout the explant (Figure 20b). Explants subcultured directly in the proliferation media presented tissues with a watery texture at first, which started to stiffen and to acquire a yellowish color through subculturing (Figure 20c). When the embryogenic-like tissue was detached from the explant and subcultured in filter paper, a more compact tissue was observed. Nevertheless, clusters with both brown, hard to disaggregate tissue, and whiter, softer tissue could be observed in the S4 and S5 proliferation media (Figure 20d,e), with some calli showing a texture and color similar to the embryogenic ones (Figure 20e). However, acetocarmine staining (2% w/v) (Figure 20f,g) indicated that this callus remained non-embryogenic.

Different from the above-mentioned explants, apical shoot buds with open scales (represented in Figure 18b) first developed a white-green soft embryogenic-like tissue at the upper wounded area, which then, growing only at this location of the explant, started to stiffen and acquire a yellowish color before the first subculture (Figure 20h,i). When comparing the differences obtained from the calli proliferated at 23 ℃ and 28 ℃, these calli presented a darker color and stiffer morphology when cultured at 28 ℃ (Figure 20j). All of the shoot slices from the reinvigorated axillary shoots cultured in the SE induction media were able to produce a non-embryogenic callus.

The tissue obtained in the S11 medium (Figure 20k) was brown, stiffer, and harder to disaggregate when compared to calli produced in the S10 induction medium (Figure 20l), which presented a lighter color, were softer, and had the easiest morphology to disaggregate. The calli induced in the S2 induction medium presented an intermediate aspect.

As described above, proliferation was consistent in all of the different initial explants and proliferation treatments. However, variations in the consistency, texture, and color of the developed tissue were observed between treatments. Also, during proliferation, tissue had similar characteristics to an embryogenic callus as it started growing, but with time it started losing those characteristics, becoming darker, stiffer, and developing non-embryogenic cells. In this sense, the initially developed cells were collected in an attempt at maturation but no somatic embryos could be obtained.

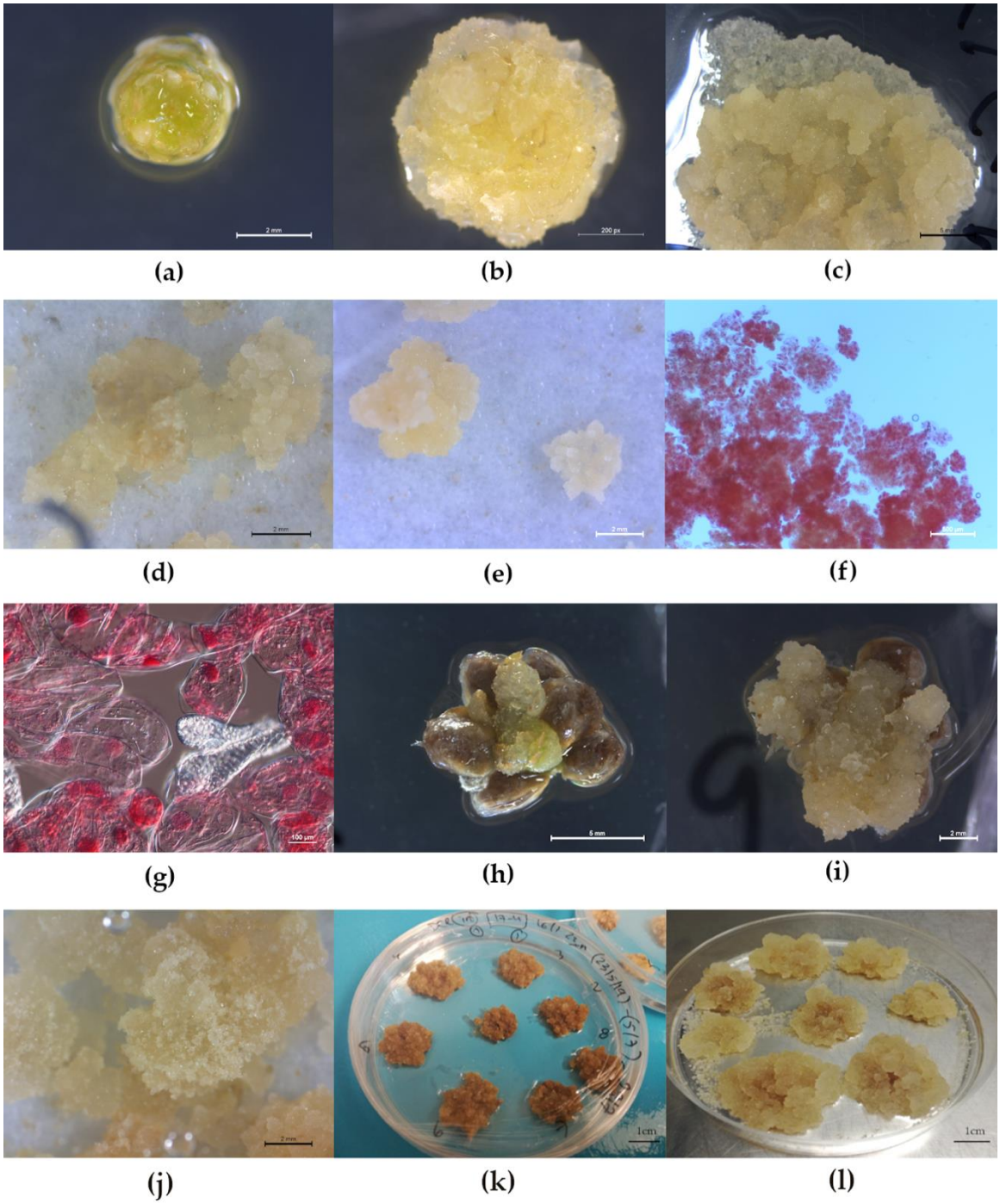

Figure 20. Induction response of apical shoot buds and axillary shoots to somatic embryogenesis (SE) **(a)** bud slice in the SE induction medium; **(b)** tissue development throughout the explant; **(c)** later proliferation of directly subcultured non-embryogenic callus; **(d)** filtered cultured tissue on the proliferation medium with 50 nM phytosulfokine; **(e)** example of non-embryogenic calli with distinct morphology in the same sample: the callus at the bottom right has more similarities with the embryogenic one; **(f)** cells collected from the lower cluster represented above, stained with acetocarmine (2% w/v) and observed using a Leica DMS1000, showing non-polarized cells; **(g)** observation of previous cells using a Nikon ECLIPSE 80i, demonstrating the non-embryogenic state of the calli; **(h)** bud slice in the SE induction medium with tissue development in the upper wounded area of the explant; **(i)** tissue development progress in the upper area of the explant with no tissue development throughout the whole explant; **(j)** filtered cultured tissue proliferating at 28 ºC; **(k)** non-embryogenic calli formed in the S11 induction medium; **(l)** non-embryogenic calli formed in the S10 induction medium.

5. Discussion

Organogenic process

The common criteria to identify reinvigoration or rejuvenation of explants are based on morphology, morphogenic and rooting capacity, and the ability to produce cones or flowers (Wendling et al. 2014). However, uncertainties remain over whether true rejuvenation can be reached by artificial methods, or whether these methods merely provide reinvigoration through the continuous *in vitro* subculture of the shoots. In the present study, for the first time, we were able to obtain reinvigorated axillary shoots through organogenesis, from the two BA treatments tested (22 and 44 µM), using apical shoot buds as explants. Then, successfully acclimatized plants were obtained.

Three different sterilization protocols were used, employing ethanol, commercial bleach, and silver nanoparticles, and the highest level of decontamination was obtained with bleach. The effective elimination of contamination could contribute to the better establishment of the shoot buds. This must be achieved with the least possible damage since a minor injury caused during sterilization can block the future growth and development of the explants. As reviewed in Sarmast (2018), ethanol and sodium hypochlorite are two of the most common chemicals used to decontaminate woody species. However, silver nanoparticles are quite effective at controlling physiochemical changes, preventing bacterial infections, and actively blocking ethylene through the release of silver ions, which could improve the induction of explants. Despite the fact that nanoparticle sterilization was not efficient in our case, changes to time or concentration could lead to better results and explant quality (Bello-Bello et al. 2017; Kim et al. 2017).

The evaluation of the organogenic response was made by considering the percentage of explants forming shoots (EFS) (%) and the number of shoots formed per explant (NS/E). The results showed that no statistically significant differences between treatments were obtained for EFS (%). When the mature zygotic embryos were used as initial explants in this species (Lambardi et al. 1993), a cytokinin alone, specially BA at the higher concentration tested (10 µM), also proved satisfactory for bud induction. Likewise, BA, either used alone or in combination with other cytokinins, was the most used growth regulator in organogenesis and its concentration played an important role in the explant response (De Diego et al. 2008). Several micropropagation protocols for the induction of axillary shoots in *Pinus* species supplement the culture media with different concentrations of BA ranging from 1 to 50 µM (Lambardi et al. 1993; Stojičić et al. 1999; Kalia et al. 2007; Cortizo et al. 2009; Montalbán et al. 2011b). When the induction medium was supplemented with 44 µM BA, the NS/E obtained from the explants was more than double that of the explants induced at 22 µM BA. These results agree with those obtained in *Pinus pinea* (Moncaleán et al. 2005), where higher concentrations of BA (44.4 µM), as compared to regular doses of 4.4 and 10 µM, led to a significantly higher number of buds being formed per explant during the first 16 days of culture, and no differences between the three concentrations tested after 35 days in culture. In *Pinus roxburghii* (Kalia et al. 2007), *P. pinaster* (De Diego et al. 2008), and

Pinus radiata (Montalbán et al. 2011b) higher concentrations of BA promoted lower organogenic capacity or lower elongation rates. In *P. elliottii* (Nunes et al. 2018), it was also shown that high levels of cytokinins may interfere with the normal development of axillary shoots and, despite the promotion of bud induction, they may compromise cell elongation and shoot elongation. It appears that the toxic environment created by the excess of BA seen in those species did not happen in our case and that the use of activated charcoal (AC) in our elongation medium proved efficient to detoxify the culture medium at both concentrations tested (22 and 44 µM BA). As has been reviewed previously by Pan and Van Staden (1998), some of the positive effects of the use of AC in micropropagation can be attributed to the removal of inhibitory substances from the media itself and of toxic plant metabolites released from the tissue into the culture. Taking all the above-mentioned data into account, the induction of explants with 44 µM of BA and the addiction of AC to the elongation medium appears to be a good strategy for Aleppo pine organogenic induction.

It is widely recognized that different genotypes and genetic backgrounds may lead to differences in terms of the *in vitro* performance and cloning capacity in different conifer species (Von Aderkas and Bonga 2000; Bonga et al. 2010). Previously, studies developed by our group on the organogenesis of different *Pinus* species (De Diego et al. 2008; Montalbán et al. 2011b, 2013a), and somatic embryogenesis in *Pinus halepensis* (Montalbán et al. 2013b), also corroborated this effect. In this sense, no statistical analysis was performed concerning the genotype effect. Despite that fact, the mean results obtained for different genotypes presented, in general, a higher EFS (%) and NS/E for the explants cultured at 44 µM BA, and no differences were obtained regarding acclimatization between different genotypes.

The root induction treatment applied in this study, with long exposure to Indole- 3-butyric acid (IBA), was not effective. Contrary, both pulses of IBA for five days in a solid medium and liquid pulses for four hours have previously proven efficient in the development of *in vitro* roots in this species (Lambardi et al. 1993). For many years, IBA has been applied to different plant species to induce adventitious roots (Ragonezi et al. 2010), however, the use of 1-Naphthaleneacetic acid (NAA), combined with IBA or alone, has proved successful for inducing root meristem differentiation in *Pinus* species (Álvarez et al. 2009; Montalbán et al. 2013a). Also, a study focused on the rooting of cuttings of mature *Pinus halepensis* (Riov et al. 2020), has shown that pulses for four hours of IBA alone, auxin combinations, and the use of the quick-dip method with IBA alone, are efficient for root development and further acclimatization of the cuttings. Our plants were able to produce *ex vitro* roots and acclimatize successfully. In this sense, further testing of different auxins, either alone or in different combinations, and of different induction times could improve this step of the Aleppo pine regeneration protocol. The application of short pulses or the quick-dip method could lead to a substantial reduction of time needed for the attainment of acclimatized true-to-type plants.

Attempts to Induce Embryogenic Tissue

In this work, we used various explants for the induction of embryogenic tissue, including apical shoot buds from both somatic and zygotic trees and reinvigorated axillary shoots developed during organogenesis. Woody species suffer a "phase change" or ontogenetic aging during their development, defined as a shift from the juvenile state to the adult state, which is usually characterized by a decrease in growth and the start of flowering (Von Aderkas and Bonga 2000; Díaz-Sala 2019). Once this shift occurs, there is a significant loss of organogenic and embryogenic capacity. Also, initial explants had been considered the most important factor for mature SE accomplishment and it has been suggested that culture-derived material could be more responsive in tissue cultures (Von Aderkas and Bonga 2000; Klimaszewska et al. 2011).

In addition to explants, plant growth regulators, culture conditions and media composition also have a great influence on the embryogenic response (Corredoira et al. 2019). Various induction media with different combinations of auxins (2,4-Dichlorophenoxyacetic acid and NAA) along with lower concentrations of cytokinins (BA and kinetin) were tested for the induction of the explants. As mentioned above, the ratio between auxins and cytokinins can be determinant to the developmental fate of explants *in vitro* (Skoog and Miller 1957). Cytokinins, or a higher ratio of cytokinin to auxin, are usually required for the induction of shoot organogenesis, while higher ratios of auxin to cytokinins typically favor SE (Zhang and Lemaux 2004). Our basal media were based on one used in *Pinus contorta* (Park et al. 2010) because they were able to induce embryogenic-like tissue from the shoot buds of mature trees, and one used for SE induction from immature megagametophytes of *P. halepensis*, as previously established in our laboratory (Montalbán et al. 2013b; Pereira et al. 2016).

All embryogenic-like tissue obtained initially produced non-embryogenic calli in the proliferation stage and no somatic embryos were produced. The primary objective of the induction phase is for the somatic cells of the explant to acquire embryogenic competence and, reprogramming the gene expression followed by polarized growth of the cells is required for that purpose (Corredoira et al. 2019). The success of this step is essential for the entire process (Stasolla and Thorpe 2011). Nonetheless, the non-embryogenic tissue obtained had proliferation capacity, since it presented the ability to continuously originate new tissue throughout all subcultures performed in the proliferation media. Likewise, in *Pinus contorta* (Park et al. 2010), they were able to develop calli with proliferation capacity and different morphologies, some of them with an embryogenic-like structure, that at the end were not able to produce somatic embryos. Non-embryogenic calli in other *Pinus* species have also been described as white-yellowish friable tissue containing spherical cells with prominent nuclei and without evidence of polarity that grow darker and necrotic with time (Klubicová et al. 2017; Salaj et al. 2019). Also, a study developed in our laboratory (Tavares 2019), tested different explants at different development stages with similar induction mediums.

Finally, we tested the influence of phytosulfokine, a small sulfated peptide involved in the initial step of cellular dedifferentiation, proliferation and re-differentiation, in the induction

medium (Igasaki et al. 2003). It did not lead to the ultimate formation of somatic embryos. However, it helped maintain the induced calli which were proliferating with a lighter color, and had the softer and easiest morphology to disaggregate. In *Daucus carota* (Kobayashi et al. 1999), *Cryptomeria japonica* (Igasaki et al. 2003), and *Pinus elliottii* (Yang et al. 2020) phytosulfokine also significantly increased cell division, proliferation, and the number of somatic embryos developed.

6. Conclusions

This is the first report of successful *in vitro* regeneration of *Pinus halepensis* adult trees. The regeneration of *P. halepensis* through organogenesis using apical shoot buds as explants was achieved. Reinvigorated shoots from both juvenile somatic trees and adult trees were obtained, and a proliferative chain of microshoots coming from the buds of the adult trees was developed. In this sense, true-to-type plants from five different genotypes (H8, H32, 17.3, P1, and P8) were successfully obtained and plants acclimatized to ex vitro conditions were developed.

Despite our efforts to induce embryogenic tissue from mature trees, we were not able to produce somatic embryos. Nonetheless, we were able to produce proliferating embryogenic-like tissue and identify morphological differences with the application of different concentrations of phytosulfokine. Further experiments should be done, modifying the chemical and physical conditions of proliferation and the maturation of the embryogenic-like tissue.

General Conclusions and Future Perspectives

The endless socio-economic and ecological value inherent to forest ecosystems, together with the anthropological and climatic threats that they are constantly exposed to, raise the need to increase the quality and productivity of forest trees. In this regard, comprehend how climatic factors impact tree's function, survival and adaptation is vital to predict the consequences that the expected extreme environmental events may have on these ecosystems. Aleppo pine is a Mediterranean conifer with significant ecological plasticity that has been extensively used for afforestation programs, and SE has been proved to be an efficient means to study embryo development as well as to learn the various mechanisms involved in stress response and adaptation of plants.

With this purpose, alongside the fact that an effective protocol for SE of *P. halepensis* has been previously described, the main goal of this work was to trigger the formation of a long-lasting metabolic and epigenetic "stress memory", through the application of high temperatures during the initiation stage of *Pinus halepensis* SE. Moreover, to study the influence of heat stress regarding the success of the SE process and the use of that technique as a tool to understand the mechanisms underlying stress-response in conifers were the objectives. For this matter, different temperature treatments were applied during the induction of EMS (40 ℃ for 4 h, 50 ℃ for 30 min, and 60 ℃ for 5 min).

It was possible not only to obtain plants from all induction treatments, but also to assess that there were no significant differences between initiation, proliferation, maturation, or germination rates for the different treatments assayed and the standard conditions (23 ℃ for 9 weeks). This indicates that not only it is possible to induce SE under heat stress in *P. halepensis*, but also that the application of high temperature pulses during the initiation phase of SE does not translate into genetic variety loss.

In the same line, concerning the morphological and ultrastructural characterization of the embryogenic cultures, heat stress did not provoke visible changes in the cell types or organization levels at the observed PEMs. And, the small differences found at the amounts of storage (starch grains and lipidic bodies) and phenolic compounds could not be directly linked with the control of the embryogenic process or the success of SE.

At the maturation stage, data regarding the morphology and number of somatic embryos showed significant differences; nevertheless, the somatic embryos were well formed, and the differences in size found in different treatments did not influence their germination capacity. In fact, the only substantial variation detected along the SE process was the number of somatic embryos produced, where the highest number was obtained at samples initiated at 60 ℃ (5 min). In this sense, this specific temperature treatment appears to have triggered a positive effect on the efficiency of *P. halepensis* SE; adding to the fact that a similar number of ECLs could be produced, maintaining the expected genetic diversity, a higher number of plants could be obtained from the same ECL. Contrarily, the 40 ℃ (4 h) and 50 ℃ (30 min) treatments led to significantly lower

numbers of somatic embryos. Consequently, short-term pulses of high temperatures appear to be a good strategy to increase the number and quality of somatic embryos produced.

Regarding the analysis of endogenous concentration of CKs in EMs, different temperatures at the initiation phase of SE led to different hormonal profiles. As a general trend, a significantly higher concentration of isoprenoid CKs was found at EMs induced at 50 ℃ (30 min) when compared to the control; samples from 40 ℃ (4 h) and 60 ℃ (5 min) presented intermediate concentrations. Regarding aromatic CKs, samples from 40 ℃ (4 h) generally presented substantially lower concentrations than those initiated under other temperature treatments. Given the different induction times of the treatments, it seems that these results corroborate the concept that short-term or mild stresses stimulate CKs accumulation, while prolonged or more severe stresses (40 ℃ for 4 h) are generally associated with downregulation of active CKs levels. Also, a clear correlation between temperature stress and the accumulation of *o*T and *c*Z types was found.

Alongside the clear effect that high temperatures had at the concentration of CKs as a stress consequence *per se*, specific hormonal profiles could relate to differences seen at the SE efficiency; samples from 60 ℃ (5 min) and the control had similar low concentration of *c*Z, iP and DHZR, and these treatments produced higher numbers of somatic embryos. In this regard, these results emphasize the idea that the CKs are directly involved in temperature stress response and may alone function as regulators of the embryogenic process.

In order to validate the epigenetic memory premise, the effect of different induction treatments on the global DNA methylation patterns was evaluated. However, no significant differences were found concerning DNA methylation levels. Nevertheless, at proliferating EMs a difference of 3.3% was found between the 60 ℃ (5 min) treatment, that presented the lowest concentrations of 5mC, and the 50 ℃ (30 min) treatment that had the highest methylation rate. Considering that it has been previously suggested that DNA methylation is critical for the success of SE, and it is commonly found at lower values in embryogenic tissues with respect to the non-embryogenic tissues, this could correlate to the differences obtained at embryo formation.

As a consequence of stress, plants can also modulate the expression of specific genes, and it was found that the differential expression patterns of stress-related genes changed along different stages of SE. A gradual increase at the relative expression of *DI19* gene along the higher temperature treatments was found in EMs, while the relative expression of *P444* and *SOD* was lower in *in vitro* somatic plants coming from EMs primed with high temperatures. This suggests that in *P. halepensis*, stress-related gene overexpression may happen during and/or shortly after the heat stress occurs, with the priming effect leading to their stabilization and lower expression over time.

Again, SOD was significantly repressed in needles sampled in plants derived from 50 ℃ (30 min), presenting a similar pattern to the one found for endogenous concentration of isoprenoid CKs, and reinforcing the concept that short or mild stress activate different mechanisms than more prolonged / severe stresses.

Finally, the effect of heat stress in the proteome and the concentration of soluble sugars, sugar alcohols and amino acids of *P. halepensis* EMs was assessed, and significant proteomic and metabolic reorganization was found.

The reorganization of basal and secondary metabolic pathways such as glycolysis, the tricarboxylic acid cycle, and secondary metabolites production has been found in different pine species as a general stress-response. 27 proteins related with heat stress response were identified in this work, and, accordingly, several enzymes directly involved in metabolic pathways were up-accumulated at samples from higher temperatures.

In addition, proteins previously accepted to be involved in temperature stress response such as histones (histone H4 variant TH091 and histone H2A.2.2), ribosomal proteins (40S ribosomal protein S15a-1 and 60S ribosomal protein L18-3) and the HSP chaperonin CPN60 were up-accumulated at higher temperatures. Strangely, 20 kDa chaperonin, a HSP that functions as a co-chaperone along with CPN60, was down- accumulated at samples from heat stress conditions. However, this co-chaperone, alone, has been reported to induce the upregulation of superoxide dismutase genes. In this regard, earlier results showed that no significant differences could be found regarding *SOD* concentrations at EMs, but a down-regulation was indeed found at the *in vitro* somatic plants obtained from stressful conditions.

Also, no significant differences were found at the transcription assay performed in this study. Altogether, this data suggests that the majority of the differences found at the proteomic profiles may result from posttranscriptional regulation rather than directly from transcription.

Overall, although the mechanisms in which they are involved are not clear so far, it is strongly accepted that a great variety of metabolites of low molecular mass can prevent the damaging change in cellular components and restore homeostasis under stress. In agreement, lower concentrations of sucrose, glycine and cysteine, and a higher concentration of glutamine, were present at higher temperatures. Highlighting the direct involvement of these primary metabolites in temperature stress response.

In conclusion, all the work presented exposed valuable information regarding temperature-induced priming. While no epigenetic memory could be confirmed, it appears that a metabolic one might be. The application of heat stress at the initial stage of SE provoked long-lasting effects throughout the SE process, and allowed to pinpoint specific CKs, proteins, stress-related genes and metabolites involved in the intricate mechanisms underlying stress response and/or the embryogenic process in conifers.

Lastly, to genetically replicate a specific donor tree, protocols for both organogenesis and somatic embryogenesis from adult explants were tested. When woody species suffer the “phase change” during their development, defined as a shift from the juvenile state to the adult state, it usually leads to a significant loss of organogenic and embryogenic capacity. In this sense, because of its proven effectiveness the initial explants for SE of Aleppo pine were megagametophytes containing immature embryos. Nonetheless, these explants do not allow the selection of specific genotypes, as they were collected from open pollinated trees, and the phenotypic characteristics of

the originated plants would not be seen until years later. Likewise, regarding the organogenesis protocol previously described for *P. halepensis*, mature somatic embryos were used as explants, which raises the same difficulty.

To resolve this issue, the culture of mature explants to induce organogenesis and SE was performed in order to clone mature trees of *P. halepensis*. Regarding SE induction, the various explants analysed led to the formation of an embryogenic-like tissue that proliferated into non-embryogenic calli and no somatic embryos were obtained. Notwithstanding, it was possible to obtain reinvigorated axillary shoots through organogenesis using apical shoot buds as explants from the two BA treatments tested (22 and 44 µM), and to successfully acclimatize the obtained plants. In this sense, this is the first report of a successful protocol for *in vitro* regeneration of *P. halepensis* adult trees. And, since a considerably higher number of shoots could be obtained from the same explant at 44 µM of BA, this seems to be the best treatment to increase the efficiency of the organogenic process.

Altogether, several breakthroughs have been accomplished in this research. This work has shed new insights into the mechanism underlying stress response, as well as heat stress "memory", and allowed the improvement and establishment of SE and organogenesis protocols for Aleppo pine.

In the future, further studies should be conducted to test the plasticity of plants coming from EMs initiated at different temperatures. No data regarding *ex vitro* plants was presented here as this work focused on the *in vitro* stages of the SE process. However, physiological, morphological and -omic analysis carried out in the resulting plants, under stressful periods in the greenhouse, would be of great importance. This analysis could confirm that the phenotypic characteristics could be preserved over time and that an enhanced resistance to higher temperatures and better adaptation to climate change may perhaps have been obtained.

Also, additional analyses to attest the formation of an epigenetic memory should be performed, as it was not possible to do it here. The global DNA methylation analysis was accomplished and no significant differences were found, but specific genes or sections of the DNA could be differentially methylated and that study was not performed. Also, there are other epigenetic changes like histone modifications, and possibly combined mechanisms between different epigenetic changes, that could support our initial theory.

References

Abdullah A, Yeoman M, Grace J (1987) Micropropagation of mature Calabrian pine (*Pinus brutia* Ten.) from fascicular buds. Tree Physiol 136:123–136. https://doi.org/10.1093/treephys/3.2.123

Abrahamsson M, Valladares S, Merino I, Larsson E, von Arnold S (2017) Degeneration pattern in somatic embryos of *Pinus sylvestris* L. In Vitro Cell Dev Biol - Plant 53:86–96. https://doi.org/10.1007/s11627-016-9797-y

Aitken-Christie J, Singh AP, Davies H (1988) Multiplication of meristematic tissue: A new tissue culture system for radiata pine. In: Hanover JW, Keathley DE, Wilson CM, Kuny G (eds) Genetic Manipulation of Woody Plants. Springer US, Boston, pp 413–432

Almeselmani M, Deshmukh PS, Sairam RK, Kushwaha SR, Singh TP (2006) Protective role of antioxidant enzymes under high temperature stress. Plant Sci 171:382–388. https://doi.org/10.1016/J.PLANTSCI.2006.04.009

Alvarez C, Valledor L, Sáez P, Hasbún R, Sánchez-Olate M, Cañal MJ, Ríos D (2016) Changes in gene expression in needles and stems of *Pinus radiata* rootstock plants of different ontogenic age. Am J Plant Sci 07:1205–1216. https://doi.org/10.4236/ajps.2016.78116

Alvarez JM, Bueno N, Cuesta C, Feito I, Ordás RJ (2020) Hormonal and gene dynamics in *de novo* shoot meristem formation during adventitious caulogenesis in cotyledons of *Pinus pinea*. Plant Cell Rep 39:527–541. https://doi.org/10.1007/s00299-020-02508-0

Álvarez JM, Majada J, Ordás RJ (2009) An improved micropropagation protocol for maritime pine (*Pinus pinaster* Ait.) isolated cotyledons. Forestry 82:175–184. https://doi.org/10.1093/forestry/cpn052

Amaral-Silva P, Clarindo W, Guilhen J, de Jesus Passos A, Sanglard N, Ferreira A (2021) Global 5-methylcytosine and physiological changes are triggers of indirect somatic embryogenesis in *Coffea canephora*. Protoplasma 258:45–57. https://doi.org/10.1007/S00709-020-01551-8

Amaral J, Ribeyre Z, Vigneaud J, Dia Sow R, Fichot R, Messier C, Pinto G, Nolet P, Maury S (2020) Advances and promises of epigenetics for forest trees. Forests 11:976. https://doi.org/10.3390/f11090976

Anjo SI, Santa C, Manadas B (2015) Short GeLC-SWATH: A fast and reliable quantitative approach for proteomic screenings. Proteomics 15:757–762. https://doi.org/10.1002/pmic.201400221

Arbona V, Manzi M, de Ollas C, Gómez-Cadenas A (2013) Metabolomics as a tool to investigate abiotic stress tolerance in plants. Int J Mol Sci 14:4885–4911. https://doi.org/10.3390/ijms14034885

Arnholdt-Schmitt B (2004) Stress-induced cell reprogramming. A role for global genome regulation? Plant Physiol 136:2579–2586. https://doi.org/10.1104/pp.104.042531

Arrillaga I, Morcillo M, Zanón I, Lario F, Segura J, Sales E (2019) New approaches to optimize somatic embryogenesis in maritime pine. Front Plant Sci 10:1–14.

https://doi.org/10.3389/fpls.2019.00138

Auler PA, do Amaral MN, Braga EJB, Maserti B (2021) Drought stress memory in rice guard cells: Proteome changes and genomic stability of DNA. Plant Physiol Biochem 169:49–62. https://doi.org/10.1016/j.plaphy.2021.10.028

Awada R, Campa C, Gibault E, Déchamp E, Georget F, Lepelley M, Abdallah C, Erban A, Martinez-Seidel F, Kopka J, Legendre L, Léran S, Conéjéro G, Verdeil JL, Crouzillat D, Breton D, Bertrand B, Etienne H (2019) Unravelling the metabolic and hormonal machinery during key steps of somatic embryogenesis: A case study in coffee. Int J Mol Sci 20:4665. https://doi.org/10.3390/ijms20194665

Ayari A, Khouja ML (2014) Ecophysiological variables influencing Aleppo pine seed and cone production: A review. Tree Physiol 34:426–437. https://doi.org/10.1093/treephys/tpu022

Ayari A, Zubizarreta-Gerendiain A, Tome M, Tome J, Garchi S, Henchi B (2012) Variables de parcela, árbol y copa que afectan la producción de piñas y piñones en bosques de pino carrasco de túnez. For Syst 21:128–140. https://doi.org/10.5424/fs/2112211-11463

Baránek M, Křižan B, Ondrušíková E, Pidra M (2010) DNA-methylation changes in grapevine somaclones following *in vitro* culture and thermotherapy. Plant Cell Tissue Organ Cult 101:11–22. https://doi.org/10.1007/s11240-009-9656-1

Baroja-Fernández E, Aguirreolea J, Martínková H, Hanuš J, Strnad M (2002) Aromatic cytokinins in micropropagated potato plants. Plant Physiol Biochem 40:217–224. https://doi.org/10.1016/S0981-9428(02)01362-1

Bäurle I (2018) Can't remember to forget you: Chromatin-based priming of somatic stress responses. Semin Cell Dev Biol 83:133–139. https://doi.org/10.1016/j.semcdb.2017.09.032

Becwar MR, Nagmani R, Wann SR (1990) Initiation of embryogenic cultures and somatic embryo development in loblolly pine (*Pinus taeda*). Can J For Res 20:810–817. https://doi.org/10.1139/x90-107

Bello-Bello JJ, Chavez-Santoscoy RA, Lecona-Guzmán CA, Bogdanchikova N, Salinas-Ruíz J, Gómez-Merino FC, Pestryakov A (2017) Hormetic response by silver nanoparticles on *in vitro* multiplication of sugarcane (*Saccharum* spp. Cv. Mex 69-290) using a temporary immersion system. Dose-Response 15:1–9. https://doi.org/10.1177/1559325817744945

Bieleski RL (1964) The problem of halting enzyme action when extracting plant tissues. Anal Biochem 9:431–442. https://doi.org/10.1016/0003-2697(64)90204-0

Blödner C, Skroppa T, Johnsen Ø, Polle A (2005) Freezing tolerance in two Norway spruce (*Picea abies* [L.] Karst.) progenies is physiologically correlated with drought tolerance. J Plant Physiol 162:549–558. https://doi.org/10.1016/J.JPLPH.2004.09.005

Boisvenue C, Running SW (2006) Impacts of climate change on natural forest productivity - evidence since the middle of the 20th century. Glob Chang Biol 12:862–882. https://doi.org/10.1111/j.1365-2486.2006.01134.x

Bonga JM (2015) A comparative evaluation of the application of somatic embryogenesis, rooting of cuttings, and organogenesis of conifers. Can J For Res 45:379–383.

https://doi.org/10.1139/cjfr-2014-0360

Bonga JM (2017) Can explant choice help resolve recalcitrance problems in *in vitro* propagation, a problem still acute especially for adult conifers? Trees - Struct Funct 31:781–789. https://doi.org/10.1007/s00468-016-1509-z

Bonga JM, Klimaszewska KK, von Aderkas P (2010) Recalcitrance in clonal propagation, in particular of conifers. Plant Cell. Tissue Organ Cult. 100:241–254

Borges A, Jiménez-Arias D, Expósito-Rodríguez M, Sandalio LM, Pérez JA (2014) Priming crops against biotic and abiotic stresses: MSB as a tool for studying mechanisms. Front Plant Sci 5:642. https://doi.org/10.3389/fpls.2014.00642

Borji M, Bouamama-Gzara B, Chibani F, Teyssier C, Ammar A Ben, Mliki A, Zekri S, Ghorbel A (2018) Micromorphology, structural and ultrastructural changes during somatic embryogenesis of a Tunisian oat variety (*Avena sativa* L. var 'Meliane'). Plant Cell Tissue Organ Cult 132:329–342. https://doi.org/10.1007/s11240-017-1333-1

Botella L, Santamaría O, Diez JJ (2010) Fungi associated with the decline of *Pinus halepensis* in Spain. Fungal Divers 40:1–11. https://doi.org/10.1007/s13225-010-0025-5

Boyko A, Blevins T, Yao Y, Golubov A, Bilichak A, Ilnytskyy Y, Hollander J, Meins FJ, Kovalchuk I (2010) Transgenerational adaptation of *Arabidopsis* to stress requires DNA methylation and the function of Dicer-Like proteins. PLoS One 5:e9514. https://doi.org/10.1371/JOURNAL.PONE.0009514

Boyko A, Kovalchuk I (2008) Epigenetic control of plant stress response. Environ Mol Mutagen 49:61–72. https://doi.org/10.1002/em.20347

Bräutigam K, Vining KJ, Lafon-Placette C, Fossdal CG, Mirouze M, Gutiérrez Marcos J, Fluch S, Fraga MF, Guevara MÁ, Abarca D, Johnsen Ø, Maury S, Strauss SH, Campbell MM, Rohde A, Díaz-Sala C, Cervera MT (2013) Epigenetic regulation of adaptive responses of forest tree species to the environment. Ecol Evol 3:399–415. https://doi.org/10.1002/ece3.461

Bravo S, Bertín A, Turner A, Sepúlveda F, Jopia P, Parra MJ, Castillo R, Hasbún R (2017) Differences in DNA methylation, DNA structure and embryogenesis-related gene expression between embryogenic and non embryogenic lines of *Pinus radiata* D. don. Plant Cell Tissue Organ Cult 130:521–529. https://doi.org/10.1007/s11240-017-1242-3

Bruce TJA, Matthes MC, Napier JA, Pickett JA (2007) Stressful "'memories'" of plants: evidence and possible mechanisms. Plant Sci 173:603–608. https://doi.org/10.1016/j.plantsci.2007.09.002

Calvo L, García-Domínguez C, Naranjo A, Arévalo JR (2013) Effects of light/darkness, thermal shocks and inhibitory components on germination of *Pinus canariensis*, *Pinus halepensis* and *Pinus pinea*. Eur J For Res 132:909–917. https://doi.org/10.1007/s10342-013-0729-7

Canhoto JM (2010) Biotecnologia Vegetal da Clonagem de Plantas à Transformação Genética. Imprensa da Universidade de Coimbra, Coimbra, Portugal

Carneros E, Celestino C, Klimaszewska K, Park YS, Toribio M, Bonga JM (2009) Plant regeneration in Stone pine (*Pinus pinea* L.) by somatic embryogenesis. Plant Cell Tissue

Organ Cult 98:165–178. https://doi.org/10.1007/s11240-009-9549-3

Carnicer J, Barbeta A, Sperlich D, Coll M, Penuelas J (2013) Contrasting trait syndromes in angiosperms and conifers are associated with different responses of tree growth to temperature on a large scale. Front Plant Sci 4:409. https://doi.org/10.3389/fpls.2013.00409

Castander-Olarieta A, Montalbán IA, De Medeiros Oliveira E, Dell'aversana E, D'amelia L, Carillo P, Steiner N, Fraga HPDF, Guerra MP, Goicoa T, Ugarte MD, Pereira C, Moncaleán P (2019) Effect of thermal stress on tissue ultrastructure and metabolite profiles during initiation of radiata pine somatic embryogenesis. Front Plant Sci 9:1–16. https://doi.org/10.3389/fpls.2018.02004

Castander-Olarieta A, Moncaleán P, Montalbán IA (2020a) *Pinus canariensis* plant regeneration through somatic embryogenesis. For Syst 29:61–66. https://doi.org/10.5424/fs/2020291-16136

Castander-Olarieta A, Pereira C, Sales E, Meijón M, Arrillaga I, Cañal MJ, Goicoa T, Ugarte MD, Moncaleán P, Montalbán IA (2020b) Induction of radiata pine somatic embryogenesis at high temperatures provokes a long-term decrease in DNA methylation/hydroxymethylation and differential expression of stress-related genes. Plants 9:1–16. https://doi.org/10.3390/plants9121762

Castander-Olarieta A, Moncaleán P, Pereira C, Pěnčík A, Petřík I, Pavlović I, Novák O, Strnad M, Goicoa T, Ugarte MD, Montalbán IA (2021a) Cytokinins are involved in drought tolerance of *Pinus radiata* plants originating from embryonal masses induced at high temperatures. Tree Physiol 41:912–926. https://doi.org/10.1093/TREEPHYS/TPAA055

Castander-Olarieta A, Pereira C, Montalbán I, Mendes VM, Correia S, Suárez-Álvarez S, Manadas B, Canhoto J, Moncaleán P (2021b) Proteome-wide analysis of heat-stress in *Pinus radiata* somatic embryos reveals a combined response of sugar metabolism and translational regulation mechanisms. Front Plant Sci 12:631239. https://doi.org/10.3389/fpls.2021.631239

Castander-Olarieta A, Pereira C, Montalbán IA, Pěnčík A, Petřík I, Pavlović I, Novák O, Strnad M, Moncaleán P (2021c) Quantification of endogenous aromatic cytokinins in *Pinus radiata* embryonal masses after application of heat stress during initiation of somatic embryogenesis. Trees - Struct Funct 35:1075–1080. https://doi.org/10.1007/s00468-020-02047-x

Castander-Olarieta A, Pereira C, Mendes VM, Correia S, Manadas B, Canhoto J, Montalbán IA, Moncaleán P (2022) Thermopriming-associated proteome and sugar content responses in *Pinus radiata* embryogenic tissue. Plant Sci 321:111327. https://doi.org/10.1016/j.plantsci.2022.111327

Celestino C, Hernández I, Carneros E, Toribio DLM (2005) La embriogénesis somática como elemento central de la biotecnología forestal. Investig Agrar Sist y Recur For 14:345–357

Chalupa V (1985) Somatic embryogenesis and plantlet regeneration from cultured immature and mature embryos of *Picea abies* (L.) Karst. Commun Inst For Cech 14:57–63.

Chang SH, Ho CK, Chen ZZ, Tsay JY (2001) Micropropagation of *Taxus mairei* from mature trees. Plant Cell Rep 20:496–502. https://doi.org/10.1007/s002990100362

Charity JA, Holland L, Grace LJ, Walter C (2005) Consistent and stable expression of the *npt*II, *uid*A and *bar* genes in transgenic *Pinus radiata* after *Agrobacterium tumefaciens*-mediated transformation using nurse cultures. Plant Cell Rep 23:606–616. https://doi.org/10.1007/s00299-004-0851-6

Chen Q, Wang B, Ding H, Zhang J, Li S (2019) Review: The role of NADP-malic enzyme in plants under stress. Plant Sci 281:206–212. https://doi.org/10.1016/j.plantsci.2019.01.010

Chevalier F, Rossignol M (2011) Proteomic analysis of *Arabidopsis thaliana* ecotypes with contrasted root architecture in response to phosphate deficiency. J Plant Physiol 168:1885–1890. https://doi.org/10.1016/j.jplph.2011.05.024

Ciura J, Kruk J (2018) Phytohormones as targets for improving plant productivity and stress tolerance. J Plant Physiol 229:32–40. https://doi.org/10.1016/j.jplph.2018.06.013

Coninck T De, Van Damme EJM (2021) Review : The multiple roles of plant lectins. Plant Sci 313:111096. https://doi.org/10.1016/j.plantsci.2021.111096

Conrath U (2011) Molecular aspects of defence priming. Trends Plant Sci 16:524–531. https://doi.org/10.1016/J.TPLANTS.2011.06.004

Corredoira E, Merkle SA, Martínez MT, Toribio M, Canhoto JM, Correia SI, Ballester A, Vieitez AM (2019) Non-zygotic embryogenesis in hardwood species. CRC Crit Rev Plant Sci 38:29–97. https://doi.org/10.1080/07352689.2018.1551122

Correia B, Valledor L, Meijón M, Rodriguez JL, Dias MC, Santos C, Cañal MJ, Rodriguez R, Pinto G (2013) Is the interplay between epigenetic markers related to the acclimation of cork oak plants to high temperatures? PLoS One 8:. https://doi.org/10.1371/journal.pone.0053543

Correia S, Vinhas R, Manadas B, Lourenço AS, Veríssimo P, Canhoto JM (2012) Comparative proteomic analysis of auxin-induced embryogenic and nonembryogenic tissues of the solanaceous tree *Cyphomandra betacea* (tamarillo). J Proteome Res 11:1666–1675. https://doi.org/10.1021/pr200856w

Cortizo M, de Diego N, Moncaleán P, Ordás RJ (2009) Micropropagation of adult Stone Pine (*Pinus pinea* L.). Trees - Struct Funct 23:835–842. https://doi.org/10.1007/s00468-009-0325-0

Crisp PA, Ganguly D, Eichten SR, Borevitz JO, Pogson BJ (2016) Reconsidering plant memory: Intersections between stress recovery, RNA turnover, and epigenetics. Sci Adv 2:e1501340. https://doi.org/10.1126/sciadv.1501340

Cuesta C, Novák O, Ordás RJ, Fernández B, Strnad M, Doležal K, Rodríguez A (2012) Endogenous cytokinin profiles and their relationships to between-family differences during adventitious caulogenesis in *Pinus pinea* cotyledons. J Plant Physiol 169:1830–1837. https://doi.org/10.1016/j.jplph.2012.08.012

Davis JM, Becwar MR (2017) Examples of current implementation of cloning technology worldwide. In Page A (Ed.), Developments in Tree Cloning, Pira International Ltd, Leatherhead, UK, pp. 32-33

De-la-Peña C, Nic-Can GI, Galaz-Ávalos RM, Avilez-Montalvo R, Loyola-Vargas VM (2015) The

role of chromatin modifications in somatic embryogenesis in plants. Front Plant Sci 6:635. https://doi.org/10.3389/FPLS.2015.00635

de Almeida M, de Almeida CV, Graner EM, Brondani GE, de Abreu-Tarazi MF (2012) Pre-procambial cells are niches for pluripotent and totipotent stem-like cells for organogenesis and somatic embryogenesis in the peach palm: A histological study. Plant Cell Rep 31:1495–1515. https://doi.org/10.1007/s00299-012-1264-6

de Araújo Silva-Cardoso IM, Meira FS, Gomes ACMM, Scherwinski-Pereira JE (2020) Histology, histochemistry and ultrastructure of pre-embryogenic cells determined for direct somatic embryogenesis in the palm tree *Syagrus oleracea*. Physiol Plant 168:845–875. https://doi.org/10.1111/ppl.13026

De Diego N, Montalbán IA, Fernandez De Larrinoa E, Moncaleán P (2008) *In vitro* regeneration of *Pinus pinaster* adult trees. Can J For Res 38:2607–2615. https://doi.org/10.1139/X08-102

De Diego N, Montalbán IA, Moncaleán P (2010) *In vitro* regeneration of adult *Pinus sylvestris* L. trees. South African J Bot 76:158–162. https://doi.org/10.1016/j.sajb.2009.09.007

Díaz-Sala C (2014) Direct reprogramming of adult somatic cells toward adventitious root formation in forest tree species: The effect of the juvenile-adult transition. Front Plant Sci 5:1–8. https://doi.org/10.3389/fpls.2014.00310

Díaz-Sala C (2019) Molecular dissection of the regenerative capacity of forest tree species: Special focus on conifers. Front Plant Sci 9:1–10. https://doi.org/10.3389/fpls.2018.01943

do Nascimento AMM, Barroso PA, do Nascimento NFF, Goicoa T, Ugarte MD, Montalbán IA, Moncaleán P (2020) *Pinus* spp. somatic embryo conversion under high temperature: Effect on the morphological and physiological characteristics of plantlets. Forests 11:1181. https://doi.org/10.3390/f11111181

do Nascimento AMM, Polesi LG, Back FP, Steiner N, Guerra MP, Castander-Olarieta A, Moncaleán P, Montalbán IA (2021) The chemical environment at maturation stage in *Pinus* spp. somatic embryogenesis: implications in the polyamine profile of somatic embryos and morphological characteristics of the developed plantlets. Front Plant Sci 12:1–19. https://doi.org/10.3389/fpls.2021.771464

Dobrá J, Černý M, Štorchová H, Dobrev P, Skalák J, Jedelský PL, Lukšanová H, Gaudinová A, Pešek B, Malbecka J, Vanek T, Brzobohatý B, Vanková R (2015) The impact of heat stress targeting on the hormonal and transcriptomic response in *Arabidopsis*. Plant Sci 231:52–61. https://doi.org/10.1016/J.PLANTSCI.2014.11.005

Dodeman VL, Ducreux G, Kreis M (1997) Zygotic embryogenesis versus somatic embryogenesis. J Exp Bot 48:1493–1509. https://doi.org/10.1093/jxb/48.8.1493

Edreva A, Velikova V, Tsonev T, Dagnon S, Gürel A, Aktaş L, Gesheva E (2008) Stress-protective role of secondary metabolites: diversity of functions and mechanisms. Gen Appl Plant Physiol 34:67–78

Efeoğlu B (2009) Heat shock proteins and heat shock response in plants. Gazi Univ J Sci 22:67–75

Eliášová K, Vondráková Z, Malbeck J, Trávníčková A, Pešek B, Vágner M, Cvikrová M (2017)

Histological and biochemical response of Norway spruce somatic embryos to UV-B irradiation. Trees - Struct Funct 31:1279–1293. https://doi.org/10.1007/s00468-017-1547-1

Elvira NJ, Lloret F, Jaime L, Margalef-Marrase J, Pérez Navarro MÁ, Batllori E (2021) Species climatic niche explains post-fire regeneration of Aleppo pine (*Pinus halepensis* Mill.) under compounded effects of fire and drought in east Spain. Sci Total Environ 798:149308. https://doi.org/10.1016/j.scitotenv.2021.149308

Escandón M, Cañal MJ, Pascual J, Pinto G, Correia B, Amaral J, Meijón M (2015) Integrated physiological and hormonal profile of heat-induced thermotolerance in *Pinus radiata*. Tree Physiol 36:63–77. https://doi.org/10.1093/treephys/tpv127

Escandón M, Valledor L, Pascual J, Pinto G, Cañal MJ, Meijón M (2017) System-wide analysis of short-term response to high temperature in *Pinus radiata*. J Exp Bot 68:3629–3641. https://doi.org/10.1093/jxb/erx198

Escudero A, Sanz MV, Pita JM, Pérez-García F (1999) Probability of germination after heat treatment of native spanish pines. Ann For Sci 56:511–520. https://doi.org/10.1051/forest:19990608

Evans HF, McNamara DG, Braasch H, Chadoeuf J, Magnusson C (1996) Pest Risk Analysis (PRA) for the territories of the European Union (as PRA area) on *Bursaphelenchus xylophilus* and its vectors in the genus *Monochamus*. EPPO Bull 26:199–249. https://doi.org/10.1111/j.1365-2338.1996.tb00594.x

Fahad S, Hussain S, Matloob A, Khan FA, Khaliq A, Saud S, Hassan S, Shan D, Khan F, Ullah N, Faiq M, Khan MR, Tareen AK, Khan A, Ullah A, Ullah N, Huang J (2015) Phytohormones and plant responses to salinity stress: a review. Plant Growth Regul. 75:391–404. https://doi.org/10.1016/j.envexpbot.2017.11.003

Falahi H, Sharifi M, Maivan HZ, Chashmi NA (2018) Phenylethanoid glycosides accumulation in roots of *Scrophularia striata* as a response to water stress. Environ Exp Bot 147:13–21. https://doi.org/10.1016/j.envexpbot.2017.11.003

FAO, (2022) SOFO The state of the world´s forests 2022, https://www.fao.org/3/cb9360en/online/cb9360en.html

Farjon A (2018) Conifers of the World. Kew Bull 73:8. https://doi.org/10.1007/S12225-018-9738-5

Feher A, Ötvös K, Pasternak TP, Pettkó-Szandtner A (2008) The involvement of reactive oxygen species (ROS) in the cell cycle activation (G0-to-G1 transition) of plant cells . Plant Signal Behav 3:823–826. https://doi.org/10.4161/PSB.3.10.5908

Fehér A (2015) Somatic embryogenesis - stress-induced remodeling of plant cell fate. Biochim Biophys Acta - Gene Regul Mech 1849:385–402. https://doi.org/10.1016/j.bbagrm.2014.07.005

Ferguson L, Grafton-Cardwell E (2014) *Citrus* production manual. ANR Catalog, University of California, USA

Filonova LH, Bozhkov P V., Brukhin VB, Daniel G, Zhivotovsky B, von Arnold S (2000) Two

waves of programmed cell death occur during formation and development of somatic embryos in the gymnosperm, Norway spruce. J Cell Sci 113:4399–4411

Fraga HP de F, Vieira L do N, Puttkammer CC, dos Santos HP, Garighan J de A, Guerra MP (2016) Glutathione and abscisic acid supplementation influences somatic embryo maturation and hormone endogenous levels during somatic embryogenesis in *Podocarpus lambertii* Klotzsch ex Endl. Plant Sci 253:98–106. https://doi.org/10.1016/j.plantsci.2016.09.012

Fraga HPF, Vieira LN, Puttkammer CC, Oliveira EM, Guerra MP (2015) Time-lapse cell tracking reveals morphohistological features in somatic embryogenesis of *Araucaria angustifolia* (Bert) O. Kuntze. Trees - Struct Funct 29:1613–1623. https://doi.org/10.1007/s00468-015-1244-x

Fraga MF, Cañal M, Rodríguez R (2002) Phase-change related epigenetic and physiological changes in *Pinus radiata* D. Don. Planta 2002 2154 215:672–678. https://doi.org/10.1007/S00425-002-0795-4

Frébort I, Kowalska M, Hluska T, Frébortová J, Galuszka P (2011) Evolution of cytokinin biosynthesis and degradation. J Exp Bot 62:2431–2452. https://doi.org/10.1093/jxb/err004

Frugis G, Giannino D, Mele G, Nicolodi C, Chiappetta A, Bitonti MB, Innocenti AM, Dewitte W, Van Onckelen H, Mariotti D (2001) Overexpression of *KNAT1* in lettuce shifts leaf determinate growth to a shoot-like indeterminate growth associated with an accumulation of isopentenyl-type cytokinins. Plant Physiol 126:1370–1380. https://doi.org/10.1104/pp.126.4.1370

Gallusci P, Dai Z, Génard M, Gauffretau A, Leblanc-Fournier N, Richard-Molard C, Vile D, Brunel-Muguet S (2017) Epigenetics for plant improvement: Current knowledge and modeling avenues. Trends Plant Sci 22:610–623. https://doi.org/10.1016/j.tplants.2017.04.009

Garcia-Mendiguren O, Montalbán IA, Stewart D, Moncaleán P, Klimaszewska K, Rutledge RG (2015) Gene expression profiling of shoot-derived calli from adult radiata pine and zygotic embryo-derived embryonal masses. PLoS One 10:1–19. https://doi.org/10.1371/journal.pone.0128679

García-Mendiguren O, Montalbán IA, Correia S, Canhoto J, Moncaleán P (2016a) Different environmental conditions at initiation of radiata pine somatic embryogenesis determine the protein profile of somatic embryos. Plant Biotechnol 33:143–152. https://doi.org/10.5511/plantbiotechnology.16.0520a

García-Mendiguren O, Montalbán IA, Goicoa T, Ugarte MD, Moncaleán P (2016b) Environmental conditions at the initial stages of *Pinus radiata* somatic embryogenesis affect the production of somatic embryos. Trees - Struct Funct 30:949–958. https://doi.org/10.1007/s00468-015-1336-7

Gazol A, Ribas M, Gutiérrez E, Camarero JJ (2017) Aleppo pine forests from across Spain show drought-induced growth decline and partial recovery. Agric For Meteorol 232:186–194. https://doi.org/10.1016/j.agrformet.2016.08.014

Ghafari H, Hassanpour H, Jafari M, Besharat S (2020) Physiological, biochemical and gene-expressional responses to water deficit in apple subjected to partial root-zone drying (PRD). Plant Physiol Biochem 148:333–346. https://doi.org/10.1016/j.plaphy.2020.01.034

Ghazghazi H, Riahi L, Yangui I, Messaoud C, Rzigui T, Nasr Z (2022) Effect of drought stress on physio-biochemical traits and secondary metabolites production in the woody species *Pinus halepensis* Mill. at a juvenile development stage. J Sustain For 41:878–894. https://doi.org/10.1080/10549811.2022.2048263

Gil L, Aránzazu P (1993) Pines as basic species for restoration of forests in the Mediterranean environment. Ecol 7:113–125

Gomez MP, Segura J (1995) Axillary shoot proliferation in cultures of explants from mature *Juniperus oxycedrus* trees. Tree Physiol 15:625–628. https://doi.org/10.1093/treephys/15.9.625

González-Zamora Á, Almendra-martín L, de Luis M, Martínez-Fernández J (2021) Influence of soil moisture vs. climatic factors in *Pinus Halepensis* growth variability in Spain : A study with remote sensing and modeled data. Remote Sens 13:757. https://doi.org/https://doi.org/10.3390/rs13040757

Gupta PK, Durzan DJ (1986) Plantlet regeneration via somatic embryogenesis from subcultured callus of mature embryos of *Picea abies* (Norway spruce). Vitr Cell Dev Biol 22:685–688. https://doi.org/10.1007/bf02623484

Haider S, Raza A, Iqbal J, Shaukat M, Mahmood T (2022) Analyzing the regulatory role of heat shock transcription factors in plant heat stress tolerance: a brief appraisal. Mol Biol Rep 49:5771–5785. https://doi.org/10.1007/s11033-022-07190-x

Hakman I, Fowke LC, von Arnold S, Eriksson T (1985) The development of somatic embryos in tissue cultures initiated from immature embryos of *Picea abies* (Norway Spruce). Plant Sci 38:53–59. https ://doi.org/10.1016/0168-9452(85)90079-2

Hamayun M, Hussain A, Khan SA, Irshad M, Khan AL, Waqas M, Shahzad R, Iqbal A, Ullah N, Rehman G, Kim HY, Lee IJ (2015) Kinetin modulates physio-hormonal attributes and isoflavone contents of soybean grown under salinity stress. Front Plant Sci 6:1–11. https://doi.org/10.3389/fpls.2015.00377

Harfouche A, Meilan R, Altmane A (2011) Tree genetic engineering and applications to sustainable forestry and biomass production. Trends Biotechnol 29:9–17. https://doi.org/10.1016/j.tibtech.2010.09.003

Hargreaves C, Reeves C, Gough K, Montalbán IA, Low C, van Ballekom S, Dungey HS, Moncaleán P (2017) Nurse tissue for embryo rescue: testing new conifer somatic embryogenesis methods in a F1 hybrid pine. Trees - Struct Funct 31:273–283. https://doi.org/10.1007/s00468-016-1482-6

Hasanuzzaman M, Nahar K, Alam MM, Roychowdhury R, Fujita M (2013) Physiological, biochemical, and molecular mechanisms of heat stress tolerance in plants. Int J Mol Sci 14:9643–9684. https://doi.org/10.3390/ijms14059643

Hauser MT, Aufsatz W, Jonak C, Luschnig C (2011) Transgenerational epigenetic inheritance in plants. Biochim Biophys Acta - Gene Regul Mech 1809:459–468. https://doi.org/10.1016/J.BBAGRM.2011.03.007

Havlová M, Dobrev PI, Motyka V, Štorchová H, Libus J, Dobrá J, Malbeck J, Gaudinová A, Vanková R (2008) The role of cytokinins in responses to water deficit in tobacco plants over-expressing *trans*-zeatin *O*-glucosyltransferase gene under 35S or SAG12 promoters. Plant, Cell Environ 31:341–353. https://doi.org/10.1111/j.1365-3040.2007.01766.x

Hazubska-Przybył T (2019) Propagation of *Juniper* species by plant tissue culture: A mini-review. Forests 10: 1028. https://doi.org/10.3390/f10111028

Hemantaranjan A, Nishant Bhanu A, Singh M, Yadav D, Patel P, Singh R, Katiyar D (2014) Heat stress responses and thermotolerance. Adv Plants Agric Res 1:62–70. https://doi.org/10.15406/apar.2014.01.00012

Hu B, Sakakibara H, Takebayashi Y, Peters FS, Schumacher J, Eiblmeier M, Arab L, Kreuzwieser J, Polle A, Rennenberg H (2017) Mistletoe infestation mediates alteration of the phytohormone profile and anti-oxidative metabolism in bark and wood of its host *Pinus sylvestris*. Tree Physiol 37:676–691. https://doi.org/10.1093/treephys/tpx006

Igasaki T, Akashi N, Ujino-Ihara T, Matsubayashi Y, Sakagami Y, Shinohara K (2003) Phytosulfokine stimulates somatic embryogenesis in *Cryptomeria japonica*. Plant Cell Physiol 44:1412–1416. https://doi.org/10.1093/pcp/pcg161

Jaouadi W, Naghmouchi S, Alsubeie M (2019) Should the silviculture of Aleppo pine (*Pinus halepensis* Mill.) stands in northern Africa be oriented towards wood or seed and cone production? Diagnosis and current potentiality. iForest - Biogeosciences For 12:297–305. https://doi.org/10.3832/ifor2965-012

Jia J, Zhou J, Shi W, Cao X, Luo J, Polle A, Luo Z Bin (2017) Comparative transcriptomic analysis reveals the roles of overlapping heat-/drought-responsive genes in poplars exposed to high temperature and drought. Sci Rep 7:1–17. https://doi.org/10.1038/srep43215

Johnsen Ø, Dæhlen OG, Østreng G, Skrøppa T (2005a) Daylength and temperature during seed production interactively affect adaptive performance of *Picea abies* progenies. New Phytol 168:589–596. https://doi.org/10.1111/j.1469-8137.2005.01538.x

Johnsen Ø, Fossdal CG, Nagy N, MØlmann Jø, Dæhlen OG, SkrØppa T (2005b) Climatic adaptation in *Picea abies* progenies is affected by the temperature during zygotic embryogenesis and seed maturation. Plant, Cell Environ 28:1090–1102. https://doi.org/10.1111/j.1365-3040.2005.01356.x

Joy IV RW, Yeung EC, Kong L, Thorpe TA (1991) Development of white spruce somatic embryos: I. Storage product deposition. Vitr Cell Dev Biol - Plant 27:32–41. https://doi.org/10.1007/BF02632059

Juarez-Escobar J, Bojórquez-Velázquez E, Elizalde-Contreras JM, Guerrero-Analco JA, Loyola-Vargas VM, Mata-Rosas M, Ruiz-May E (2021) Current proteomic and metabolomic knowledge of zygotic and somatic embryogenesis in plants. Int J Mol Sci 22:11807

Kalia RK, Arya S, Kalia S, Arya ID (2007) Plantlet regeneration from fascicular buds of seedling shoot apices of *Pinus roxburghii* Sarg. Biol Plant 51:653–659. https://doi.org/10.1007/s10535-007-0138-1

Kim DH, Gopal J, Sivanesan I (2017) Nanomaterials in plant tissue culture: The disclosed and undisclosed. RSC Adv 7:36492–36505. https://doi.org/10.1039/c7ra07025j

Klein T, Cohen S, Yakir D (2011) Hydraulic adjustments underlying drought resistance of *Pinus halepensis*. Tree Physiol 31:637–648. https://doi.org/10.1093/TREEPHYS/TPR047

Klimaszewska K, Trontin J-F, Becwar MR, Devillard C, Park Y-S, Lelu-Walter M-A (2007) Recent progress in somatic embryogenesis of four *Pinus* spp. Tree For Sci Biotechnol 1:11–25

Klimaszewska K, Overton C, Stewart D, Rutledge RG (2011) Initiation of somatic embryos and regeneration of plants from primordial shoots of 10-year-old somatic white spruce and expression profiles of 11 genes followed during the tissue culture process. Planta 233:635–647. https://doi.org/10.1007/s00425-010-1325-4

Klubicová K, Uvácková L, Danchenko M, Nemecek P, Skultéty L, Salaj J, Salaj T (2017) Insights into the early stage of *Pinus nigra* Arn. somatic embryogenesis using discovery proteomics. J Proteomics 169:99–111. https://doi.org/10.1016/j.jprot.2017.05.013

Kobayashi T, Eun CH, Hanai H, Matsubayashi Y, Sakagami Y, Kamada H (1999) Phytosulphokine-α, a peptidyl plant growth factor, stimulates somatic embryogenesis in carrot. J Exp Bot 50:1123–1128. https://doi.org/10.1093/jxb/50.336.1123

Korotko U, Chwiałkowska K, Sańko-Sawczenko I, Kwasniewski M (2021) DNA demethylation in response to heat stress in *Arabidopsis thaliana*. Int J Mol Sci 22:1–20. https://doi.org/10.3390/ijms22041555

Kotak S, Larkindale J, Lee U, Koskull-do P Von, Vierling E, Scharf K (2007) Complexity of the heat stress response in plants. Curr Opin Plant Biol 10:310–316. https://doi.org/10.1016/j.pbi.2007.04.011

Kumar S, Kumari R, Sharma V, Sharma V (2013) Roles, and establishment, maintenance and erasing of the epigenetic cytosine methylation marks in plants. J Genet 92:629–666. https://doi.org/10.1007/s12041-013-0273-8

Kumari A, Baskaran P, Plačková L, Omámiková H, Nisler J, Doležal K, Van Staden J (2018) Plant growth regulator interactions in physiological processes for controlling plant regeneration and *in vitro* development of *Tulbaghia simmleri*. J Plant Physiol 223:65–71. https://doi.org/10.1016/j.jplph.2018.01.005

Kuo WY, Huang CH, Liu AC, Cheng CP, Li SH, Chang WC, Weiss C, Azem A, Jinn TL (2012) CHAPERONIN 20 mediates iron superoxide dismutase (*FeSOD*) activity independent of its co-chaperonin role in *Arabidopsis* chloroplasts. New Phytol 197:99–110. https://doi.org/10.1111/j.1469-8137.2012.04369.x

Lambardi M, Sharma KK, Thorpe TA (1993) Optimization of *in vitro* bud induction and plantlet formation from mature embryos of Aleppo pine (*Pinus halepensis* Mill.). Vitr Cell Dev Biol - Plant 29:189–199. https://doi.org/10.1007/BF02632034

Lamelas L, Valledor L, Escandón M, Pinto G, Cañal MJ, Meijón M (2020) Integrative analysis of the nuclear proteome in *Pinus radiata* reveals thermopriming coupled to epigenetic regulation. J Exp Bot 71:2040–2057. https://doi.org/10.1093/jxb/erz524

Lämke J, Bäurle I (2017) Epigenetic and chromatin-based mechanisms in environmental stress adaptation and stress memory in plants. Genome Biol 18:1–11. https://doi.org/10.1186/s13059-017-1263-6

Lee K, Seo PJ (2018) Dynamic epigenetic changes during plant regeneration. Trends Plant Sci 23:235–247. https://doi.org/10.1016/j.tplants.2017.11.009

Lelu-Walter MA, Thompson D, Harvengt L, Sanchez L, Toribio M, Pâques LE (2013) Somatic embryogenesis in forestry with a focus on Europe: State-of-the-art, benefits, challenges and future direction. Tree Genet Genomes 9:883–899. https://doi.org/10.1007/s11295-013-0620-1

Letham DS (1984) Cytokinins as phytohormones — Sites of biosynthesis, translocation, and function of translocated cytokinin. In: Mok DWS, Mok MC (eds) Cytokinins: Chemistry, Activity, and Function. CRC Press, New York, USA, pp 57–80

Lewis SL, Edwards DP, Galbraith D (2015) Increasing human dominance of tropical forests. Science 349, 827–832 https://doi.org/10.1126/science.aaa9932

Lin Y, I MRW, Heidmann LJ (1991) *In vitro* formation of axillary buds by immature shoots of Ponderosa pine. Plant Cell Tissue Organ Cult 26:161–166. https://doi.org/10.1007/BF00039938

Lindner M, Maroschek M, Netherer S, Kremer A, Barbati A, Garcia-Gonzalo J, Seidl R, Delzon S, Corona P, Kolström M, Lexer MJ, Marchetti M (2010) Climate change impacts, adaptive capacity, and vulnerability of European forest ecosystems. For Ecol Manage 259:698–709. https://doi.org/10.1016/j.foreco.2009.09.023

Ling Y, Serrano N, Gao G, Atia M, Mokhtar M, Woo YH, Bazin J, Veluchamy A, Benhamed M, Crespi M, Gehring C, Reddy ASN, Mahfouz MM (2018) Thermopriming triggers splicing memory in *Arabidopsis*. J Exp Bot 69:2659–2675. https://doi.org/10.1093/JXB/ERY062

Lira-Medeiros CF, Parisod C, Fernandes RA, Mata CS, Cardoso MA, Ferreira PCG (2010) Epigenetic variation in mangrove plants occurring in contrasting natural environment. PLoS One 5:e10326. https://doi.org/10.1371/JOURNAL.PONE.0010326

Liu CJ, Zhao Y, Zhang K (2019a) Cytokinin transporters: Multisite players in cytokinin homeostasis and signal distribution. Front Plant Sci 10:1–9. https://doi.org/10.3389/fpls.2019.00693

Liu W, Xu J, Fu W, Wang X, Lei C, Chen Y (2019b) Evidence of stress imprinting with population-level differences in two moss species. Ecol Evol 9:6329–6341. https://doi.org/10.1002/ece3.5205

Liu WX, Zhang FC, Zhang WZ, Song LF, Wu WH, Chen YF (2013) *Arabidopsis* Di19 functions as a transcription factor and modulates *PR1*, *PR2*, and *PR5* expression in response to drought stress. Mol Plant 6:1487–1502. https://doi.org/10.1093/mp/sst031

Livak KJ, Schmittgen TD (2001) Analysis of relative gene expression data using real-time quantitative PCR and the 2(-Delta Delta C(T)) Method. Methods 25:402–408. https://doi.org/10.1006/METH.2001.1262

López-Escamilla AL, Olguín-Santos LP, Márquez J, Chávez VM, Bye R (2000) Adventitious bud formation from mature embryos of *Picea chihuahuana* Martínes, an endangered mexican spruce tree. Ann Bot 86:921–927. https://doi.org/10.1006/anbo.2000.1257

Lu C, Harry IS, Thompson MR, Thorpe TA (1991) Plantlet regeneration from cultured embryos and seedling parts of red spruce (*Picea rubens* Sarg.). Bot Gaz 152:42–50

Ludvigsen M, Honoré B (2018) Transcriptomics and proteomics: integration? eLS 1–7. https://doi.org/10.1002/9780470015902.a0006188.pub2

Mahdavi-Darvari F, Noor NM, Ismanizan I (2015) Epigenetic regulation and gene markers as signals of early somatic embryogenesis. Plant Cell Tissue Organ Cult 120:407–422. https://doi.org/10.1007/s11240-014-0615-0

Marondedze C, Thomas L, Gehring C, Lilley KS (2019) Changes in the *Arabidopsis* RNA-binding proteome reveal novel stress response mechanisms. BMC Plant Biol 19:139. https://doi.org/10.1186/s12870-019-1750-x

Maruyama TE, Hosoi Y (2019) Progress in somatic embryogenesis of Japanese pines. Front Plant Sci 10:1–15. https://doi.org/10.3389/fpls.2019.00031

Matsubayashi Y, Ogawa M, Kihara H, Niwa M, Sakagami Y (2006) Disruption and overexpression of *Arabidopsis* phytosulfokine receptor gene affects cellular longevity and potential for growth. Plant Physiol 142:45–53. https://doi.org/10.1104/pp.106.081109

Matysiak K, Kierzek R, Siatkowski I, Kowalska J, Krawczyk R, Miziniak W (2020) Effect of exogenous application of amino acids L-Arginine and glycine on maize under temperature stress. Agronomy 10:769. https://doi.org/10.3390/agronomy10060769

Mauri A, Leo M Di, Rigo D De, Caudullo G (2016) *Pinus halepensis* and *Pinus brutia* in Europe: distribution, habitat, usage and threats. In: San-Miguel-Ayanz J, de Rigo D, Caudullo G, Houston Durrant T, Mauri A (eds) European Atlas of Forest Tree Species. European Comission, pp 122–123

Mazzucotelli E, Mastrangelo AM, Crosatti C, Guerra D, Stanca AM, Cattivelli L (2008) Abiotic stress response in plants : when post-transcriptional and post-translational regulations control transcription. Plant Sci 174:420–431. https://doi.org/10.1016/j.plantsci.2008.02.005

Milla MA, Townsend J, Chang IF, Cushman JC (2006) The *Arabidopsis AtDi19* gene family encodes a novel type of Cys2/His2 zinc-finger protein implicated in ABA-independent dehydration, high-salinity stress and light signaling pathways. Plant Mol Biol 61:13–30. https://doi.org/10.1007/S11103-005-5798-7

Mirouze M, Paszkowski J (2011) Epigenetic contribution to stress adaptation in plants. Curr Opin Plant Biol 14:267–274. https://doi.org/10.1016/j.pbi.2011.03.004

MITECO (2015) Los pinares de pino carrasco https://www.miteco.gob.es/es/biodiversidad/temas/inventariosnacionales/phalepensis_tcm30

-153816.pdf

Mittler R, Finka A, Goloubinoff P (2012) How do plants feel the heat? Trends Biochem Sci 37:118–125. https://doi.org/10.1016/J.TIBS.2011.11.007

Moncaleán P, Alonso P, Centeno ML, Cortizo M, Rodríguez A, Fernández B, Ordás RJ (2005) Organogenic responses of *Pinus pinea* cotyledons to hormonal treatments: BA metabolism and cytokinin content. Tree Physiol 25:1–9. https://doi.org/10.1093/treephys/25.1.1

Moncaleán P, García-Mendiguren O, Novák O, Strnad M, Goicoa T, Ugarte MD, Montalbán IA (2018) Temperature and water availability during maturation affect the cytokinins and auxins profile of radiata pine somatic embryos. Front Plant Sci 9:1–13. https://doi.org/10.3389/fpls.2018.01898

Montalbán I a., De Diego N, Moncaleán P (2010) Bottlenecks in *Pinus radiata* somatic embryogenesis: improving maturation and germination. Trees 24:1061–1071. https://doi.org/10.1007/s00468-010-0477-y

Montalbán I a., De Diego N, Moncaleán P (2011a) Enhancing initiation and proliferation in radiata pine (*Pinus radiata* D. Don) somatic embryogenesis through seed family screening, zygotic embryo staging and media adjustments. Acta Physiol Plant 34:451–460. https://doi.org/10.1007/s11738-011-0841-6

Montalbán IA, De Diego N, Moncaleán P (2011b) Testing novel cytokinins for improved *in vitro* adventitious shoots formation and subsequent *ex vitro* performance in *Pinus radiata*. Forestry 84:363–373. https://doi.org/10.1093/forestry/cpr022

Montalbán IA, de Diego N, Moncaleán P (2012) Enhancing initiation and proliferation in radiata pine (*Pinus radiata* D. Don) somatic embryogenesis through seed family screening, zygotic embryo staging and media adjustments. Acta Physiol Plant 34:451–460. https://doi.org/10.1007/s11738-011-0841-6

Montalbán IA, Novák O, Rolčik J, Strnad M, Moncaleán P (2013a) Endogenous cytokinin and auxin profiles during *in vitro* organogenesis from vegetative buds of Pinus radiata adult trees. Physiol Plant 148:214–231. https://doi.org/10.1111/j.1399-3054.2012.01709.x

Montalbán IA, Setién-Olarra A, Hargreaves CL, Moncaleán P (2013b) Somatic embryogenesis in *Pinus halepensis* Mill.: an important ecological species from the Mediterranean forest. Trees 27:1339–1351. https://doi.org/10.1007/s00468-013-0882-0

Montalbán IA, García-Mendiguren O, Goicoa T, Ugarte MD, Moncaleán P (2015) Cold storage of initial plant material affects positively somatic embryogenesis in *Pinus radiata*. New For 46:309–317. https://doi.org/10.1007/s11056-014-9457-1

Montalbán IA, Moncaleán P (2017) Long term conservation at -80ºC of *Pinus radiata* embryogenic cell lines: Recovery, maturation and germination. Cryo-Letters 38:202–209

Montalbán IA, Olarieta AC, Pereira C, Canhoto J, Moncaleán P (2020) Use of biotechnology in forestry breeding programs for natural resources and biodiversity conservation : Creating super trees for the future. In: Chong P, Newman D, Steinmacher D (eds) Agricultural, Forestry and Bioindustry Biotechnology and Biodiscovery, Springer, Cham, pp 103–115

Montalbán IA, Castander-Olarieta A, Hargreaves CL, Gough K, Reeves CB, Ballekom S van, Goicoa T, Ugarte MD, Moncaleán P (2021) Hybrid pine (*Pinus attenuata* × *Pinus radiata*) somatic embryogenesis: What do you prefer, mother or nurse? Forests 12:1–12. https://doi.org/10.3390/f12010045

Montero JL, Alcanda P (1993) Reforestación y biodiversidad. Montes, 33:57-76.

Morel A, Teyssier C, Trontin JF, Eliášová K, Pešek B, Beaufour M, Morabito D, Boizot N, Le Metté C, Belal-Bessai L, Reymond I, Harvengt L, Cadene M, Corbineau F, Vágner M, Label P, Lelu-Walter MA (2014) Early molecular events involved in *Pinus pinaster* Ait. somatic embryo development under reduced water availability: Transcriptomic and proteomic analyses. Physiol Plant 152:184–201. https://doi.org/10.1111/ppl.12158

Morin X, Fahse L, Jactel H, Scherer-Lorenzen M, Garcia-Valdés R, Bugmann H (2018) Long-term response of forest productivity to climate change is mostly driven by change in tree species composition. Sci Rep 8:5627. https://doi.org/10.1038/s41598-018-23763-y

Nakabayashi R, Saito K (2015) Integrated metabolomics for abiotic stress responses in plants. Curr Opin Plant Biol 24:10–16. https://doi.org/10.1016/j.pbi.2015.01.003

Ne'eman G, Goubitz S, Nathan R (2004) Reproductive traits of *Pinus halepensis* in the light of fire- A critical review. Plant Ecol 171:69–79. https://doi.org/10.1023/B:VEGE.0000029380.04821.99

Nehra NS, Becwar MR, Rottmann WH, Pearson L, Chowdhury K, Chang S, Wilde HD, Kodrzycki RJ, Zhang C, Gause KC, Parks DW, Hinchee MA (2005) Forest biotechnology: Innovative methods, emerging opportunities. Vitr Cell Dev Biol - Plant 41:701–717. https://doi.org/10.1079/IVP2005691

Neilson KA, Gammulla CG, Mirzaei M, Imin N, Haynes PA (2010) Proteomic analysis of temperature stress in plants. Proteomics 10:828–845. https://doi.org/10.1002/pmic.200900538

Nishiyama R, Watanabe Y, Fujita Y, Le DT, Kojima M, Werner T, Vankova R, Yamaguchi-Shinozaki K, Shinozaki K, Kakimoto T, Sakakibara H, Schmülling T, Tran LSP (2011) Analysis of cytokinin mutants and regulation of cytokinin metabolic genes reveals important regulatory roles of cytokinins in drought, salt and abscisic acid responses, and abscisic acid biosynthesis. Plant Cell 23:2169–2183. https://doi.org/10.1105/tpc.111.087395

Noceda C, Salaj T, Pérez M, Viejo M, Cañal MJ, Salaj J, Rodriguez R (2009) DNA demethylation and decrease on free polyamines is associated with the embryogenic capacity of *Pinus nigra* Arn. cell culture. Trees 2009 236 23:1285–1293. https://doi.org/10.1007/S00468-009-0370-8

Nunes S, Sousa D, Pereira VT, Correia S, Marum L, Santos C, Dias MC (2018) Efficient protocol for *in vitro* mass micropropagation of slash pine. Vitr Cell Dev Biol - Plant 54:175–183. https://doi.org/10.1007/s11627-018-9891-4

Olivar J, Rais A, Pretzsch H, Bravo F (2022) The impact of climate and adaptative forest management on the intra-annual growth of *Pinus halepensis* based on long-term dendrometer recordings. Forests 13:1–11. https://doi.org/10.3390/f13060935

Osem Y, Yavlovich H, Zecharia N, Atzmon N, Moshe Y, Schiller G (2013) Fire-free natural regeneration in water limited *Pinus halepensis* forests: a silvicultural approach. Eur J For Res 132:679–690. https://doi.org/10.1007/s10342-013-0704-3

Oseni OM, Pande V, Nailwal TK (2018) A review on plant tissue culture, a technique for propagation and conservation of endangered plant species. Int J Curr Microbiol Appl Sci 7:3778–3786. https://doi.org/10.20546/ijcmas.2018.707.438

Pan MJ, Van Staden J (1998) The use of charcoal in *in vitro* culture - A review. Plant Growth Regul 26:155–163. https://doi.org/10.1023/A:1006119015972

Pan Y, Birdsey RA, Phillips OL, Jackson RB (2013) The structure, distribution, and biomass of the world´s forests. Annu Rev Ecol Evol Syst 44:593–622. https://doi.org/10.1146/annurev-ecolsys-110512-135914

Pang Z, Chong J, Li S, Xia J (2020) Metaboanalystr 3.0: Toward an optimized workflow for global metabolomics. Metabolites 10:186. https://doi.org/10.3390/metabo10050186

Park SY, Klimaszewska K, Park JY, Mansfield SD (2010) Lodgepole pine: The first evidence of seed-based somatic embryogenesis and the expression of embryogenesis marker genes in shoot bud cultures of adult trees. Tree Physiol 30:1469–1478. https://doi.org/10.1093/treephys/tpq081

Park Y-S (2002) Implementation of conifer somatic embryogenesis in clonal forestry: technical requirements and deployment considerations. Ann For Sci 59:651–656. https://doi.org/10.1051/forest

Park Y, Ding C, Lenz P, Nadeau S, Adams G, Millican S, Beaulieu J, Bousquet J (2019) Implementing genomic selection for multi-varietal forestry of white spruce Implementing genomic selection for multi-varietal forestry of white spruce (*Picea glauca*) in New Brunswick , Canada. The 5th International Conference of the IUFRO Unit 2.09.02.pp.230-233

Pereira C, Montalbán IA, García-Mendiguren O, Goicoa T, Ugarte MD, Correia S, Canhoto JM, Moncaleán P (2016) *Pinus halepensis* somatic embryogenesis is affected by the physical and chemical conditions at the initial stages of the process. J For Res 21:143–150. https://doi.org/10.1007/s10310-016-0524-7

Pereira C, Montalbán IA, Goicoa T, Ugarte MD, Correia S, Canhoto JM, Moncaleán P (2017) The effect of changing temperature and agar concentration at proliferation stage in the final success of Aleppo pine somatic embryogenesis. For Syst 26:3–6. https://doi.org/10.5424/fs/2017263-11436

Pereira C, Castander-Olarieta A, Montalbán IA, Pěnčík A, Petřík I, Pavlović I, Oliveira EDM, Fraga HP de F, Guerra MP, Novák O, Strnad M, Canhoto J, Moncaleán P (2020) Embryonal masses induced at high temperatures in Aleppo pine: cytokinin profile and cytological characterization. Forests 11:807. https://doi.org/10.3390/F11080807

Pereira C, Castander-Olarieta A, Sales E, Montalbán IA, Canhoto J, Moncaleán P (2021) Heat stress in *Pinus halepensis* somatic embryogenesis induction : effect in DNA methylation and differential expression of stress-related genes. Plants 10:2333.

https://doi.org/10.3390/plants10112333

Pérez-Oliver MA, Haro JG, Pavlović I, Novák O, Segura J, Sales E, Arrillaga I (2021) Priming maritime pine megagametophytes during somatic embryogenesis improved plant adaptation to heat stress. Plants 10:1–26. https://doi.org/10.3390/plants10030446

Perrella G, Bäurle I, van Zanten M (2022) Epigenetic regulation of thermomorphogenesis and heat stress tolerance. New Phytol 234:1144–1160. https://doi.org/10.1111/nph.17970

Pinheiro C, Guerra-Guimarães L, David TS, Vieira A (2014) Proteomics: state of the art to study Mediterranean woody species under stress. Environ Exp Bot 103:117–127. https://doi.org/10.1016/j.envexpbot.2014.01.010

Podlešáková K, Ugena L, Spíchal L, Doležal K, De Diego N (2019) Phytohormones and polyamines regulate plant stress responses by altering GABA pathway. N Biotechnol 48:53–65. https://doi.org/10.1016/j.nbt.2018.07.003

Pulido CM, Harry IS, Thorpe TA (1994) Effect of various bud induction treatments on elongation and rooting of adventitious shoots of Canary Island pine (*Pinus canariensis*). Plant Cell Tissue Organ Cult 39:225–230. https://doi.org/10.1007/BF00035974

Pullman GS, Buchanan M (2003) Loblolly pine (*Pinus taeda* L.): Stage-specific elemental analyses of zygotic embryo and female gametophyte tissue. Plant Sci 164:943–954. https://doi.org/10.1016/S0168-9452(03)00080-3

Puértolas Simón J, Prada Sáez MA, Climent Maldonado J, Oliet Palá J, Del Campo Garcia AD

(2012) *Pinus halepensis* Mill. In: García JP, Navarro Cerrillo RM, Nicolás Peragón JL, Prada Sáez MA, Serrada Hierro R. (Eds) Producción y manejo de semillas y plantas forestales. Organismo Autónomo Parques Nacionales Ministerio de Agricultura. Alimentación y Medio Ambiente. pp. 885-880.

Qin L-X, Li Y, Li · Deng-Di, Xu W-L, Zheng Y, Li X-B (2014) *Arabidopsis* drought-induced protein Di19-3 participates in plant response to drought and high salinity stresses. Plant Mol Biol 86:609–625. https://doi.org/10.1007/s11103-014-0251-4

Qu A, Ding Y, Jiang Q, Zhu C (2013) Molecular mechanisms of the plant heat stress response. Biochem Biophys Res Commun 432:203–207. https://doi.org/10.1016/j.bbrc.2013.01.104

Quan R, Shang M, Zhang H, Zhao Y, Zhang J (2004) Engineering of enhanced glycine betaine synthesis improves drought tolerance in maize. Plant Biotechnol J 2:477–486. https://doi.org/10.1111/j.1467-7652.2004.00093.x

Quoirin M, Lepoivre P (1977) Improved media for *in vitro* culture of *Prunus* sp. Acta Hortic 78:437–442. https://doi.org/10.17660/ActaHortic.1977.78.54

Ragonezi C, Klimaszewska K, Castro MR, Lima M, de Oliveira P, Zavattieri MA (2010) Adventitious rooting of conifers: Influence of physical and chemical factors. Trees - Struct Funct 24:975–992. https://doi.org/10.1007/s00468-010-0488-8

Ramage CM, Williams RR (2002) Mineral nutrition and plant morphogenesis. Vitr Cell Dev Biol - Plant 38:116–124. https://doi.org/10.1079/IVP2001269

Ramarosandratana A, Harvengt L, Bouvet A, Calvayrac R, Pâques M (2001) Influence of the

embryonal-suspensor mass (ESM) sampling on development and proliferation of maritime pine somatic embryos. Plant Sci 160:473–479. https://doi.org/10.1016/S0168-9452(00)00410-6

Rank R, Maneta M, Higuera P, Holden Z, Dobrowski S, Gardiner BA (2022) Conifer seedling survival in response to high surface temperature events of varying intensity and duration. Front. For. Glob. Change 4: 731267. https://doi.org/10.3389/ffgc.2021.731267

Reinert J (1959) Über die Kontrolle der Morphogenese und die Induktion von Adventivembryonen an Gewebekulturen aus Karotten. Planta 53:318–333

Reis E, Batista MT, Canhoto JM (2008) Effect and analysis of phenolic compounds during somatic embryogenesis induction in *Feijoa sellowiana* Berg. Protoplasma 232:193–202. https://doi.org/10.1007/s00709-008-0290-2

Renau-morata B, Ollero J, Arrillaga I, Segura J (2005) Factors influencing axillary shoot proliferation and adventitious budding in cedar. Tree Physiol 25:477–486. https://doi.org/10.1093/treephys/25.4.477

Reynolds ES (1963) The use of lead citrate at high pH as an electron-opaque stain in electron microscopy. J Cell Biol 17:208–212. https://doi.org/10.1083/jcb.17.1.208

Ribeiro T, Viegas W, Morais-Cecílio L (2009) Epigenetic marks in the mature pollen of *Quercus suber* L. (*Fagaceae*). Sex Plant Reprod 22:1–7. https://doi.org/10.1007/s00497-008-0083-y

Riov J, Foxa H, Attiasa R, Shklar G, Farkash-Haim L, Sitbon R, Moshe Y, Abu-Abied M, Sadot E, David-Schwartz R (2020) Improved method for vegetative propagation of mature *Pinus halepensis* and its hybrids by cuttings. Isr J Plant Sci 67:5–15. https://doi.org/10.1163/22238980-20191118

Rittenberg D, Foster G (1940) A new procedure for quantitative analysis by isotope dilution, with application to the determination of amino acids and fatty acids. J Biol Chemestry 133:737–744

Rodríguez SM, Ordás RJ, Alvarez JM (2022) Conifer Biotechnology: An overview. Forests. 13:1061. https://doi.org/10.3390/f13071061

Rojas-Vargas A, Castander-Olarieta A, Montalbán IA, Moncaleán P (2022) Influence of physico-chemical factors on the efficiency and metabolite profile of adult *Pinus radiata* D. Don bud organogenesis. Forests 13:1455. https://doi.org/10.3390/f13091455

Sáenz L, Jones LH, Oropeza C, Vláčil D, Strnad M (2003) Endogenous isoprenoid and aromatic cytokinins in different plant parts of *Cocos nucifera* (L.). Plant Growth Regul 39:205–215. https://doi.org/10.1023/A:1022851012878

Sakakibara H (2010) Cytokinin biosynthesis and metabolism. In: Davies P (ed) Plant Hormones: Biosynthesis, Signal Transduction, Action! Springer Netherlands, pp 95–114

Salaj T, Klubicová K, Matusova R, Salaj J (2019) Somatic embryogenesis in selected conifer trees *Pinus nigra* arn. And abies hybrids. Front Plant Sci 10:1–13. https://doi.org/10.3389/fpls.2019.00013

Sánchez-González A (2008) Una visión actual de la diversidad y distribución de los pinos de

México. Madera y Bosques 14:107–120. https://doi.org/10.21829/myb.2008.1411222

Sánchez-Salguero R, Navarro-Cerrillo RM, Camarero JJ, Fernández-Cancio Á (2012) Selective drought-induced decline of pine species in southeastern Spain. Clim Change 113:767–785. https://doi.org/10.1007/s10584-011-0372-6

Sarmast MK (2018) *In vitro* propagation of conifers using mature shoots. J For Res 29:565–574. https://doi.org/10.1007/s11676-018-0608-7

Sarris D, Christodoulakis D, Körner C (2011) Impact of recent climatic change on growth of low elevation eastern Mediterranean forest trees. Clim Change 106:203–223. https://doi.org/10.1007/s10584-010-9901-y

Schlaen RG, Mancini E, Sanchez SE, Perez-Santángelo S, Rugnone ML, Simpson CG, Brown JWS, Zhang X, Chernomoretz A, Yanovsky MJ (2015) The spliceosome assembly factor GEMIN2 attenuates the effects of temperature on alternative splicing and circadian rhythms. Proc Natl Acad Sci U S A 112:9382–9387. https://doi.org/10.1073/pnas.1504541112

Schwarzerová K, Vondráková Z, Fischer L, Bořík̆ová P, Bellinvia E, Eliášová K, Havelková L, Fišerová J, Vágner M, Opatrný Z (2010) The role of actin isoforms in somatic embryogenesis in Norway spruce. BMC Plant Biol 10:. https://doi.org/10.1186/1471-2229-10-89

Shi D, Ali I, Tang J, Yang W (2017) New insights into 5hmC DNA modification: generation, distribution and function. Front. Genet. 8:1–11. https://doi.org/10.3389/fgene.2017.00100

Simón JP, Sáez MAP, Maldonado JC, Palá JO, Garcia ADDC (2012) *Pinus halepensis* Mill. In: García JP, Cerrillo RMN, Peragón JLN, Sáez MAP, Hierro RS (Eds.). Producción y Manejo de Semillas y Plantas Forestales. Ministerio de Agricultura, Alimentación y Medio Ambiente, Madrid, pp. 885-880.

Skoog F, Miller CO (1957) Chemical regulation of growth and organ formation in plant tissues cultured. Symp Soc Exp Biol 11:118–131

Skordilis A, Thanos CA (1997) Comparative ecophysiology of seed germination strategies in the seven pine species naturally growing in Greece. In: Ellis RH, Black M, Murdoch AJ, Hong,TD (Eds). Basic and Applied Aspects of Seed Biology. Springer, Dordrecht, pp. 623-632.

Smertenko A, Bozhkov P V (2014) Somatic embryogenesis: life and death processes during apical-basal patterning. J Exp Bot 65:1343–60. https://doi.org/10.1093/jxb/eru005

Smulders MJM, Klerk GJ de (2010) Epigenetics in plant tissue culture. Plant Growth Regul 2010 632 63:137–146. https://doi.org/10.1007/S10725-010-9531-4

Sow MD, Allona I, Ambroise C, Conde D, Fichot R, Gribkova S, Jorge V, Le-Provost G, Pâques L, Plomion C, Salse J, Sanchez-Rodriguez L, Segura V, Tost J, Maury S (2018) Epigenetics in forest trees: State of the art and potential implications for breeding and management in a context of climate change. Adv Bot Res 88:387–453. https://doi.org/10.1016/bs.abr.2018.09.003

Spíchal L (2012) Cytokinins - Recent news and views of evolutionally old molecules. Funct Plant Biol 39:267–284. https://doi.org/10.1071/FP11276

Spurr AR (1969) A low-viscosity epoxy resin embedding medium for electron microscopy. J Ultrasructure Res 26:31–43. https://doi.org/10.1016/S0022-5320(69)90033-1

Stasolla C, Thorpe T (2011) Tissue culture: historical perspectives and applications. Appl Plant Biotechnol 15–305

Stasolla C, Yeung EC (2003) Recent advances in conifer somatic embryogenesis: Improving somatic embryo quality. Plant Cell Tissue Organ Cult 74:15–35. https://doi.org/10.1023/A:1023345803336

Steiner N, Farias-Soares FL, Schmidt ÉC, Pereira MLT, Scheid B, Rogge-Renner GD, Bouzon ZL, Schmidt D, Maldonado S, Guerra MP (2016) Toward establishing a morphological and ultrastructural characterization of proembryogenic masses and early somatic embryos of *Araucaria angustifolia* (Bert.) O. Kuntze. Protoplasma 253:487–501. https://doi.org/10.1007/s00709-015-0827-0

Steward FC (1958) Growth and organized development of cultured cells. III. interpretations of the growth from free cell to carrot plant. Am J Bot 45:709-713.

Stojičić D, Budimir S, Ćulafić L (1999) Micropropagation of *Pinus heldreichii*. Plant Cell Tissue Organ Cult 59:147–150. https://doi.org/10.1023/A:1006373218772

Sugiyama M (2015) Historical review of research on plant cell dedifferentiation. J Plant Res 128:349–359. https://doi.org/10.1007/s10265-015-0706-y

Svačinová J, Novák O, Plačková L, Lenobel R, Holík J, Strnad M, Doležal K (2012) A new approach for cytokinin isolation from *Arabidopsis* tissues using miniaturized purification: pipette tip solid-phase extraction. Plant Methods 8:1–14. https://doi.org/10.1186/1746-4811-8-17

Taïbi K, del Campo AD, Vilagrosa A, Bellés JM, López-Gresa MP, Pla D, Calvete JJ, López-Nicolás JM, Mulet JM (2017) Drought tolerance in *Pinus halepensis* seed sources as identified by distinctive physiological and molecular markers. Front Plant Sci 8:1202. https://doi.org/10.3389/fpls.2017.01202

Tavares JJDM (2019) *In vitro* morphogenesis assays in *Pinus halepensis* Mill. Master's Thesis, University of Coimbra, Coimbra, Portugal

Tesniere C, Torregrosa L, Pradal M, Souquet J-M, Gilles C, dos Santos K, Chatelet P, Gunata Z (2006) Effects of genetic manipulation of alcohol dehydrogenase levels on the response to stress and the synthesis of secondary metabolites in grapevine leaves. J Exp Bot 57:91–99. https://doi.org/10.1093/jxb/erj007

Thomas SG, Huang S, Li S, Staiger CJ, Franklin-Tong VE (2006) Actin depolymerization is sufficient to induce programmed cell death in self-incompatible pollen. J Cell Biol 174:221–229. https://doi.org/10.1083/jcb.200604011

Trindade CS, Canas S, Inácio ML, Pereira-Lorenzo S, Sousa E, Naves P (2022) Phenolic Compounds Regulating the Susceptibility of Adult Pine Species to *Bursaphelenchus xylophilus*. Forests 13:1–14. https://doi.org/10.3390/f13040500

Trontin J, Klimaszewska K, Morel A, Hargreaves C, Lelu-Walter M-A (2016) Molecular aspects

of conifer zygotic and somatic embryo development: a review of genome-wide approaches and recent insights. In: Germana MA, Lambardi M (eds) *In vitro* embryogenesis in higher plants. Methods in Molecular Biology, Humana Press, NY pp 167–207

Us-Camas R, Rivera-Solís G, Duarte-Aké F, De-la-Peña C (2014) *In vitro* culture: an epigenetic challenge for plants. Plant Cell, Tissue Organ Cult 2014 1182 118:187–201. https://doi.org/10.1007/S11240-014-0482-8

Valledor L, Escandón M, Meijón M, Nukarinen E, Cañal MJ, Weckwerth W (2014) A universal protocol for the combined isolation of metabolites, DNA, long RNAs, small RNAs, and proteins from plants and microorganisms. Plant J 79:173–180. https://doi.org/10.1111/tpj.12546

Valledor L, Hasbún R, Meijón M, Rodríguez JL, Santamaría E, Viejo M, Berdasco M, Feito I, Fraga MF, Cañal MJ, Rodríguez R (2007) Involvement of DNA methylation in tree development and micropropagation. Plant Cell Tissue Organ Cult 91:75–86. https://doi.org/10.1007/s11240-007-9262-z

Valledor L, Jorrín J V., Rodríguez JL, Lenz C, Meijón M, Rodríguez R, Cañal MJ (2010) Combined proteomic and transcriptomic analysis identifies differentially expressed pathways associated to *Pinus radiata* needle maturation. J Proteome Res 9:3954–3979. https://doi.org/10.1021/pr1001669

Van Damme EJM, Barre A, Rougé P, Peumans WJ (2004) Cytoplasmic/nuclear plant lectins: A new story. Trends Plant Sci 9:484–489. https://doi.org/10.1016/j.tplants.2004.08.003

Varis S, Klimaszewska K, Aronen T (2018) Somatic embryogenesis and plant regeneration from primordial shoot explants of *Picea abies* (L.) H. Karst. Somatic trees. Front Plant Sci 871:1–8. https://doi.org/10.3389/fpls.2018.01551

Vasil IK (2008) A history of plant biotechnology: From the cell theory of Schleiden and Schwann to biotech crops. Plant Cell Rep. 27:1423–1440. https://doi.org/10.1007/s00299-008-0571-4

Vennetier M, Ripert C, Rathgeber C, Bellot J, Maestre FT, Chirino E, Hernández N, De Urbina JO, Botella L, Santamaría O, Diez JJ, Javier Diez J, Aka H, Darici C (2010) Afforestation with *Pinus halepensis* reduces native shrub performance in a Mediterranean semiarid area. Fungal Divers 41:9–18. https://doi.org/10.1016/j.ejsobi.2005.05.001

Viejo M, Santamaría ME, Rodríguez JL, Valledor L, Meijón M, Pérez M, Pascual J, Hasbún R, Fraga MF, Berdasco M, Toorop PE, Cañal MJ, Fernández RR (2012) Epigenetics, the role of DNA methylation in tree development. Methods Mol Biol 877:277–301. https://doi.org/10.1007/978-1-61779-818-4_22

Voll LM, Zell MB, Engelsdorf T, Saur A, Wheeler MG, Maria F, Weber APM, Maurino VG (2012) Loss of cytosolic NADP-malic enzyme 2 in *Arabidopsis thaliana* is associated with enhanced susceptibility to *Colletotrichum higginsianum*. New Phytol 195:189–202. https://doi.org/10.1111/j.1469-8137.2012.04129.x

Von Aderkas P, Bonga JM (2000) Influencing micropropagation and somatic embryogenesis in mature trees by manipulation of phase change, stress and culture environment. Tree Physiol

20:921–928. https://doi.org/10.1093/treephys/20.14.921

von Arnold S, Clapham D, Abrahamsson M (2019) Embryology in conifers. In: Cánovas FM (ed) Advances in Botanical Research, Elsevier Ltd, pp 157–184

von Arnold S, Eriksson T (1984) Effect of agar concentration on growth and anatomy of adventitious shoots of *Picea abies* (L.) Karst. Plant Cell Tissue Organ Cult 3:257–264

von Arnold S, Sabala I, Bozhkov P, Dyachok J, Filonova L (2002) Developmental pathways of somatic embryogenesis. Plant Cell Tissue Organ Cult 69:233–249. https://doi.org/10.1023/A:1015673200621

Vondrakova Z, Dobrev PI, Pesek B, Fischerova L, Vagner M, Motyka V (2018) Profiles of endogenous phytohormones over the course of norway spruce somatic embryogenesis. Front Plant Sci 9:1–13. https://doi.org/10.3389/fpls.2018.01283

Walter C, Find JI, Grace LJ (2005) Somatic embryogenesis and genetic transformation in *Pinus radiata*. In: Jain SM, Gupta PK (eds) Protocol for Somatic Embryogenesis in Woody Plants. Springer, Dordrecht, pp 11–24

Wang L, Yu C, Chen C, He C, Zhu Y, Huang W (2014) Identification of rice Di19 family reveals OsDi19-4 involved in drought resistance. Plant Cell Reports 2014 3312 33:2047–2062. https://doi.org/10.1007/S00299-014-1679-3

Weber C, Nover L, Fauth M (2008) Plant stress granules and mRNA processing bodies are distinct from heat stress granules. Plant J 56:517–530. https://doi.org/10.1111/j.1365-313X.2008.03623.x

Weiss G, Emery MR, Corradini G, Živojinovi I (2020) New Values of Non-Wood Forest Products. Forests 11:165. https://doi.org/10.3390/f11020165

Wendling I, Trueman SJ, Xavier A (2014) Maturation and related aspects in clonal forestry-part II: Reinvigoration, rejuvenation and juvenility maintenance. New For 45:473–486. https://doi.org/10.1007/s11056-014-9415-y

Weng Y, Park YS, Krasowski MJ, Tosh KJ, Adams G (2008) Partitioning of genetic variance and selection efficiency for alternative vegetative deployment strategies for white spruce in eastern Canada. Tree Genet. Genomes 4:809-819. https://doi.org/10.1007/s11295-008-0154-0

Weng Y, Park YS, Krasowski MJ (2010) Managing genetic gain and diversity in clonal deployment of white spruce in New Brunswick, Canada. Tree Genet Genomes 6:367–376. https://doi.org/10.1007/s11295-009-0255-4

Wheeler MCG, Arias CL, Tronconi MA, Maurino VG, Andreo CS, Drincovich MF (2008) *Arabidopsis thaliana* NADP-malic enzyme isoforms: high degree of identity but clearly distinct properties. Plant Mol Biol 67:231–242. https://doi.org/10.1007/s11103-008-9313-9

Wheeler MCG, Arias CL, Maurino VG, Andreo CS, Drincovich MF (2009) Identification of domains involved in the allosteric regulation of cytosolic *Arabidopsis thaliana* NADP-malic enzymes. FEBS J 276:5665–5677. https://doi.org/10.1111/j.1742-4658.2009.07258

Wolyn DJ, Jelenkovic G (1990) Nucleotide sequence of an alcohol dehydrogenase gene in

octoploid strawberry (Fragaria × Ananassa Duch.). Plant Mol Biol 14:855–857. https://doi.org/10.1007/BF00016518

Wu J, Wang J, Hui W, Zhao F, Wang P, Su C, Gong W (2022) Physiology of plant responses to water stress and related genes: a review. Forests 13:324. https://doi.org/10.3390/f13020324

Yadav R, Saini R, Adhikary A, Kumar S (2022) Unravelling cross priming induced heat stress, combinatorial heat and drought stress response in contrasting chickpea varieties. Plant Physiol Biochem 180:91–105. https://doi.org/10.1016/j.plaphy.2022.03.030

Yakovlev IA, Carneros E, Lee YK, Olsen JE, Fossdal CG (2016) Transcriptional profiling of epigenetic regulators in somatic embryos during temperature induced formation of an epigenetic memory in Norway spruce. Planta 243:1237–1249. https://doi.org/10.1007/s00425-016-2484-8

Yakovlev IA, Gackowski D, Abakir A, Viejo M, Ruzov A, Olinski R, Starczak M, Fossdal CG, Krutovsky K V. (2019) Mass spectrometry reveals the presence of specific set of epigenetic DNA modifications in the Norway spruce genome. Sci Reports 2019 91 9:1–7. https://doi.org/10.1038/s41598-019-55826-z

Yang F, Xia XR, Ke X, Ye J, Zhu L (2020) Somatic embryogenesis in slash pine (*Pinus elliottii* Engelm): improving initiation of embryogenic tissues and maturation of somatic embryos. Plant Cell Tissue Organ Cult 143:159–171. https://doi.org/10.1007/s11240-020-01905-3

Yildirim T, Kaya Z, Işik K (2006) Induction of embryogenic tissue and maturation of somatic embryos in *Pinus brutia* TEN. Plant Cell Tissue Organ Cult 87:67–76. https://doi.org/10.1007/s11240-006-9137-8

Zang QL, Zhang Y, Han SY, Li WF, Qi LW (2021) Transcriptional and post-transcriptional regulation of the miR171-LaSCL6 module during somatic embryogenesis in *Larix kaempferi*. Trees - Struct Funct 35:145–154. https://doi.org/10.1007/s00468-020-02026-2

Zavattieri MA, Frederico AM, Lima M, Sabino R, Arnholdt-Schmitt B (2010) Induction of somatic embryogenesis as an example of stress-related plant reactions. Electron J Biotechnol 13:1–9. https://doi.org/10.2225/vol13-issue1-fulltext-4

Zhang S, Lemaux PG (2004) Molecular analysis of *in vitro* shoot organogenesis. CRC Crit Rev Plant Sci 23:325–335. https://doi.org/10.1080/07352680490484569

Zhang X-F, Jiang T, Wu Z, Du S-Y, Yu Y-T, Jiang S-C, Lu K, Feng X-J, Wang X-F, Zhang D-P (2013) Cochaperonin CPN20 negatively regulates abscisic acid signaling in *Arabidopsis*. Plant Mol Biol 83:205–218. https://doi.org/10.1007/s11103-013-0082-8